DOCTOR OF PHILOSOPHY

Patterns and Fronts in Cross-Diffusion Systems

Aldandani, Mohammed

Award date:
2021

Patterns and Fronts in Cross-Diffusion Systems

By

Mohammed Aldandani

A Thesis submitted for the degree of Doctor of Philosophy

Division of Mathematics

University of Dundee

Dundee

May 2021

Contents

List of figures

List of tables

Acknowledgements

My sincere and profound gratitude goes first and foremost to my supervisor, Prof. Fordyce Davidson for his valuable suggestions, inspired guidance, insightful criticism, extraordinary patience and constant encouragement and support throughout the entire period of my PhD study. The profound and invaluable knowledge that I gained from him will benefit me in my future life and career.

I want to thank the members of the Division of Mathematics at the University of Dundee for their support and kindness.

I sincerely thank my father Mutrib, mother Aminh, brothers, sisters and friends for their encouragement and support all through my studies. My sincerest thanks to my wife, Rahaf, for being so understanding and for tolerating me through my research.

I also would like to thank my lovely son, Abdullah, who joined us when I was working on this PhD thesis, for giving me unlimited happiness and pleasure.

Furthermore, my deepest gratitude is extended to Jouf University, whose funding has graciously allowed me to study in Scotland.

Declaration

I declare that the following thesis is my own composition and that it has not been submitted before in application for a higher degree.

Mohammed Aldandani

Certification

This is to certify that Mohammed Aldandani has complied with all the requirements for the submission of this Doctor of Philosophy thesis to the University of Dundee.

Prof. Fordyce Davidson

Abstract

Reaction-diffusion systems continue to attract increasing attention from the scientific community, with investigators seeking insights into the patterns that occur in living organisms, in ecological systems, in geochemistry, and in physiochemical systems. Cross-diffusion is a special case of reaction-diffusion system and refers to the phenomenon in which a gradient in the concentration of one species induces a flux of another species.

Pattern formation is a sub-area of complexity science, where non-linear spatial process dynamics are studied. Reaction-diffusion systems are at the core of the mathematical analysis of pattern formation and appear as relevant models for such processes.

A travelling wave is a solution of a partial differential equation with a constant profile (shape) and a constant propagation speed. A key precursor of a developmental process seems to be the appearance of a travelling wave front of chemical concentration in many phenomena in biology.

The aim of this thesis is to better understand how cross-diffusion influences the formation and characteristics of patterns and fronts in reaction-diffusion systems. In particular, we are interested in the mechanism of pattern formations and wave fronts in cross-diffusion systems. We do this by taking an approach that combines mathematical modelling, analysis, and numerical simulations. First, we discuss the derivation

of a cross-diffusion system; in particular, we investigate whether all cross-diffusion systems of two interacting species can be derived from the microscopic master equation. Next, we consider the impact of cross-diffusion on the stability of a spatially uniform equilibrium. Then, we derive a new non-linear cross-diffusion system based on mathematical modelling for tightly packed biomass, and we study the travelling wave solution for this model. Using mathematical modelling, analysis, and numerical simulations, we conclude that cross-diffusion plays a key role in forming spatial patterns for competitive model, and we show that the cross-diffusion model gives rise to the travelling wave solution. The cross-diffusion can generate patterns and can change the sign of travelling fronts speed comparing to standard diffusion.

Chapter 1

Introduction

In this chapter, we begin with a brief mathematical background of topics relating to the project to motivate the work undertaken. We then present an outline of the thesis.

1.1 Cross-Diffusion Models

The reaction-diffusion equation is the mathematical model representation that demonstrates the dispersion of substance concentration under the influence of local reactions and diffusion processes. Diffusion is the movement of particles from a region of higher concentration to a region of lower concentration until equilibrium is reached [3]. There are also number of other physical factors which influence the movement of particles other than diffusion process such as advection, chemotaxis and haptotaxis for more details see [9, 12, 16, 20, 22, 22, 56, 61, 64, 73, 78, 87, 90, 91, 95]. In local reactions, the interaction of substances with each other takes place while in diffusion process, substances disperse in space.

Cross-diffusion, the phenomenon in which a gradient in the concentration of one species

induces a flux of another chemical species [95]. Cross-diffusion can arise in genuinely practical models. For examples see [43, 65, 75]. In general, the cross-diffusion coefficient can be positive, negative, or zero. The positive means that the movement of the species in the direction of lower concentration of another species, and the negative means that one species tends to diffuse in the direction of higher concentration of another species.

The general macroscopic model consisting of two partial differential equations with cross-diffusion has been derived in [39, 72]. They derived macroscopic models for ecological or biological systems in which two interacting species occupy the same spatial environment. They start with micro-level assumptions about the probability of individuals moving from one discrete site into another one, depending on the current population densities of both species in both sites.

These days the investigation of pattern formation is very interested topic in chemistry, physics, and biology. Patterns occur in population dynamics, and are usually investigated through reaction-diffusion models, which consider the diffusion of each species depends only on the gradients of the concentration of the species itself [5, 6, 11, 19, 36, 52]. On the contrary, when a gradient in the concentration of one species induces a flux of another species, one must take into account also the cross-diffusion terms. Cross-diffusion plays an important role in patterns formation of reaction-diffusion systems, and large attention has recently been given to studying the stability behaviour of a system of interacting populations, taking into account the effects of self and cross-diffusion [31, 55]. We will present some existing models for which pattern formation has been shown.

The principal ingredients of reaction-diffusion models are equation of the form

$$\mathbf{u}_t = \nabla \cdot (D(\mathbf{u})\nabla \mathbf{u}) + \mathbf{f}(\mathbf{u}), \tag{1.1.1}$$

where f can be associated with the representation of death and/or birth process, while u can be associated with representation of population density. $D(\mathbf{u})$ in equation (1.1.1) denotes the matrix of diffusion coefficients (a diagonal matrix if no cross-diffusion). Since, $\nabla\mathbf{u}$ in equation (1.1.1) is a tensor, therefore, $\nabla \cdot D(\mathbf{u})\nabla\mathbf{u}$ will be a vector, see [59]. In the case D is space-dependent are more often observed within the biomedical modelling domain such as organisms diffusion within heterogeneous environments and growth of brain tumors; more details in [84, 85, 86].

In special case, we can have diffusion matrix as a diagonal matrix. For instance, in the case of a two-species model, self-diffusion matrix takes the form

$$\begin{pmatrix} D_{11} & 0 \\ 0 & D_{22} \end{pmatrix}. \tag{1.1.2}$$

We note that cross-diffusion will be discussed in much more depth later, which refers to the fact that the flux of one species is triggered by the concentration gradient of another species. The cross-diffusion coefficients are the diffusion matrix elements that are not diagonal, meaning that a minimum of one non-diagonal diffusion matrix element in a cross-diffusion setting is different from zero [95]. We can have a diffusion matrix as a full constant matrix. For instance, in special case of a two-species model, cross-diffusion matrix takes the form

$$\begin{pmatrix} D_{11} & D_{12} \\ D_{21} & D_{22} \end{pmatrix}. \tag{1.1.3}$$

1.2 Derivation of Reaction-Diffusion Equations / Conservation of Mass

Towards the derivation of the reaction-diffusion equation following [22, 64], let us account for diffusion in three-dimension space with an arbitrary surface (S) with volume (V). As per the definition of conservation equation, the overall rate of change of material within volume V will be the same as the rate of flow of material across the surface S plus any new material created within the volume V. Mathematically, this can be expressed as presented in equation (1.2.1).

$$\frac{\partial}{\partial t}\int_V u(\mathbf{x},t)dV = -\int_S \mathbf{J}\cdot\mathbf{dS} + \int_V f dV, \tag{1.2.1}$$

where $\mathbf{J}$ denotes the material flux and f denotes the source of material, which may be a function of $u, \mathbf{x}$ and t. Considering that $u(\mathbf{x},t)$ is continuous and implementing divergence theorem to the surface integral, equation (1.2.1) will transform into

$$\int_V \left[\frac{\partial u}{\partial t} + \nabla\cdot\mathbf{J} - f(u,\mathbf{x},t)\right] dV = 0. \tag{1.2.2}$$

As it is known that volume V is arbitrary, therefore, the integrand must result in zero. As a result, conservation equation for u can be expressed as the following

$$u_t = -\nabla\cdot\mathbf{J} + f(u,\mathbf{x},t). \tag{1.2.3}$$

Equation (1.2.3) is valid for any general value of $\mathbf{J}$. For instance, in case of classical transport process, $\mathbf{J}$ is

$$\mathbf{J} = -D\nabla u, \tag{1.2.4}$$

which called Fickian diffusion.

Hence, equation (1.2.3) with (1.2.4) will become

$$u_t = \nabla \cdot (D\nabla u) + f(u, \mathbf{x}, t), \tag{1.2.5}$$

where D might be a function of $\mathbf{x}$ and u or t.

Let us now generalize the equation (1.2.5) for multiple interacting substances. In that case, $u_i(\mathbf{x},t), i = 1,\ldots,m$ will represent the concentration of the interacting substances and D_i will represent the diffusion coefficient of each substance. Equation (1.2.5) will now transform into equation (1.2.6) for the multiple interacting substances.

$$\mathbf{u}_t = \nabla \cdot (D(\mathbf{u})\nabla \mathbf{u}) + \mathbf{f}(\mathbf{u}), \tag{1.2.6}$$

1.3 Derivation of Cross-Diffustion from Random Walk

In this section, we show an alternative method of derivation of PDEs particularly cross-diffusion models. We derive PDEs from a random walk. This derivation can lead to the same equation we derive in section 1.2. Our goal is to derive a cross-diffusion system based on a continuous in time, discrete in space master equation that has done before in [39, 72]. We re-derive it because we use this derivation as start point of our work in Chapter 2. We will investigate whether all cross-diffusion systems of two interacting species can be a special case of this derivation. Khassehkhan in [72] showed that some examples of cross-diffusion systems are special case of this derivation, however we

will continue this investigation by considering other examples. Before that, we show the derivation of a continuous in time, discrete in space master equation.

We will only consider the spatial case 1-D in space for simplicity, although we could use this method for the case n-D. To start the derivation, we first derive a scalar PDEs, where the jump probabilities are simple. Let the variable $p(x,t)$ be defined as the probability of a randomly chosen individual being found on the interval $(x, x+\Delta x)$ at the time t [46], where Δx is a small space interval, Thus, for a population size N with population density $u(x,t)$,

$$p(x,t) = \frac{1}{N}\int_x^{x+\Delta x} u(\xi,t)d\xi \longrightarrow \frac{\Delta x\, u(x,t)}{N} \quad as \quad \Delta x \longrightarrow 0. \tag{1.3.1}$$

During time interval Δt an individual may move Δx to the right with probability $q^+(x,t)$, Δx to the left with probability $q^-(x,t)$, and may remain stationary with probability $1-q^+(x,t)-q^-(x,t)$. If there are no births and deaths then then $p(x,t+\Delta t)$ satisfies

$$\begin{aligned} p(x,t+\Delta t) =& p(x,t) + q^+(x-\Delta x,t)p(x-\Delta x,t) \\ &+ q^-(x+\Delta x,t)p(x+\Delta x,t) - (q^+(x,t)+q^-(x,t))p(x,t). \end{aligned} \tag{1.3.2}$$

Expanding L.H.S in (1.3.2) only in time t yields

$$\begin{aligned} p(x,t) + \frac{\partial}{\partial t}p(x,t)\ \triangle t + H.O.T =& p(x,t) + q^+(x-\Delta x,t)p(x-\Delta x,t) \\ &+ q^-(x+\Delta x,t)p(x+\Delta x,t) - (q^+(x,t)+q^-(x,t))p(x,t). \end{aligned}$$

Cancelling $p(x,t)$ from both sides, we have

$$\frac{\partial}{\partial t}p(x,t)\Delta t = q^{+}_{k-1}p(x-\Delta x,t) + q^{-}_{k+1}p(x+\Delta x,t) - (q^{+}_{k}+q^{-}_{k})p(x,t),$$

where $q^{\pm}_{k} = q^{\pm}(x,t)$ and $q^{\pm}_{k\mp1} = q^{\pm}(x\mp\Delta x,t)$.

Taking the appropriate limit as Δt converge to zero ($\Delta t \longrightarrow 0$ so that $\frac{q^{\pm}_{k}}{\Delta t} \longrightarrow \tau^{\pm}_{k}$), and using (1.3.1) gives the continuous in time, discrete in space master equation which defined over an infinite domain grid in the unbounded domain is

$$\frac{du_k}{dt} = \tau^{+}_{k-1}u_{k-1} + \tau^{-}_{k+1}u_{k+1} - (\tau^{+}_{k}+\tau^{-}_{k})u_k. \tag{1.3.3}$$

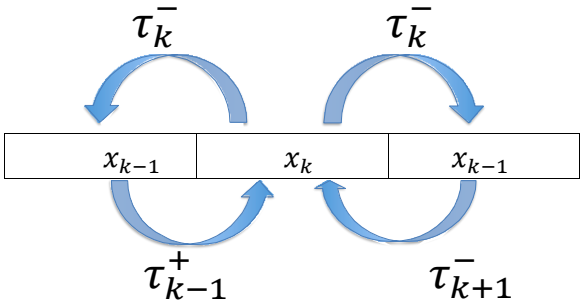

Figure 1.1: Schematic of movement of biomass between neighbouring lattice cells. The probability for biomass to move from cell x_k into cell $x_{k\pm1}$ is denoted by $\tau^{\pm}_{k}$ etc.

Note that $x_{k-1} = x_k - \Delta x$ and $x_{k+1} = x_k + \Delta x$.

u_k, u_{k-1} and u_{k+1} are the biomass density of species u, at the locations x_k, x_{k-1} and x_{k+1} respectively. Here a biomass of u in the location k_k can move to the left or to the right to exit, with the transfer rate τ^{-}_{k} or τ^{+}_{k}, respectively. The biomass in a neighbouring location (x_{k-1} or x_{k+1}) can move into location x_k either from the left with transfer rate τ^{+}_{k-1} or from the right with τ^{-}_{k+1}. Note that $\tau^{\pm}_{k} = \lim_{\Delta t\to 0}\frac{q^{\pm}_{k}}{\Delta t}$, and $q^{\pm}_{k}$ represents the probability of a jump from location x_k to location $x_{k\pm1}$. Equation (1.3.3) is a lot used

in mathematical biology [1, 39, 51, 65, 68, 70, 72, 72, 83, 94], to derive population-level macroscopic partial differential equation models from microscopic behavioural rules.

If u_k is interpreted as a quantity in the cell center x_k, the grid function u_k can be interpolated with a smooth function u with $u(t,x_k) = u_k(t)$ and similarly, $q^{\pm}(x_k) = q_k^{\pm}$. For given t we expand $u(t,x_{k\pm1})$ and $q^{\pm}(x_{k\pm1})$ by Taylor series:

$$u(t,x_{k\pm1}) = u(t,x_k) \pm \Delta x \frac{\partial u(t,x_k)}{\partial x} + \frac{(\Delta x)^2}{2}\frac{\partial^2 u(t,x_k)}{\partial x^2} + H.O.T, \tag{1.3.4}$$

and

$$q^{\pm}(x_{k\pm1}) = q_k^{\pm} \pm \Delta x \frac{\partial q_k^{\pm}}{\partial x} + \frac{(\Delta x)^2}{2}\frac{\partial^2 q_k^{\pm}}{\partial x^2} + H.O.T. \tag{1.3.5}$$

Substituting these expressions into (1.3.3) and dropping H.O.T, we obtain:

$$\begin{aligned}\frac{\partial u}{\partial t} =& \frac{\Delta x}{\Delta t}\Big[(q^- - q^+)\frac{\partial u}{\partial x} + u(\frac{\partial q^-}{\partial x} - \frac{\partial q^+}{\partial x})\Big] \\ &+ \frac{(\Delta x)^2}{\Delta t}\Big[(\frac{1}{2}q^- + \frac{1}{2}q^+)\frac{\partial^2 u}{\partial x^2} + (\frac{\partial^2 q^-}{\partial x^2} + \frac{\partial^2 q^+}{\partial x^2})\frac{\partial u}{\partial x} + u(\frac{1}{2}\frac{\partial^2 q^+}{\partial x^2} + \frac{1}{2}\frac{\partial^2 q^-}{\partial x^2})\Big].\end{aligned} \tag{1.3.6}$$

q^+ and q^- are probabilities. In this section, we investigate simplest case where q^+ and q^- are constants. However we can choose q^+ and q^- as functions which lead to more complex PDEs, we will investigate this case in section 1.3.1.

We investigate possible cases for q^+ and q^- which end up with scalar equations such as diffusion and advection-diffusion equation.

Constant Jump Probability

For q^+ and q^- as constants, (1.3.6) will be

$$\begin{aligned}\frac{\partial u}{\partial t} =& \frac{\Delta x}{\Delta t}\Big[(q^- - q^+)\frac{\partial u}{\partial x}\Big] \\ &+ \frac{(\Delta x)^2}{\Delta t}\Big[(\frac{1}{2}q^- + \frac{1}{2}q^+)\frac{\partial^2 u}{\partial x^2}\Big].\end{aligned} \tag{1.3.7}$$

We have the following cases for q^+ and q^- :

1. Unbiased random walk $q^+ = q^- = \frac{1}{2}$,

$$\frac{\partial u}{\partial t} = \frac{(\Delta x)^2}{\Delta t}\Big[(\frac{1}{2}.\frac{1}{2} + \frac{1}{2}.\frac{1}{2})\frac{\partial^2 u}{\partial x^2}\Big],$$

if we take

$$\lim_{\Delta x \to 0} \frac{(\Delta x)^2}{2\Delta t} = D > 0.$$

Thus, we obtain the diffusion equation

$$\frac{\partial u}{\partial t} = D\frac{\partial^2 u}{\partial x^2}. \tag{1.3.8}$$

2. Biased random walk $q^+ \neq q^-$,

$$\begin{aligned}\frac{\partial u}{\partial t} =& \frac{\Delta x}{\Delta t}\Big[(q^- - q^+)\frac{\partial u}{\partial x}\Big] \\ &+ \frac{(\Delta x)^2}{2\Delta t}\Big[\frac{\partial^2 u}{\partial x^2}\Big],\end{aligned}$$

if we take

$$\lim_{\substack{\Delta x \to 0 \\ \Delta t \to 0}} [q^- - q^+]\frac{\Delta x}{\Delta t} = v, \quad \lim_{\substack{\Delta x \to 0 \\ \Delta t \to 0}} \frac{(\Delta x)^2}{2\Delta t} = D.$$

Thus, we obtain advection-diffusion equation:

$$\frac{\partial u}{\partial t} = v\frac{\partial u}{\partial x} + D\frac{\partial^2 u}{\partial x^2}. \tag{1.3.9}$$

We compare the diffusion and advection-diffusion equations (1.3.8) and (1.3.9) (continuous) with a random walk (discrete) (1.3.2) numerically in Figures 1.2 1.3. Clearly, after several steps, the probability distribution spreads out and becomes approximately PDEs solution. We solve PDEs in MATLAB (PDEPE) with zero flux boundary condition, and we solve (1.3.2) in MATLAB (see code in Appendix B.2).

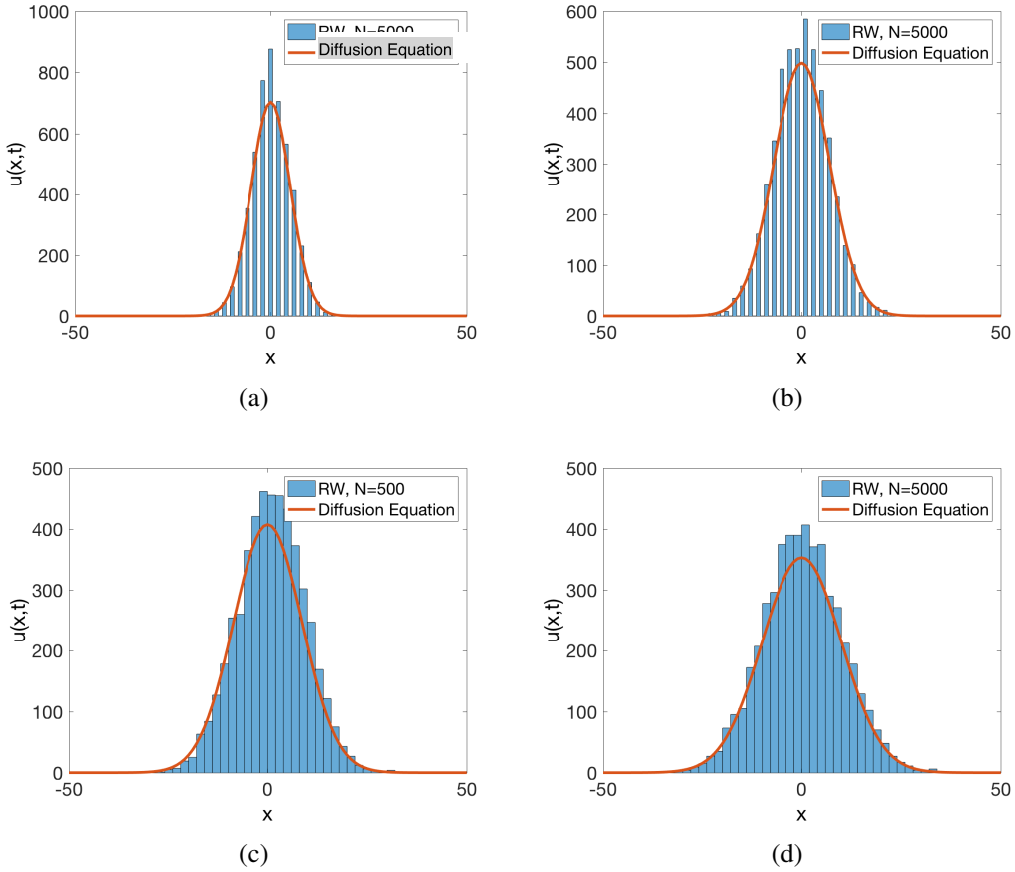

Figure 1.2: Comparing the diffusion equation (1.3.8) and random walk. This figure shows the solution to the diffusion equation, in red. To obtain the teal histogram, 5000 walkers with random walk were simulated for 100 time steps. As a result, each bar represents the number of walkers whose final position was in that bin : (a) At time t=25; (b) At time t=50; (c) At time t=75; and, (d) At time t=100. Parameter values are shown in Table 1.1.

Parameter	Value
D	0.5
q^+	0.5
q^-	0.5

Table 1.1: Table showing the parameter values that used to solve diffusion equation (1.3.8) and master equation (1.3.2).

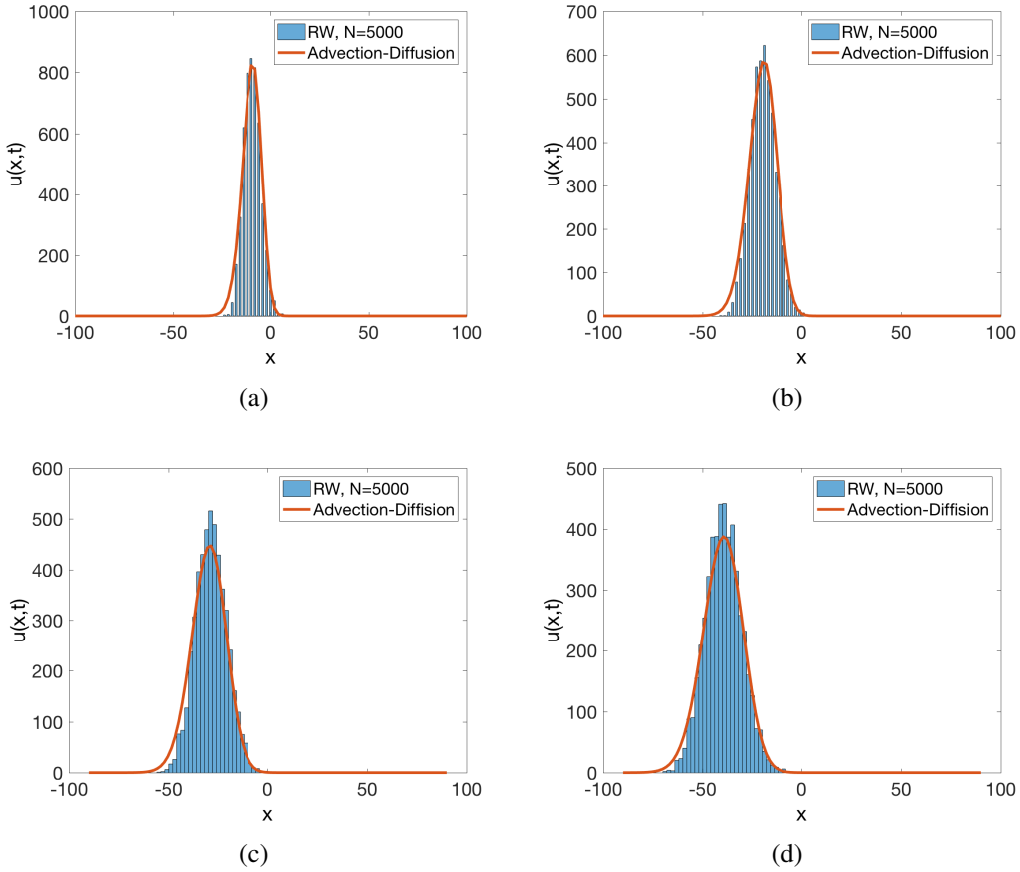

Figure 1.3: Comparing the advection-diffusion equation (1.3.9) and random walk.. This figure shows the solution to the advection-diffusion equation, in red with $I.C = (5000)e^{(-x^2)}$. To obtain the teal histogram, 5000 walkers with random walk were simulated for 100 time steps. As a result, each bar represents the number of walkers whose final position was in that bin : (a) At time t=25; (b) At time t=50; (c) At time t=75; and, (d) At time t=100. Parameter values are shown in Table 1.2.

Parameter	Value
D	0.5
v	0.4
q^+	0.3
q^-	0.7

Table 1.2: Table showing the parameter values that used to solve diffusion equation (1.3.9) and master equation (1.3.2).

1.3.1 Derivation of Cross-Diffusion from a Continuous in Time, Discrete in Space Master Equation

In theoretical ecology and other areas of mathematical biology, a continuous in time, discrete in space master equation is commonly used for single-species communities to derive population-level macroscopic partial differential equation models from microscopic behavioral rules [1, 51, 65, 68, 70, 83, 94, 97]. In Khassehkhan paper [39] , it was demonstrated that a single-species biofilm model could be derived as the macroscopic limit of a microscopic continuous in time, discrete in space master equation in which biomass movement from one site to another is governed by microscopic behavioural rules that account for biomass already present in both sites. This modelling approach is based on a strategy commonly used in spatially structured populations or directed cell movement, such as chemotaxis [1, 51, 65, 68, 94, 97]. For general dual-species systems with spatially interacting populations, this was worked out in Ostrander [67]. Rahman in [72] extend Ostrander derivations to dual-species biofilm systems, following the same master equation approach. A simpler dual-species model was previously derived in [71], where it was implicitly assumed that individual movement is not restricted by the presence of others and that interaction between species takes place through reactions, in which case one obtains a semi-linear model with Fickian diffusion. In Rahman work, they account for the effect that the presence of other cells has on individual movement. In a biofilm, where cells are often packed tightly, this is an important aspect.

In section 1.3, we showed the derivation of a scalar PDE with a simple jump probabilities which are constants. jump probabilities can be functions that lead to different PDEs. In this thesis, we interested two-species cross-diffusion system. So, the derivation of cross-diffusion system must be from two continuous in time, discrete in space master equations. Note a scalar master equation leads to a scalar PDE. The constant

jump probabilities will not lead to cross-diffusion system. For cross-diffusion, jump probabilities need to functions that depend on densities of the two-species.

A derivation of cross-diffusion from a continuous in time, discrete in space master equations is summarized here, using the same approach as outlined in [39, 72], to obtain a better understanding of the origin of cross-diffusion terms in a two-species model, and what they mean in relation to the movement of individuals.

For two interacting species u and v, the continuous in time, discrete in space master equation which defined over an infinite domain grid in the unbounded domain is

$$\begin{aligned} \frac{du_k}{dt} &= \tau^+_{k-1}u_{k-1} + \tau^-_{k+1}u_{k+1} - (\tau^+_k + \tau^-_k)u_k, \\ \frac{dv_k}{dt} &= \beta^+_{k-1}v_{k-1} + \beta^-_{k+1}v_{k+1} - (\beta^+_k + \beta^-_k)v_k. \end{aligned} \tag{1.3.10}$$

Note that equation for v can be derived in similar way we did for u in (1.3.3). u_k, u_{k-1} and u_{k+1} are the biomass density of species u, at the locations x_k, x_{k-1} and x_{k+1} respectively. Similarly for v equation. The master equation (1.3.10) describes the population change in a particular site in a particular species.

In general, the transfer rate $\tau^\pm_k$, $\beta^\pm_k$ can depend on the density of both populations in sites x_k and $x_k \pm 1$. One choice of $\tau^\pm_k$, $\beta^\pm_k$, motived by Eberl [72] is

$$\begin{aligned} \tau^\pm_k &= \gamma q_1(u_k, v_k)p_1(u_{k\pm1}, v_{k\pm1}), \\ \beta^\mp_k &= \mu q_2(u_k, v_k)p_2(u_{k\pm1}, v_{k\pm1}), \end{aligned} \tag{1.3.11}$$

that is a separation of variable approach. Functions q_1, p_1, q_2 and p_2 are the "jump probabilities". q_1 and p_1 are non-negative and continuous functions with $0 \leq q_1, p_1 \leq 1$ that control the local movement from one site to a neighbouring site for species u.

Similarly, q_2 , p_2 for species v. The incentive for species u and v to leave lattice site k is measured by the functions $q_{1,2}(u_k, v_k)$. The function $p_{1,2}(u_k, v_k)$ represent how suitable the lattice site k is for incoming individuals of species u and v.

Functions q_1, p_1, q_2 and p_2 can be understood as probabilities for an individual to move between sites x_k and $x_{k\pm1}$. The coefficient γ is a scaling factor that depends on length-scale and time-scale, i.e. distance between two sites Δx. More specifically, for diffusion problems γ scales with$(\Delta x)^2$, such that $\lim_{\Delta x\to 0} \gamma(\Delta x)^2 = \gamma_0 > 0$, Similarly, for β.

We first introduce two continuous functions $u(t,x)$ and $v(t,x)$ that interpolate the grid functions $u(t,x_k) = u_k(t)$, $v(t,x_k) = u_k(t)$, in order to make the transition from a spatially discrete to a continuous model.

To express $u(t,x_{k\pm1})$ and $v(t,x_{k\pm1})$, we will use the expansion of the Taylor series.

$$\begin{aligned} u(t,x_{k\pm1}) &= u(t,x_k) \pm \Delta x \frac{\partial u(t,x_k)}{\partial x} + \frac{(\Delta x)^2}{2}\frac{\partial^2 u(t,x_k)}{\partial x^2} + H.O.T, \\ v(t,x_{k\pm1}) &= v(t,x_k) \pm \Delta x \frac{\partial v(t,x_k)}{\partial x} + \frac{(\Delta x)^2}{2}\frac{\partial^2 v(t,x_k)}{\partial x^2} + H.O.T, \end{aligned} \tag{1.3.12}$$

where $H.O.T.$ represents higher order terms and Δx is the small distance between grid points.

Also, we can use the Taylor series to describe $q_{1,2}(u_{k\pm1}, v_{k\pm1}), p_{1,2}(u_{k\pm1}, v_{k\pm1})$ as follows

$$
\begin{aligned}
q_{1,2}(u_{k\pm1}, v_{k\pm1}) &= q_{1,2}(u_k, v_k) + (u_{k\pm1} - u_k)\frac{\partial q_{1,2}(u_k, v_k)}{\partial u_k} + (v_{k\pm1} - v_k)\frac{\partial q_{1,2}(u_k, v_k)}{\partial v_k} \\
&+ \frac{1}{2}\left[(u_{k\pm1} - u_k)^2\frac{\partial^2 q_{1,2}(u_k, v_k)}{\partial u_k^2} + (v_{k\pm1} - v_k)^2\frac{\partial^2 q_{1,2}(u_k, v_k)}{\partial v_k^2}\right. \\
&+ \left. 2(u_{k\pm1} - u_k)(v_{k\pm1} - v_k)\frac{\partial q_{1,2}(u_k, v_k)}{\partial u_k \partial v_k}\right] + H.O.T, \qquad (1.3.13)
\end{aligned}
$$

and

$$
\begin{aligned}
p_{1,2}(u_{k\pm1}, v_{k\pm1}) &= p_{1,2}(u_k, v_k) + (u_{k\pm1} - u_k)\frac{\partial p_{1,2}(u_k, v_k)}{\partial u_k} + (v_{k\pm1} - v_k)\frac{\partial p_{1,2}(u_k, v_k)}{\partial v_k} \\
&+ \frac{1}{2}\left[(u_{k\pm1} - u_k)^2\frac{\partial^2 p_{1,2}(u_k, v_k)}{\partial u_k^2} + (v_{k\pm1} - v_k)^2\frac{\partial^2 p_{1,2}(u_k, v_k)}{\partial v_k^2}\right. \\
&+ \left. 2(u_{k\pm1} - u_k)(v_{k\pm1} - v_k)\frac{\partial p_{1,2}(u_k, v_k)}{\partial u_k \partial v_k}\right] + H.O.T. \qquad (1.3.14)
\end{aligned}
$$

Substituting these expressions in the equation (1.3.10) the previously calculated Taylor expansions and taking the limits as $\Delta t \to 0$ and $\Delta x \to 0$, a continuous equation describing the rate of change of u can be found, without taking into account higher order terms. Thus,

$$
\begin{aligned}
u_t &= \gamma(\Delta x)^2\left[q_1 p_1 + u\left(p_1\frac{\partial q_1}{\partial u} - q_1\frac{\partial p_1}{\partial u}\right)\right]\frac{\partial^2 u}{\partial x^2} + \gamma(\Delta x)^2\left[u\left(p_1\frac{\partial q_1}{\partial v} - q_1\frac{\partial p_1}{\partial v}\right)\right]\frac{\partial^2 v}{\partial x^2} \\
&+ \gamma(\Delta x)^2\left[2\frac{\partial^2 q_1}{\partial u}p_1 + u\left(p_1\frac{\partial^2 q_1}{\partial v^2} - q_1\frac{\partial^2 p_1}{\partial v^2}\right)\right]\left(\frac{\partial u}{\partial x}\right)^2 \\
&+ \gamma(\Delta x)^2\left[up_1\frac{\partial^2 q_1}{\partial v^2} - uq_1\frac{\partial^2 p_1}{\partial v^2}\right]\left(\frac{\partial v}{\partial x}\right)^2 \\
&+ \gamma(\Delta x)^2\left[2\frac{\partial q_1}{\partial v}p_1 + 2u\left(p_1\frac{\partial^2 q_1}{\partial u \partial v} - q_1\frac{\partial^2 p_1}{\partial u \partial v}\right)\right]\frac{\partial u}{\partial x}\frac{\partial v}{\partial x}, \qquad (1.3.15)
\end{aligned}
$$

passing to continuous limit, $\Delta x \to 0$ such as $\lim_{\Delta x \to 0} \gamma(\Delta x)^2 = \gamma_0 > 0$ rearranging the order of term we obtain

$$u_t = \gamma_0 \nabla \cdot \left[\left(q_1 p_1 + u \left(p_1 \frac{\partial q_1}{\partial u} - q_1 \frac{\partial p_1}{\partial u} \right) \right) \nabla u + u \left(p_1 \frac{\partial q_1}{\partial v} - q_1 \frac{\partial p_1}{\partial v} \right) \nabla v \right], \tag{1.3.16}$$

which is now recognisable as a cross-diffusion equation, where

$$D_{11} = q_1 p_1 + u \left(p_1 \frac{\partial q_1}{\partial u} - q_1 \frac{\partial p_1}{\partial u} \right), \qquad D_{12} = u \left(p_1 \frac{\partial q_1}{\partial v} - \alpha_1 \frac{\partial p_1}{\partial v} \right). \tag{1.3.17}$$

In an analogous way, we can apply the same methodology to calculate $\partial v / \partial t$.

$$v_t = \mu_0 \nabla \cdot \left[\left(q_2 p_2 + v \left(p_2 \frac{\partial q_2}{\partial v} - q_2 \frac{\partial p_2}{\partial v} \right) \right) \nabla v + v \left(p_2 \frac{\partial q_2}{\partial u} - q_2 \frac{\partial p_2}{\partial u} \right) \nabla u \right] \tag{1.3.18}$$

$$D_{21} = v \left(p_2 \frac{\partial q_2}{\partial u} - q_2 \frac{\partial p_2}{\partial u} \right), \qquad D_{22} = q_2 p_2 + v \left(p_2 \frac{\partial q_2}{\partial v} - q_2 \frac{\partial p_2}{\partial v} \right). \tag{1.3.19}$$

This derivation has been investigated before in [39, 66, 72]. The question is, can any cross-diffusion system can be a special case of this derivation. Ostrander shows that some examples of cross-diffusion systems are special case of this derivation such as the cross diffusion model of Shigesada, Kawasaki, and Teramoto (SKT) and the cross diffusion model of Chattopadhyay and Chatterjee in [66]. They conclude that their

approach in the inverse problem could likely be used to find jump probabilities which recover many other reaction-diffusion systems. Therefore, we extend their work to recover two different systems in Chapter 2, which are the simplest cross-diffusion and new non-linear cross-diffusion system in similar way. By considering these examples, we try to answer whether all cross-diffusion system can be special case of this derivation. In addition, we extend their work on SKT model by comparing the solution of SKT with the solution of the master equation (1.3.10).

1.4 Pattern Formation in Reaction-Diffusion Equations

Chapter 3 deals with the effect of pattern formation on cross-diffusion models, so we introduce pattern formation in this section. In biological sciences, there are number of phenomena and mechanisms which result in temporal or spatial patterns. Furthermore, in terms of variability, these processes occur in different scales among a different range of species for different purposes [102]. Although, there are number of differences and variations in different biological pattern formation mechanisms [33], however, they can be collectively represented through a mathematical expression. The reaction-diffusion equation is the key in developing the mathematical relationship since it represents the evolution of spatio-temporal densities of materials forming the patterns [18, 21, 34, 35, 40, 41, 95]. Each equation includes the diffusion term (Fickian diffusion, porous diffusion) and reaction term (interaction among substance) [64].

Let us assume that diffusion is standard Fickian, then, system can be expressed mathematically as given follows

$$\mathbf{u}_t = \nabla \cdot (D\nabla \mathbf{u}) + f(\mathbf{u}),$$

where $\mathbf{u} = (u_1, \ldots, u_n)^T \in \mathbb{R}^n_+$ is the representation of chemical substance concentrations and bifurcations on the system eigenvalues.

There are three principle type of instabilities including wave, Turing and Hopf in such kind of diffusion-reaction systems [7, 57].

- **Wave bifurcation:** Generates time oscillatory and spatially periodic type of patterns.
- **Turing bifurcation:** Generated time stationary and spatially periodic type of patterns.
- **Hopf bifurcation:** Generates time oscillatory and spatially homogeneous type of patterns.

However, the combination of instabilities may increase the wealth of patterns. There is the possibility of having a periodic pattern in space and time without having a wave instability, as when both Turing and Hopf instabilities are present, leading to oscillatory Turing patterns [34, 107].

The Turing mechanism discovered 1952 has been considered the most common towards mathematically describing biological pattern formation mechanism under constant diffusion coefficients [93] .

Typically, it is assumed that the diffusion process influences the system differential equations towards making it stable. However, in the case of Turing pattern formation, the opposite is true. Process of Turing pattern formation occurs when a system (previously stable in the absence of diffusion) becomes spatially unstable under the diffusion process. This process is referred to as diffusion-driven instability and results in non-homogeneous pattern formation. For the sake of mathematical representation, this process must need to involve two substances with different diffusion constant; an

activator with D_A and an inhibitor with D_I. Non-linear reaction terms corresponding to these diffusion constants will become $F(A,I)$ and $G(A,I)$, respectively. Overall, the system will be transformed as follows

$$A_t = \nabla \cdot (D_A \nabla A) + F(A,I),$$
$$I_t = \nabla \cdot (D_I \nabla I) + G(A,I).$$

For the case of diffusion-drive instability, the reaction-diffusion equations can be expressed accordingly in their non-dimensional form as given in system (1.4.1).

$$\begin{aligned} u_t &= \nabla \cdot (\nabla u) + \gamma f(u,v), \\ v_t &= \nabla \cdot (d \nabla u) + \gamma g(u,v), \end{aligned} \tag{1.4.1}$$

where $\gamma \in \mathbb{R}_+$ is the term added by scale length and is the representation of domain size, and $d = \frac{D_I}{D_A}$ is the ratio between two diffusion coefficients. In [93], Alan Turing showed how a reaction-diffusion system could exhibit such instabilities to form patterns. For a two-component reaction-diffusion system, a key requirement for diffusion-driven instability is the concept of long-range inhibition and short-range activation (Gierer and Meinhardt 1972). This implies that one of the species (the inhibitor D_I) must diffuse faster (typically much faster) than the autocatalytic species (activator D_A) ($D_I > D_A \Rightarrow d > 1$), thereby fulfilling one of the necessary condition for the formation of spatial structure. In summary, Turing instability means that a stable steady state of ODE become unstable (can generate patterns) in the presence of diffusion with $d > 1$.

1.4.1 Linear Stability Analysis for Diffusion-Driven Instability

Now, we consider the linear stability analysis for the reaction-diffusion system (Turing Instability). For any steady state to be driven unstable in the presence of diffusion, certain conditions must be satisfied. To formulate the problem mathematically, we need to specify initial conditions and boundary conditions. We take these to be given initial conditions (which will be small perturbations about the steady state) and zero flux boundary conditions. Therefore the mathematical problem is

$$\begin{aligned} u_t &= \nabla \cdot (\nabla u) + \gamma f(u,v), \\ v_t &= \nabla \cdot (d\nabla v) + \gamma g(u,v), \\ (\mathbf{n}.\nabla) &\begin{bmatrix} u \\ v \end{bmatrix} = 0, \quad \mathbf{r} \text{ on } \partial\Omega; \quad u(\mathbf{r},0),\ v(\mathbf{r},0) \text{ given}, \end{aligned} \tag{1.4.2}$$

where $\partial\Omega$ is the closed boundary of the reaction-diffusion domain Ω and n is the unit outward normal to $\partial\Omega$.

The relevant homogeneous steady state (u_0, v_0) of (1.4.2) is the positive solution of

$$f(u,v) = 0, \quad g(u,v) = 0.$$

In the absence of diffusion, any homogeneous (positive) steady state must be linearly stable since we are concerned with diffusion-driven instability. It is only in the presence of diffusion that we want this steady state to be driven unstable. With no diffusion terms, we have

$$\frac{du}{dt} = \gamma f(u,v), \quad \frac{du}{dt} = \gamma g(u,v). \tag{1.4.3}$$

We consider the following perturbations to the steady state (u_0, v_0)

$$u(x,t) = u_0 + \hat{u}(t), \quad v(x,t) = v_0 + \hat{v}(t). \tag{1.4.4}$$

where $|\hat{u}(t)| << 1$ and $|\hat{v}(t)| << 1$ are small perturbations.

Substitute these into equation (1.4.3), we have

$$\frac{du}{dt} = \gamma f(u_0 + \hat{u}, v_0 + \hat{v}), \quad \frac{du}{dt} = \gamma g(u_0 + \hat{u}, v_0 + \hat{v}), \tag{1.4.5}$$

and using a Taylor expansion of f and g about (u_0, v_0) we obtain the linearised system

$$\begin{aligned} &\mathbf{w}_t = \gamma J \mathbf{w}, \\ &\text{where} \\ &J = \begin{pmatrix} f_u^o & f_v^o \\ g_u^o & g_v^o \end{pmatrix}, \quad \mathbf{w} = \begin{pmatrix} \hat{u}(t) \\ \hat{v}(t) \end{pmatrix}. \end{aligned} \tag{1.4.6}$$

The subscripts u and v denote differentiation with respect to u and v respectively, and ^{o} indicates evaluation at the equilibrium (u_0, v_0).

We look for solution $\mathbf{w} \propto e^{\lambda t}$, where λ is the eigenvalue. If $Re\lambda < 0$, the steady state $\mathbf{w} = 0$ is linearly stable since in this case the perturbation $\mathbf{w} \longrightarrow 0$ as $t \longrightarrow \infty$.

Substituting the form of solution into (1.4.6) determines the characteristic equation

$$\lambda^2 - \gamma \mathrm{tr}(J)\lambda + \gamma^2 \det(J) = 0,$$

so

$$\lambda_1, \lambda_2 = \frac{\gamma}{2}[\mathrm{tr}(J) \pm \sqrt{\mathrm{tr}(J)^2 - 4\det(J)}].$$

It can be derived that the linear stability of reaction equations is guaranteed if $Re\lambda < 0$, that is

$$\mathrm{tr}(J) = f_u^o + g_v^o < 0, \tag{1.4.7}$$

$$\det(J) = f_u^o g_v^o - f_v^o g_u^o > 0. \tag{1.4.8}$$

We now consider the whole system, including diffusion (1.4.2), and we consider the following perturbations to the steady state (u_0, v_0)

$$u(x,t) = u_0 + \hat{u}(x,t), \quad v(x,t) = v_0 + \hat{v}(x,t), \tag{1.4.9}$$

where $|\hat{u}| << 1$ and $|\hat{v}| << 1$ are small perturbations.

Substitute equation (1.4.9) into (1.4.2) and apply a Taylor expansion about (u_0, v_0) to $f(u,v)$ and $g(u,v)$ to obtain the linearised problem

$$\begin{aligned}
&\hat{u}(x,t)_t = \nabla \cdot (\hat{u}(x,t)\nabla\hat{u}(x,t)) + \gamma(f_u^o\hat{u}(x,t) + f_v^o\hat{v}(x,t)),\\
&\hat{v}(x,t)_t = \nabla \cdot (d\hat{v}(x,t)\nabla\hat{v}(x,t)) + \gamma(g_u^o\hat{u}(x,t) + g_v^o\hat{v}(x,t)),\\
&(\mathbf{n}.\nabla)\begin{bmatrix} \hat{u}(x,t) \\ \hat{v}(x,t) \end{bmatrix} = 0, \quad \mathbf{r} \text{ on } \partial\Omega.
\end{aligned} \tag{1.4.10}$$

System (1.4.10) can be written in the form

$$\begin{aligned}
&\mathbf{w}_t = \nabla \cdot (D\mathbf{w}\nabla\mathbf{w}) + \gamma J\mathbf{w}, \quad \mathbf{w} = \begin{pmatrix} \hat{u}(x,t) \\ \hat{v}(x,t) \end{pmatrix},\\
&\text{where}\\
&J = \begin{pmatrix} f_u^o & f_v^o \\ g_u^o & g_v^o \end{pmatrix}, \; D = \begin{pmatrix} 1 & 0 \\ 0 & d \end{pmatrix}.
\end{aligned} \tag{1.4.11}$$

We define $\mathbf{W}(r)$ to be the time-independent solution of the spatial eigenvalue problem defined by

$$\begin{aligned} \triangle \mathbf{W} + k^2 \mathbf{W} &= 0 \qquad \text{on } \Omega, \\ (\mathbf{n}.\nabla)\mathbf{W} &= 0 \qquad \text{on } \partial\Omega. \end{aligned} \tag{1.4.12}$$

For example, in the one-dimensional domain (e.g. $0 \leq x \leq a$) with zero flux boundary conditions, $\mathbf{W} \propto \cos(\frac{n\pi x}{a})$ (n integer) and ($k = \frac{n\pi x}{a}$, k is called the wavenumber). We define the wavelength as $\omega = \frac{2\pi}{k} = \frac{2a}{n}$.

Since n is an integer, there is a discrete set of possible wavenumbers in a finite domain. Let $\mathbf{W}_k(r)$ be the eigenfunction corresponding to the wavenumber k. Each eigenfunction $\mathbf{W}_k$ satisfies zero flux boundary conditions. Since the problem is linear, the solutions $\mathbf{w}(\mathbf{r},t)$ of (1.4.11) in the form

$$\mathbf{w}(\mathbf{r},t) = \sum_k c_k e^{\lambda t} \mathbf{W}_k(\mathbf{r}), \tag{1.4.13}$$

where the constant c_k are determined by Fourier expansion of the initial conditions in term of $\mathbf{W}_k(r)$ and λ is the eigenvalue which for temporal growth. Substituting (1.4.13) into (1.4.11) with (1.4.12) and cancelling $e^{\lambda t}$, we get, for each k

$$\begin{aligned} \lambda \mathbf{W}_k &= \gamma J \mathbf{W}_k + D \triangle \mathbf{W}_k, \\ &= \gamma J \mathbf{W}_k - D k^2 \mathbf{W}_k. \end{aligned}$$

$\mathbf{W}_k$ are required to be non-trivial solutions, thus we determine λ as roots of the characteristic polynomial

$$\det(\lambda I - \gamma J + D k^2) = 0,$$

we have

$$\lambda^2 + G(k^2)\lambda + H(k^2) = 0, \tag{1.4.14}$$

where

$$G(k^2) = k^2 \mathrm{tr}(D) - \gamma \mathrm{tr}(J),$$

and

$$H(k^2) = \det(D)k^4 - \gamma q k^2 + \gamma^2 \det(J), \tag{1.4.15}$$

with

$$q := [d f_u^o + g_v^o].$$

We require $Re(\lambda) > 0$ for exponential growth and hence for steady state to now be unstable. For the case $k = 0$ we are back to the diffusionless system, and we already imposed the constraints that the steady state is stable in the absence of any spatial effect. For the steady state to be unstable when we add diffusion we require $Re(\lambda) > 0$ for some $k \neq 0$. This can happen if either $G(k^2) < 0$ or $H(k^2) < 0$. Since we have $(f_u^o + g_v^o) < 0$ and $k^2[1+d] > 0$, then we have $G(k^2) > 0$. Therefore, h must be negative to have $Re(\lambda) > 0$, and since $d > 0$ and $|J| > 0$, the only possibility for $H(k^2) < 0$ is if $d f_u^o + g_v^o > 0$ Thus, further requirement for instability is

$$d f_u^o + g_v^o > 0 \quad \implies d \neq 1, \tag{1.4.16}$$

(1.4.16) is necessary but not sufficient for $Re(\lambda) > 0$. For $H(k^2)$ to be negative for non-zero k^2, the minimum $H(k^2)_{min}$ must be negative

$$H(k^2)_{min} = \gamma^2 [\det(J) - \frac{(d f_u^o + g_v^o)^2}{4d}],$$

thus,

$$(df_u^o + g_v^o)^2 > 4d\det(J), \tag{1.4.17}$$

note $4d\det(J) > 0$. Now we have (1.4.7), (1.4.8), (1.4.16) and (1.4.17) conditions for diffusion driven instability. Here we derive all the necessary condition for diffusion driven instability in general. In next section, we will check these condition for our specific system.

1.4.2 Cross-Diffusion and Pattern Formation

Recently, cross-diffusion effects have been recently considered in [25, 26, 49, 76, 88, 89, 108]. The effects of cross-diffusion on models for pattern formation have been studied in many theoretical papers [4, 13, 14, 27, 28, 30, 31, 38, 42, 45, 48, 50, 55, 69, 74, 76, 79, 88, 95, 105, 109]. When linear cross-diffusion terms are introduced into the Schnakenberg model, the constant steady state is destabilized even if the diffusion constant of the inhibitor is smaller or equal to the diffusion constant of the activator, as shown in [55]. Cross-diffusion has been shown to be the cause of Turing instability in a large class of predator-prey or competitive kinetics term "cross-diffusion induced instability " [29, 30, 69, 79, 92, 95]. However, other cross-diffusion models that have not been investigated yet. The purpose of Chapter 3 is to further explore Turing's diffusion-induced instability for a class of cross-diffusion systems. Assume that there is a spatially homogeneous stable steady state in the absence of self-diffusion and cross-diffusion; this steady state remains stable in the presence of self-diffusion. We investigate how this can be affected by cross-diffusion. Hence, it does not belong to the classical Turing instability scheme; however, it may become unstable when cross-diffusion enters the system; thus, it is a cross-diffusion induced instability. Here, we present some examples of work on pattern formation for cross-diffusion models related to the work in this thesis.

Shigesada, Kawasaki, and Teramoto (SKT) proposed original Cross-diffusion models to model the spatial segregation of two competing species [81]. SKT model has been studied extensively for the last three decades (see for example [15, 38, 44, 53, 58, 60, 103, 104, 106]), and the model has the following form

$$\begin{aligned} u_t &= \nabla.(d_1\nabla u + d_\alpha u\nabla u + d_\beta u\nabla v) + u(r_1 - r_a u - r_v v), \\ v_t &= \nabla.(d_2\nabla v + d_\gamma v\nabla v + d_\delta v\nabla u) + v(r_2 - r_c v - r_d u), \end{aligned} \tag{1.4.18}$$

where $u(x,t)$ and $v(x,t)$ are the population densities of the two competing species, d_j $(j = 1,2)$ are positive, and constants $d_\alpha, d_\gamma, d_\beta, d_\delta$ are non-negative. d_1 and d_2 are the random diffusion rates, d_α and d_γ are the self-diffusion rates which represent intra-specific population pressures, and d_β, d_δ are the so-called cross-diffusion rates which represent the inter-specific population pressures. The constant r_i, r_a, r_c, r_b, r_d are all positive.

The main feature of such a model is that the movement rate of each species depend on the density of both species, and one key underlying biological assumption is that the transition probability from one place to its neighbourhood depends solely on the arrival spot and is independent of the departure spot. The goal of Shigesada was to show that heterogeneity of the environment and the non-linear dispersive movements raise a spatial segregation of the populations of two similar and competing species.

In the context of biological interactions of bacterial species, such a non-linear cross-diffusion model (1.4.18) was investigated in [30, 32]. These are systems consisting of two or more bacterial species exhibiting both competitive interaction for nutrients and also diffusion that is mediated by the presence of another species and the presence of its own species. They are interested in pattern formation in reaction-diffusion equations with non-linear diffusion terms. The main interest in that paper is to understand how cross-diffusion leads to pattern formation; their emphasis is less on the modelling and

more on identifying conditions under which patterns are formed.

Many many researchers consider liner cross-diffusion flux which we called it "A Simple Cross-diffusion" with different kinetics [27, 45, 54], one example is Madzvamuse in [55] investigated Turing instability with the effect of linear cross diffusion for the following model

$$\begin{aligned} u_t &= \nabla \,.\, (\nabla u + d_v \nabla v) + a - u + u^2 v, \\ v_t &= \nabla \,.\, (d\nabla v + d_u \nabla u) + b - u^2 v, \end{aligned} \tag{1.4.19}$$

where $u(x,t)$ and $v(x,t)$ are of two chemical concentrations, and d is the ratio of the diffusion coefficients only (without cross-diffusion), and d_u and d_v are the ratios of the cross-diffusion and the diffusion coefficients, respectively. The constants $a$and b are all positive .

They showed in the presence of cross diffusion, it is no longer necessary to enforce that one of the species diffuse much faster than the other, so ($D_u = D_v \Rightarrow d = 1$).

In the previous studies, the effects of linear cross-diffusion on pattern formation has been investigated for example [27, 45, 54]. None of these focused for the case where steady state of the kinetic is stable to self-diffusion with any ratio of the coefficients and see how this can be affected by linear cross-diffusion.

Yahong propose a mathematical model for a spatial predator-prey system with Allee effect in [69]. They investigate the Turing instability and the phenomena of pattern formation of the following system

$$\begin{aligned} u_t &= \nabla.(a_1 u \nabla u + b_1 u \nabla v) + \gamma u(u-\beta)(1-u) - uv, \\ v_t &= \nabla.(a_2 v \nabla v + b v \nabla u) + uv - \delta v, \end{aligned} \tag{1.4.20}$$

where $u(x,t)$ is the prey density, $v(x,t)$ is the predator density. $a_1 > 0$, $a_2 > 0$, b_1 and b are diffusion and cross-diffusion coefficients, respectively. The constants γ, β, δ are all positive.

They showed that non-linear cross-diffusion could induce instability that pattern can form in case where the standard diffusion can not. There are still many cross-diffusion models can be investigated to understand how cross-diffusion can affect a stable steady state with standard-diffusion, and how cross-diffusion can affect pattern formation. In Chapter 3, we extend the work in this area to have a better understand of the effect of cross-diffusion on pattern formation and investigate this case for a class of cross-diffusion systems where the non-dimensional form of this class of cross-diffusion systems is

$$u_t = \nabla.[D_{11}(u,v)\nabla u + D_{12}(u,v)\nabla v] + \gamma f(u,v),$$
$$v_t = \nabla.[D_{21}(u,v)\nabla u + D_{22}(u,v)\nabla v] + \gamma g(u,v).$$

We then consider two examples, the first one is the (simple) linear cross-diffusion (1.4.19), and the other one is a new non-linear cross-diffusion model that we derive in Chapter 4. We also focus on a class of kinetics term where uniform steady state is stable with standard-diffusion, and one example of kinetic is predator-prey system with Allee effect [69].

1.5 Background of Travelling Wave

In Chapter 4, we consider travelling wave solution, so we give introduction of what is the travelling wave in this section. Travelling wave means the shape and speed of propagation of the front continually changed. Customarily a travelling wave is taken

to be a wave which travels without change of shape. So, if a solution $u(x,t)$ represents a travelling wave, the shape of the solution will be the same for all time and the speed of propagation of this shape is a constant, which we denote by c. If we look at this wave in a travelling frame moving at speed c it will appear stationary. A mathematical way of saying this is that if the solution

$$u(x,t) = u(x-ct) = u(z), \quad \text{where} \quad z = x-ct, \tag{1.5.1}$$

then $u(x,t)$ is a travelling wave, and it moves at constant speed c. If $c > 0$ then, we have a right travelling wave, and If $c < 0$ then, we have a left travelling wave. The wavespeed c generally has to be determined. The dependent variable z is sometimes called the wave variable. When we look for travelling wave solutions of an equation or system of equations in x and t in the form (1.5.1), we have $\frac{\partial u}{\partial t} = -c\frac{du}{dz}$ and $\frac{\partial u}{\partial x} = \frac{du}{dz}$. So partial differential equations in x and t become ordinary differential equations in z. To be physically realistic $u(z)$ has to be bounded for all z and non-negative with the quantities with which we are concerned, such as chemicals, populations, bacteria and cells. For more details, see [64].

1.6 Thesis Outline

The aim of this thesis is to better understand how cross-diffusion influences the formation and characteristics of patterns and fronts in reaction-diffusion systems. In particular, we are interested in the mechanism of pattern formations and wave fronts in a cross-diffusion system. The structure of the thesis is as follows.

In Chapter 2, we investigate whether all cross-diffusion system of two interacting

species can be derived from the following microscopic master equation [39, 72]

$$\frac{du_k}{dt} = \tau_{k-1}^{+}u_{k-1} + \tau_{k+1}^{-}u_{k+1} - (\tau_k^{+} + \tau_k^{-})u_k,$$
$$\frac{dv_k}{dt} = \beta_{k-1}^{+}v_{k-1} + \beta_{k+1}^{-}v_{k+1} - (\beta_k^{+} + \beta_k^{-})v_k,$$

where u_k is a biomass of u in the location x_k, and the biomass can move to the left or to the right to exit, with the transfer rate τ_k^{-} or τ_k^{+}, similarly for v_k.

In Chapter 3, our goal is to follow the ideas of Turing about diffusive instability but to consider the impact of cross-diffusion on the stability of a spatially uniform equilibrium. We perform a stability analysis for a class of cross-diffusion system

$$u_t = \nabla.[D_{11}(u,v)\nabla u + D_{12}(u,v)\nabla v] + \gamma f(u,v),$$
$$v_t = \nabla.[D_{21}(u,v)\nabla u + D_{22}(u,v)\nabla v] + \gamma g(u,v).$$

We investigate the possibility of pattern formation. Particularly, we investigate one case which is can cross-diffusion induce pattern where standard-diffusion can not. We then consider two examples which are

$$u_t = \nabla\ .\ (\nabla u + d_v\nabla v) + \gamma f(u,v),$$
$$v_t = \nabla\ .\ (d\nabla v + d_u\nabla u) + \gamma g(u,v),$$

and

$$u_t = \nabla\ .\ (D_u(1-u)\nabla u - D_v u\nabla v) + \gamma f(u,v),$$
$$v_t = \nabla\ .\ (D_v(1-v)\nabla v - D_u v\nabla u) + \gamma g(u,v).$$

In Chapter 4, we are interested in a non-linear cross-diffusion system used to model tightly packed populations [72]. We first derive the model from a mass-conservation

perspective

$$u_t = \nabla \cdot (D_u(1-u)\nabla u - D_v u \nabla v) + \gamma f(u,v),$$
$$v_t = \nabla \cdot (D_v(1-v)\nabla v - D_u v \nabla u) + \gamma g(u,v).$$

We investigate moving front solutions of this model. For ease of analysis and numeric investigation, we take $v = 0$. Thus, the system is reduced to a scalar equation, and we seek a travelling wave solution of

$$u_t = \nabla \cdot (D_u(1-u)\nabla u) + \gamma u(1-u)(u-\beta). \tag{1.6.1}$$

By studying this scalar equation, we try to understand the travelling wave solution In particular, (1.6.1) is similar to Nagumo's equation, so we also focus on the effect of the non-linear diffusion term and what difference the non-linear diffusion term makes to the travelling wave solution.

In Chapter 5, we summarise the important points presented in the thesis, and discuss possible future work.

Throughout the thesis models are formulated as systems set in physically relevant spatial domains $\Omega \subset R^3$. These domains are either considered to be unbounded or to have smooth boundary $\partial\Omega$. In the latter case, boundary conditions are assumed to be of no-flux type. For ease of computation, much of the analysis and all the numerical simulations are conducted with $\Omega \subset R$.

In this thesis, the simulations of PDEs including cross-diffusion carried out using MATLAB's pdepe B.4solver with (zero-flux) Neumann boundary conditions, we plot the dispersion relations in Chapter 3 using MATLAB (see the code in Appendix B.3), we also use MATLAB function pplane to develop the phase portraits (see the description

of pplane in Appendix B.5).

Note that we are interested in processes and mechanisms and the underlying mathematical structures with no direct applications considered. Hence, we do not provide a dimensional analysis and all systems in this thesis are non-dimensional.

Chapter 2

Inverse Problem

We discussed in Chapter 1 that cross-diffusion models could be derived from random walk arguments. This chapter investigates whether all cross-diffusion systems of two interacting species can be derived from the microscopic master equation (1.3.10). The general proof does not seem an easy. Therefore, we illustrate that there is no proof by two examples. The first one is the classical cross-diffusion model (SKT) investigated in [66], and the second example is the simplest cross-diffusion. Since the analysis of SKT model has been done before we will not go in details. In addition, since the jump probabilities are simple for SKT, we compare the solution of SKT with the solution of the master equation numerically, which has not been done before. Later, we recover the non-linear cross-diffusion which is relevant to our work in this thesis.

2.1 Shigesada, Kawasaki, and Teramoto Cross-Diffusion System

The first example we investigate is the cross-diffusion model of Shigesada, Kawasaki, and Teramoto. The partial differential equation we investigate without the environmental potential function is

$$\begin{aligned} u_t &= \nabla \cdot (D_{11}\nabla u + 2D_{12}u\nabla u + D_{13}v\nabla u + D_{13}u\nabla v), \\ v_t &= \nabla \cdot (D_{21}\nabla v + 2D_{23}v\nabla v + D_{22}v\nabla u + D_{22}u\nabla v), \end{aligned} \tag{2.1.1}$$

where D are positive coefficients. The model (2.1.1) is known as the cross-diffusion model of Shigesada, Kawasaki, and Teramoto (SKT). To recover (2.1.1) from (1.3.16) and (1.3.18), the equations that must be satisfied are

$$\begin{aligned} &D_{11} + 2D_{12}u + D_{13}v = p_1q_1 + u(p_1q_{1u} - q_1p_{1u}), \\ &D_{13} = p_1q_{1v} - q_1p_{1v}, \\ &D_{21} + D_{22}u + 2D_{23}v = p_2q_2 + v(p_2q_{2v} - q_2p_{2v}), \\ &D_{22} = p_2q_{2u} - q_2p_{2u}. \end{aligned} \tag{2.1.2}$$

By choosing p_1, p_2, q_1, q_2 as

$$\begin{aligned} p_1(u,v) &= a_1, \\ q_1(u,v) &= \frac{1}{a_1}(D_{11} + D_{12}u + D_{13}v), \\ p_2(u,v) &= a_2, \\ q_2(u,v) &= \frac{1}{a_2}(D_{21} + D_{22}u + D_{23}v). \end{aligned} \tag{2.1.3}$$

Where a_1, a_2 are constants. As a result, system (2.1.1) can be recoved from (1.3.16)

and (1.3.18). For more details see [66].

We compare the solution of master equation (1.3.10) using jump probabilities (2.1.3) with solution of the SKT model (2.1.1) in Figure 2.1. Clearly, we can see that the simulation of master equation match the solution of the SKT model. We solve PDEs in MATLAB (PDEPE) with zero flux boundary condition, and we solve the master equation in MATLAB (ODE45) (see code in Appendix B.1).

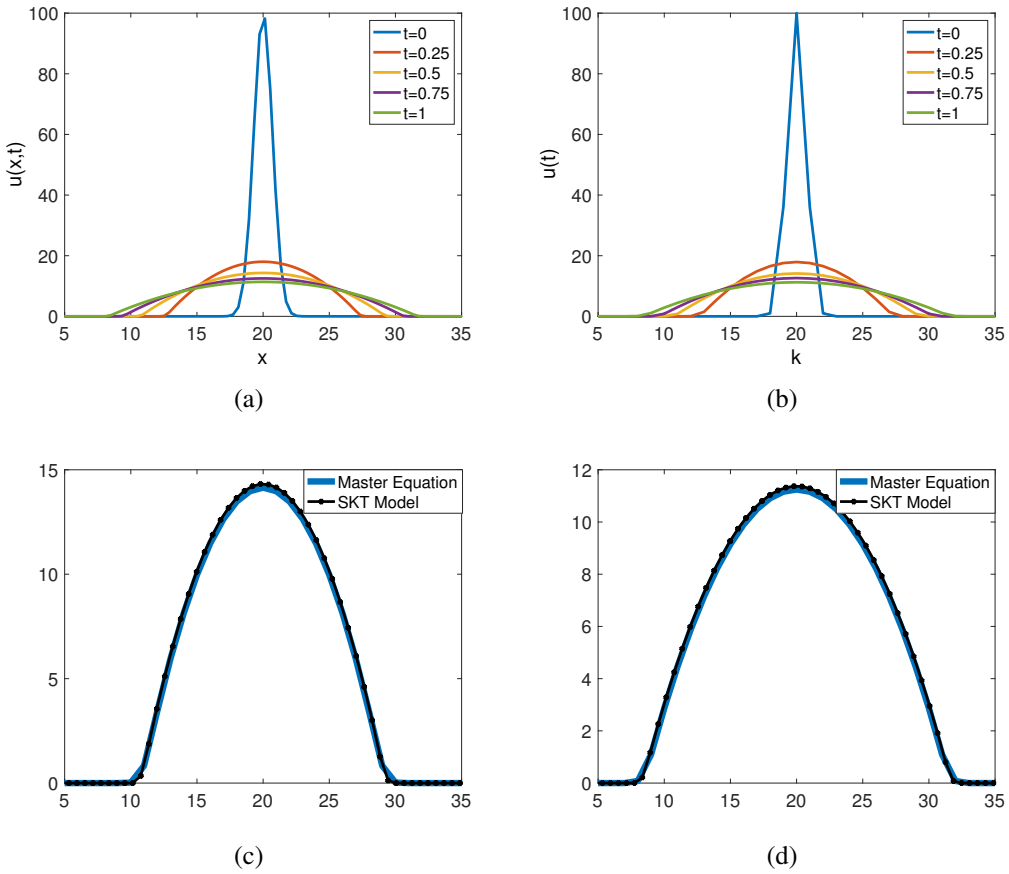

Figure 2.1: (a) Solution of u in SKT model (2.1.1) with initial condition $I.C = (100)e^{-1(x-20)^2}$. (b) Solution of u in master equation (1.3.10) using jump probabilities (2.1.3) with initial condition $I.C = (100)e^{-1(i-20)^2}$. (c) Comparing u in SKT model with master equation at time $t = 0.5$. (d) Comparing u in SKT model with master equation at time $t = 1$. Parameter values are shown in Table 2.1.

Parameter	Value
D_{11}	0
D_{12}	0
D_{21}	0
D_{23}	0
D_{13}	1
D_{22}	1
a_1	10
a_2	1
γ	1

Table 2.1: Table showing the parameter values that used to solve SKT model (2.1.1) and master equation (1.3.10) with jump probabilities (2.1.3).

Using analysis and numerical simulations, we can conclude that SKT cross-diffusion model commonly used to model dual species interaction can be derived from the random walk.

2.2 A Simple Cross-Diffusion System

In the following, we consider the simplest cross-diffusion system given by the equations

$$\begin{aligned} u_t &= \nabla \cdot (\nabla u + d_v \nabla v), \\ v_t &= \nabla \cdot (d \nabla v + d_u \nabla u). \end{aligned} \tag{2.2.1}$$

Our next goal is to recover (2.2.1) from (1.3.16) and (1.3.18). We complete this trying to find appropriate jump probabilities functions p_1, q_1, p_2, q_2. In doing this, we match the right hand side of (2.2.1) with the right hand side of (1.3.16) and (1.3.18), we get that the following equations must be satisfied for the functions p_1, q_1, p_2, q_2,

$$
\begin{aligned}
\bar{a} &= p_1 q_1 + u(p_1 q_{1u} - q_1 p_{1u}),\\
\bar{d_v} &= u(p_1 q_{1v} - q_1 p_{1v}),\\
\bar{d} &= p_2 q_2 + v(p_2 q_{2v} - q_2 p_{2v}),\\
\bar{d}u &= v(p_2 q_{2u} - q_2 p_{2u}).
\end{aligned}
\tag{2.2.2}
$$

We have included γ_0 and μ_0 in the coefficients $\bar{a},\ \bar{d_v},\ \bar{d},\ \bar{d_u}$ s.t. $\bar{a} = \frac{1}{\gamma_0},\ \bar{d_v} = \frac{d_v}{\gamma_0},\ \bar{d} = \frac{d}{\mu_0},\ \bar{d_u} = \frac{d_u}{\mu_0}$. Note that the first and second equations in (2.2.2) represent the first equation in the cross-diffusion system for the species u and the third and fourth equations represent the second equation in cross-diffusion system for the species v.
The following lemma holds.

Lemma 1. *It is not possible to recover the linear cross-diffusion system (2.2.1) in the following cases.*

1. *If p_1, q_1, p_2, q_2 are constants.*
2. *If p_1, or q_1, or p_2, or q_2 is a constant.*

Proof. 1. If all of the jump probability functions p_1, q_1, p_2, q_2 are constants, substituting in the equations (2.2.2), all is reduced to zero and therefore it is impossible to recover (2.2.1).

2. If we suppose that one of the jump probabilities is constant for example p_1, that is

$$p_1(u, v) = c, \tag{2.2.3}$$

where c is constant.

Substituting (2.2.3) into (2.2.2) we have

$$\bar{a} = cq_1 + u(cq_{1u}), \tag{2.2.4a}$$

$$\bar{d}_v = cq_{1v}. \tag{2.2.4b}$$

The equation (2.2.4a) is a first order linear ordinary differential equation with non-constant coefficients for the variable q_1 and its solution is given by

$$q_1(u,v) = \frac{\bar{a}}{c} + \frac{1}{u} f(v), \tag{2.2.5}$$

for some function $f(v)$. If we substitute (2.2.5) into (2.2.4b) we have

$$\bar{d}_v = c(\frac{1}{u} f'(v)) \implies f'(v) = \frac{\bar{d}_v u}{c}. \tag{2.2.6}$$

Clearly, this produces a contradiction to the previous assumption that f is a function only of v. Note that, we can proceed in the same way in the case that we suppose that the jump probability q_1 is constant.

□

In order to try to recover (2.2.1) from (1.3.16) and (1.3.18), we change the strategy assuming that the jump probabilities can be separated into independent functions of u and of v. In this case, we have the following proposition.

Proposition 2.2.1. *Suppose that the jump probabilities can be separated in the following way:*

$$
\begin{aligned}
p_1(u,v) &= f_1(u)g_1(v),\\
q_1(u,v) &= h_1(u)j_1(v),\\
p_2(u,v) &= f_2(u)g_2(v),\\
q_2(u,v) &= h_2(u)j_2(v).
\end{aligned}
\tag{2.2.7}
$$

In that case we can recover (2.2.1) from (1.3.16) and (1.3.18), and we have that the jump probability functions are given by

$$
\begin{aligned}
&f_1(u) = \left(\frac{\bar{d}_v}{\lambda_1(c_1 e^{\frac{\bar{a}\lambda_1 u}{2\lambda_2 \bar{d}_v}})}\right), \quad g_1(v) = \left(\frac{\lambda_2}{c_1 e^{\frac{\lambda_1 v}{2\lambda_2}}}\right), \quad h_1(u) = \left(\frac{\bar{c}_1}{u} e^{\frac{\bar{a}\lambda_1 u}{2\lambda_2 \bar{d}_v}}\right), \quad j_1(v) = \left(\bar{c}_1 e^{\frac{\lambda_1 v}{2\lambda_2}}\right),\\
&f_2(u) = \left(\frac{\lambda_4}{c_2 e^{\frac{\lambda_3 u}{2\lambda_4}}}\right), \quad g_2(v) = \left(\frac{\bar{d}_u}{\lambda_3(c_2 e^{\frac{\bar{d}\lambda_3 v}{2\lambda_4 \bar{d}_u}})}\right), \quad h_2(u) = \left(\bar{c}_2 e^{\frac{\lambda_3 u}{2\lambda_4}}\right), \quad j_2(v) = \left(\frac{\bar{c}_2}{v} e^{\frac{\bar{d}\lambda_3 v}{2\lambda_4 \bar{d}_u u}}\right),
\end{aligned}
\tag{2.2.8}
$$

so that,

$$
\begin{cases}
p_1(u,v) = f_1(u)g_1(v) = \left(\frac{\bar{d}_v}{\lambda_1 c_1} e^{-\frac{\bar{a}\lambda_1 u}{2\lambda_2 \bar{d}_v}}\right)\left(\frac{\lambda_2}{c_1} e^{-\frac{\lambda_1 v}{2\lambda_2}}\right),\\
q_1(u,v) = h_1(u)j_1(v) = \left(\frac{\bar{c}_1}{u} e^{\frac{\bar{a}\lambda_1 u}{2\lambda_2 \bar{d}_v}}\right)\left(\bar{c}_1 e^{\frac{\lambda_1 v}{2\lambda_2}}\right),\\
p_2(u,v) = f_2(u)g_2(v) = \left(\frac{\lambda_4}{c_2} e^{-\frac{\lambda_3 u}{2\lambda_4}}\right)\left(\frac{\bar{d}_u}{\lambda_3 c_2} e^{-\frac{\bar{d}\lambda_3 v}{2\lambda_4 \bar{d}_u}}\right),\\
q_2(u,v) = h_2(u)j_2(v) = \left(\bar{c}_2 e^{\frac{\lambda_3 u}{2\lambda_4}}\right)\left(\frac{\bar{c}_2}{v} e^{\frac{\bar{d}\lambda_3 v}{2\lambda_4 \bar{d}_u}}\right).
\end{cases}
$$

where $c_1, \bar{c}_1, c_2, \bar{c}_2, \lambda_1, \lambda_2, \lambda_2, \lambda_4$ are constants.

Proof. We proceed substituting (2.2.7) into (2.2.2), in doing this we denote by $\prime$ as derivative with respect u or v but taking care of what variable the function is depending, thus we have

$$
\begin{aligned}
\bar{a} &= f_1 g_1 h_1 j_1 + u(f_1 g_1 (h_1 j_1)' - h_1 j_1 (f_1 g_1)'), \\
\bar{d}_v &= u(f_1 g_1 (h_1 j_1)' - h_1 j_1 (f_1 g_1)'), \\
\bar{d} &= f_2 g_2 h_2 j_2 + v(f_2 g_2 (h_2 j_2)' - h_2 j_2 (f_2 g_2)'), \\
\bar{d}_u &= v(f_2 g_2 (h_2 j_2)' - h_2 j_2 (f_2 g_2)'),
\end{aligned}
\tag{2.2.9}
$$

since g and j are function only of v, the derivatives of these functions with respect to u are zero. Similarly, since f, h are function only of u, the derivatives with respect to v are zero, thus we can rewrite (2.2.9) in the following way

$$
\begin{aligned}
\bar{a} &= g_1 j_1 [f_1 h_1 + u(f_1 h_1' - h_1 f_1')], \\
\bar{d}_v &= u f_1 h_1 (g_1 j_1' - j_1 g_1'), \\
\bar{d} &= f_2 h_2 [g_2 j_2 + v(g_2 j_2' - j_2 g_2')], \\
\bar{d}_u &= v g_2 j_2 (f_2 h_2' - h_2 f_2').
\end{aligned}
\tag{2.2.10}
$$

Note that from the first and the second equations in (2.2.10) we can recover the first equation in (2.2.1), and from the third and fourth equations we can recover second equation in (2.2.1). We are now going to solve the first two equation in (2.2.10) in order to find g_1, j_1, f_1, h_1 which implies that the following must hold for arbitrary constants λ_1 and λ_2

$$
g_1 j_1' - j_1 g_1' = \lambda_1, \tag{2.2.11a}
$$

$$
g_1 j_1 = \lambda_2, \tag{2.2.11b}
$$

$$
f_1 h_1 = \frac{\bar{d}_v}{u\lambda_1}, \tag{2.2.11c}
$$

$$
f_1 h_1 + u(f_1 h_1' - h_1 f_1') = \frac{\bar{a}}{\lambda_2}. \tag{2.2.11d}
$$

Now we are going to calculate the functions $g_1(v)$ and $j_1(v)$. Note that the functions g_1 and g_1' can be obtained from the equation (2.2.11b), that is

$$g_1 = \frac{\lambda_2}{j_1}, \quad g_1' = \frac{-\lambda_2 j_1'}{j_1^2}. \tag{2.2.12}$$

Substituting the values given by (2.2.12) into (2.2.11a) we get

$$j_1' = \frac{\lambda_1}{2\lambda_2} j. \tag{2.2.13}$$

Equation (2.2.13) is an ordinary differential equation of the first order which solution is given by

$$j_1(v) = c_1 e^{\frac{\lambda_1 v}{2\lambda_2}}, \tag{2.2.14}$$

where c_1 is a constant. Substituting (2.2.14) into the relation found for g_1 in (2.2.12), we have

$$g_1(v) = \frac{\lambda_2}{c_1 e^{\frac{\lambda_1 v}{2\lambda_2}}}. \tag{2.2.15}$$

Now we are going to calculate the functions $f_1(u)$ and $h_1(u)$. Proceeding as before note that the functions f_1 and f_1' can be obtained from the equation (2.2.11c), in this case we have

$$f_1 = \frac{\bar{d}_v}{u h_1 \lambda_1}, \quad f_1' = \frac{-\bar{d}_v}{u^2 h_1 \lambda_1} - \frac{\bar{d}_v h_1'}{u h_1^2 \lambda_1}. \tag{2.2.16}$$

Substituting the values given by (2.2.16) for f_1 and f_1' into (2.2.11d), we have

$$(\frac{\bar{d}_v}{u h_1 \lambda_1}) h_1 + u((\frac{\bar{d}_v}{u h_1 \lambda_1}) h_1' - h_1(\frac{-\bar{d}_v}{u^2 h_1 \lambda_1} - \frac{\bar{d}_v h_1'}{u h_1^2 \lambda_1}) = \frac{\bar{a}}{\lambda_2}, \tag{2.2.17}$$

thus,

$$h_1' = h_1\left(\frac{k\lambda_1}{2\bar{d}_v\lambda_2} - \frac{1}{u}\right). \tag{2.2.18}$$

Equation (2.2.18) is an ordinary differential equation of first order with solution given by

$$h_1(u) = \frac{\bar{c}_1}{u} e^{\frac{k\lambda_1 u}{2\lambda_2 \bar{d}_v}}, \tag{2.2.19}$$

where $\bar{c}_1$ is constant. Substituting (2.2.19) into the relation founded for f_1 in (2.2.16), we have

$$f_1(u) = \frac{\bar{d}_v}{u\lambda_1\left(\frac{\bar{c}_1}{u} e^{\frac{\bar{a}\lambda_1 u}{2\lambda_2 \bar{d}_v}}\right)} = \frac{\bar{d}_v}{\lambda_1\left(\bar{c}_1 e^{\frac{\bar{a}\lambda_1 u}{2\lambda_2 \bar{d}_v}}\right)}. \tag{2.2.20}$$

Thus we get that the solutions for the first two equations of (2.2.10) are given by

$$\begin{aligned} f_1(u) &= \frac{\bar{d}_v}{\lambda_1\left(\bar{c}_1 e^{\frac{\bar{a}\lambda_1 u}{2\lambda_2 \bar{d}_v}}\right)}, \\ h_1(u) &= \frac{\bar{c}_1}{u} e^{\frac{\bar{a}\lambda_1 u}{2\lambda_2 \bar{d}_v}}, \\ g_1(v) &= \frac{\lambda_2}{c_1 e^{\frac{\lambda_1 v}{2\lambda_2}}}, \\ j_1(v) &= c_1 e^{\frac{\lambda_1 v}{2\lambda_2}}, \end{aligned} \tag{2.2.21}$$

where $c_1, \bar{c}_1$ are constants. Next, we are going to proceed in a similar way as before to find the functions f_2, h_2, g_2, j_2 solving the last two equation in (2.2.10) which implies

that the following must hold for arbitrary constants λ_3 and λ_4

$$f_2 h_2' - h_2 f_2' = \lambda_3, \tag{2.2.22a}$$

$$f_2 h_2 = \lambda_4, \tag{2.2.22b}$$

$$g_2 j_2 = \frac{\bar{d}_u}{v\lambda_3}, \tag{2.2.22c}$$

$$g_2 j_2 + v(g_2 j_2' - j_2 g_2') = \frac{\bar{d}}{\lambda_4}. \tag{2.2.22d}$$

As we can see the functions f_2 and f_2' can be obtained from (2.2.22b). Thus we have

$$f_2 = \frac{\lambda_4}{h_2}, \quad f_2' = \frac{-\lambda_4 h_2'}{h_2^2}. \tag{2.2.23}$$

Substituting this values for f_2 and f_2' given by (2.2.23) into (2.2.22a), we have

$$h_2' = \frac{\lambda_3}{2\lambda_4} h. \tag{2.2.24}$$

This is a linear ordinary differential equation of first order with solution given by

$$h_2(u) = c_2 e^{\frac{\lambda_3 u}{2\lambda_4}}, \tag{2.2.25}$$

where, c_2 is a constant. Now substituting the value of h_2 given by (2.2.25) into the relation given by (2.2.23) for the function f_2, we have

$$f_2(u) = \frac{\lambda_4}{c_2 e^{\frac{\lambda_3 u}{2\lambda_4}}}. \tag{2.2.26}$$

We are going now to calculate the values of the functions $g_2(v)$ and $j_2(v)$. As we can

see the values of the functions g_2 and g_2' that can be obtained from (2.2.22c), in this case we have

$$g_2 = \frac{\bar{d}_u}{v j_2 \lambda_3}, \quad g_2' = \frac{-\bar{d}_u}{v^2 j_2 \lambda_3} - \frac{\bar{d}_u j_2'}{v j_2^2 \lambda_3}. \tag{2.2.27}$$

Substituting the values of g_2 and g_2' given by (2.2.27) into the relation (2.2.22d) we have

$$(\frac{\bar{d}_u}{v j_2 \lambda_3}) j_2 + v((\frac{\bar{d}_u}{v j_2 \lambda_3}) j_2' - j_2(\frac{-\bar{d}_u}{v^2 j_2 \lambda_3} - \frac{\bar{d}_u j_2'}{v j_2^2 \lambda_3}) = \frac{\bar{d}}{\lambda_4}, \tag{2.2.28}$$

we have

$$j_2' = j_2(\frac{\bar{d}\lambda_3}{2\bar{d}_u \lambda_4} - \frac{1}{v}). \tag{2.2.29}$$

The equation given by (2.2.29) is a linear ordinary differential equation of the first order with solution given by

$$j_2(v) = \frac{\bar{c}_2}{v} e^{\frac{\bar{d}\lambda_3 v}{2\lambda_4 \bar{d}_u}}, \tag{2.2.30}$$

where $\bar{c}_2$ is constant. Substituting the value of j_2 given by (2.2.30) in the relation obtained for g_2 in (2.2.27) we get

$$g_2(v) = \frac{\bar{d}_u}{v\lambda_3(\frac{\bar{c}_2}{v} e^{\frac{\bar{d}\lambda_3 v}{2\lambda_4 \bar{d}_u}})} = \frac{\bar{d}_u}{\lambda_3(\bar{c}_2 e^{\frac{\bar{d}\lambda_3 v}{2\lambda_4 \bar{d}_u}})}, \tag{2.2.31}$$

and thus, we obtain the solutions

$$\begin{aligned} h_2(u) &= c_2 e^{\frac{\lambda_3 u}{2\bar{\lambda}_4}}, \\ f_2(u) &= \frac{\lambda_4}{c_2 e^{\frac{\lambda_3 u}{2\bar{\lambda}_4}}}, \\ g_2(v) &= \frac{\bar{d}_u}{\lambda_3(\bar{c}_2 e^{\frac{\bar{d}\lambda_3 v}{2\lambda_4 \bar{d}_u}})}, \\ j_2(v) &= \frac{\bar{c}_2}{v} e^{\frac{\bar{d}\lambda_3 v}{2\lambda_4 \bar{d}_u}}, \end{aligned} \tag{2.2.32}$$

where $c_2, \bar{c}_2$ are constants. Gathering all above leads us to the following jump probability functions

$$\begin{cases} p_1(u,v) = f_1(u)g_1(v) = (\frac{\bar{d}_v}{\lambda_1 c_1} e^{-\frac{\bar{a}\lambda_1 u}{2\lambda_2 \bar{d}_v}})(\frac{\lambda_2}{c_1} e^{-\frac{\lambda_1 v}{2\bar{\lambda}_2}}), \\ q_1(u,v) = h_1(u)j_1(v) = (\frac{\bar{c}_1}{u} e^{\frac{\bar{a}\lambda_1 u}{2\lambda_2 \bar{d}_v}})(\bar{c}_1 e^{\frac{\lambda_1 v}{2\bar{\lambda}_2}}), \\ p_2(u,v) = f_2(u)g_2(v) = (\frac{\lambda_4}{c_2} e^{-\frac{\lambda_3 u}{2\bar{\lambda}_4}})(\frac{\bar{d}_u}{\lambda_3 c_2} e^{-\frac{\bar{d}\lambda_3 v}{2\lambda_4 \bar{d}_u}}), \\ q_2(u,v) = h_2(u)j_2(v) = (\bar{c}_2 e^{\frac{\lambda_3 u}{2\bar{\lambda}_4}})(\frac{\bar{c}_2}{v} e^{\frac{\bar{d}\lambda_3 v}{2\lambda_4 \bar{d}_u}}). \end{cases} \tag{2.2.33}$$

Clearly with these functions, we can recover the simple cross-diffusion system (2.2.1) from the relations given by (1.3.16) and (1.3.18). □

From p_1, q_1 as defined in (2.2.33), the dispersal strategy of species u depends on both densities of its own and v in the arrival and target site. Therefore, cross-diffusion effects are introduced. The jump probability $p_1(u,v)$, which describes the wish or need of the particles u to join its neighbouring position is an exponentially decreasing function, and it is separated into two decreasing functions that one depends on u. The other depends on v. The jump probability $q_1(u,v)$, which describes the incentive for that the particles u leave their original position, is an exponentially increasing function, and it is separated into two increasing functions that one depends on u and the other depends

on v, indicating that species u preferentially seeks location with lower concentrations of both species u and v.

As we can see, $p_1(u,v)$ and $q_1(u,v)$ are complex and do not seem to have a specific meaning. In contrast to the SKT model where the flux is more complex, but the jump probabilities (2.1.3) are simpler. As a result , the simple flux does not mean that the jump probabilities are simple and the complex flux does not mean that the jump probabilities are complex. Therefore, it is not easy to prove that all cross-diffusion systems of two interacting species can be derived from the microscopic master equation (1.3.10). Similarly for jump probabilities $p_2(u,v)$ and $q_2(u,v)$ which are for species v.

2.3 New Non-linear Cross-Diffusion System

Here, we investigate the final example that is relevant to our work in this thesis

$$\begin{aligned} u_t &= \nabla \cdot (D_u(1-u)\nabla u - D_v u \nabla v), \\ v_t &= \nabla \cdot (D_v(1-v)\nabla v - D_u v \nabla u). \end{aligned} \tag{2.3.1}$$

We will leave the details of the derivation for Chapter 4; however, our next goal is to recover the non-linear cross-diffusion system (2.3.1) from (1.3.16) and (1.3.18). In other words, we investigate now whether this model can be derived from our microscopic master equation. We achieve this by trying to find appropriate jump probabilities functions p_1, q_1, p_2, q_2. In doing this, we match the right hand side of (2.3.1) with the right hand side of (1.3.16) and (1.3.18); we get that the following equations must be satisfied for the functions p_1, q_1, p_2, q_2

$$
\begin{aligned}
\bar{D}_u - \bar{D}_u u &= p_1 q_1 + u(p_1 q_{1u} - q_1 p_{1u}),\\
-\bar{D}_v &= u(p_1 q_{1v} - q_1 p_{1v}),\\
\bar{D}_v - \bar{D}_v v &= p_2 q_2 + v(p_2 q_{2v} - q_2 p_{2v}),\\
-\bar{D}_u &= (p_2 q_{2u} - q_2 p_{2u}),
\end{aligned}
\tag{2.3.2}
$$

we have included γ_0 in the coefficients $\bar{D}_u$, $\bar{D}_v$ s.t. $\bar{D}_u = \frac{D_u}{\gamma_0}$, $\bar{D}_v = \frac{D_v}{\gamma_0}$. Note that the first and second equations in (2.3.2) represent the first equation in the cross-diffusion system for the species u and the third and fourth equations represent the second equation in the cross-diffusion system for the species v.

In order to recover (2.3.1) from ((1.3.16) and (1.3.18), we assume that the jump probabilities can be separated into independent functions of u and of v. In this case, we have the following proposition.

Proposition 2.3.1. *Suppose that the jump probabilities can be separated in the following way:*

$$
\begin{aligned}
p_1(u,v) &= f_1(u) g_1(v),\\
q_1(u,v) &= h_1(u) j_1(v),\\
p_2(u,v) &= f_2(u) g_2(v),\\
q_2(u,v) &= h_2(u) j_2(v).
\end{aligned}
\tag{2.3.3}
$$

In that case, we can recover (2.3.1) from (1.3.16) and (1.3.18), and we will notice that the jump probability functions are given by

$$
\begin{aligned}
f_1(u) &= \frac{\bar{D}_v}{\lambda_1(\frac{c_1}{\sqrt{u}}e^{\frac{\bar{D}_u\lambda_1(-u+\ln u)}{2\bar{D}_v\lambda_2}})}, \quad & h_1(u) &= \frac{c_1}{\sqrt{u}}e^{\frac{\bar{D}_u\lambda_1(-u+\ln u)}{2\bar{D}_v\lambda_2}}, \\
g_1(v) &= \frac{\lambda_2}{c_1 e^{\frac{-\lambda_1 v}{2\lambda_2}}}, & j_1(v) &= c_1 e^{\frac{\lambda_1 v}{2\lambda_2}},
\end{aligned}
\tag{2.3.4}
$$

so that,

$$
\begin{cases}
p_1(u,v) = f_1(u)g_1(v) = \Big(\frac{\bar{D}_v}{\lambda_1(\frac{c_1}{\sqrt{u}}e^{\frac{\bar{D}_u\lambda_1(-u+\ln u)}{2\bar{D}_v\lambda_2}})}\Big)\Big(\frac{\lambda_2}{c_1 e^{\frac{-\lambda_1 v}{2\lambda_2}}}\Big), \\
q_1(u,v) = h_1(u)j_1(v) = \Big(\frac{c_1}{\sqrt{u}}e^{\frac{\bar{D}_u\lambda_1(-u+\ln u)}{2\bar{D}_v\lambda_2}}\Big)\Big(c_1 e^{\frac{\lambda_1 v}{2\lambda_2}}\Big),
\end{cases}
$$

where c_1, λ_1, λ_2 are constants.

Proof. We proceed by substituting (2.3.3) into (2.3.2) which we denote by $'$ as the derivative with respect to u or v with taking care of what variable the function depends on. Thus we have

$$
\begin{aligned}
\bar{D}_u - \bar{D}_u u &= f_1 g_1 h_1 j_1 + u(f_1 g_1 (h_1 j_1)' - h_1 j_1 (f_1 g_1)'), \\
-\bar{D}_v &= (f_1 g_1 (h_1 j_1)' - h_1 j_1 (f_1 g_1)'),
\end{aligned}
\tag{2.3.5}
$$

since g and j are function only of v, the derivatives of these functions with respect to u are zero. Similarly f, h are function only of u, so the derivatives with respect to v are zero. We rewrite (2.3.5) in the following way

$$
\begin{aligned}
\bar{D}_u - \bar{D}_u u &= g_1 j_1 [f_1 h_1 + u(f_1 h_1' - h_1 f_1')], \\
-\bar{D}_v &= u f_1 h_1 (g_1 j_1' - j_1 g_1'),
\end{aligned}
\tag{2.3.6}
$$

and we solve (2.3.6) to recover only the first equation in (2.3.1). We will now solve (2.3.6) in order to find g_1, j_1, f_1, h_1 which implies that the following must hold for

arbitrary constants λ_1 and λ_2

$$g_1 j_1' - j_1 g_1' = \lambda_1, \tag{2.3.7a}$$

$$g_1 j_1 = \lambda_2, \tag{2.3.7b}$$

$$f_1 h_1 = \frac{-\bar{D}_v}{\lambda_1}, \tag{2.3.7c}$$

$$f_1 h_1 + u(f_1 h_1' - h_1 f_1') = \frac{\bar{D}_u - \bar{D}_u u}{\lambda_2}. \tag{2.3.7d}$$

Now we are going to calculate the functions $g_1(v)$ and $j_1(v)$. Note that the functions g_1 and g_1' can be obtained from the equation (2.3.7b), that is

$$g_1 = \frac{\lambda_2}{j_1}, \quad g_1' = \frac{-\lambda_2 j_1'}{j_1^2}. \tag{2.3.8}$$

Substituting the values given by (2.3.8) into (2.3.7a), we have

$$j_1' = \frac{\lambda_1}{2\lambda_2} j_1. \tag{2.3.9}$$

Equation (2.3.9) is an ordinary differential equation of the first order which solution is given by

$$j_1(v) = c_1 e^{\frac{\lambda_1 v}{2\lambda_2}}, \tag{2.3.10}$$

where c_1 is a constant. Substituting (2.3.10) into the relation found for g_1 in (2.3.8), we get

$$g_1(v) = \frac{\lambda_2}{c_1 e^{\frac{\lambda_1 v}{2\lambda_2}}}, \tag{2.3.11}$$

where c_1 is a constant. Now we are going to calculate the functions $f_1(u)$ and $h_1(u)$. Proceeding as before note that the functions f_1 and f_1' can be obtained from the equation (2.3.7c), in this case we have

$$f_1 = \frac{-\bar{D}_v}{h_1\lambda_1}, \quad f_1' = \frac{\bar{D}_v h_1'}{h_1^2\lambda_1}. \tag{2.3.12}$$

Substituting the values given by (2.3.12) for f_1 and f_1' into (2.3.7d), we get

$$(\frac{-\bar{D}_v}{h_1\lambda_1})h_1 + u((\frac{-\bar{D}_v}{h_1\lambda_1})h_1' - h_1(\frac{\bar{D}_v h_1'}{h_1^2\lambda_1}) = \frac{\bar{D}_u - \bar{D}_u u}{\lambda_2}, \tag{2.3.13}$$

we have

$$-\bar{D}_v + u((\frac{-\bar{D}_v}{h_1})h_1' - (\frac{\bar{D}_v h_1'}{h_1}) = \frac{\lambda_1(\bar{D}_u - \bar{D}_u u)}{\lambda_2}, \tag{2.3.14}$$

which is

$$-\bar{D}_v - 2u\frac{-\bar{D}_v}{h_1}h_1' = \frac{\lambda_1(\bar{D}_u - \bar{D}_u u)}{\lambda_2}, \tag{2.3.15}$$

thus, we get

$$h_1' = h_1(\frac{\lambda_1\bar{D}_u(1-u)}{2\bar{D}_v u\lambda_2} - \frac{1}{2u}). \tag{2.3.16}$$

Equation (2.3.16) is an ordinary differential equation of first order with solution given by (steps of the solution are in Appendix A.3)

$$h_1(u) = \frac{c_1}{\sqrt{u}} e^{\frac{\bar{D_u}\lambda_1(-u+\ln u)}{2\bar{D_v}\lambda_2}}. \tag{2.3.17}$$

Substituting (2.3.17) into the relation founded for f_1 in (2.3.12), we have

$$f_1(u) = \frac{\bar{D_v}}{\lambda_1(\frac{c_1}{\sqrt{u}} e^{\frac{\bar{D_u}\lambda_1(-u+\ln u)}{2\bar{D_v}\lambda_2}})}, \tag{2.3.18}$$

Thus we get that the solutions for the first two equations of (2.3.6) are given by

$$\begin{aligned} f_1(u) &= \frac{\bar{D_v}}{\lambda_1(\frac{c_1}{\sqrt{u}} e^{\frac{\bar{D_u}\lambda_1(-u+\ln u)}{2\bar{D_v}\lambda_2}})}, \\ h_1(u) &= \frac{c_1}{\sqrt{u}} e^{\frac{\bar{D_u}\lambda_1(-u+\ln u)}{2\bar{D_v}\lambda_2}}, \\ g_1(v) &= \frac{\lambda_2}{c_1 e^{\frac{\lambda_1 v}{2\lambda_2}}}, \\ j_1(v) &= c_1 e^{\frac{\lambda_1 v}{2\lambda_2}}, \end{aligned} \tag{2.3.19}$$

where c_1 is constant. Gathering all above leads us to the following jump probability functions

$$\begin{cases} p_1(u,v) = f_1(u)g_1(v) = (\frac{\bar{D_v}}{\lambda_1(\frac{c_1}{\sqrt{u}} e^{\frac{\bar{D_u}\lambda_1(-u+\ln u)}{2\bar{D_v}\lambda_2}})})(\frac{\lambda_2}{c_1 e^{\frac{\lambda_1 v}{2\lambda_2}}}), \\ q_1(u,v) = h_1(u)j_1(v) = (\frac{c_1}{\sqrt{u}} e^{\frac{\bar{D_u}\lambda_1(-u+\ln u)}{2\bar{D_v}\lambda_2}})(c_1 e^{\frac{\lambda_1 v}{2\lambda_2}}). \end{cases} \tag{2.3.20}$$

Clearly with this functions, we can recover the first equation in a cross-diffusion system (2.3.1) for species u from the relations given by (1.3.16) and (1.3.18). In a similar way as before we can find the functions f_2, h_2, g_2, j_2 to recover equation for v in (2.3.1).

□

2.4 Conclusions

In Chapter 1, it was outlined how the spatially discrete master equations

$$\frac{du_k}{dt} = \tau_{k-1}^{+} u_{k-1} + \tau_{k+1}^{-} u_{k+1} - (\tau_k^{+} + \tau_k^{-}) u_k,$$
$$\frac{dv_k}{dt} = \beta_{k-1}^{+} v_{k-1} + \beta_{k+1}^{-} v_{k+1} - (\beta_k^{+} + \beta_k^{-}) v_k,$$

could be used to derive a macro scale cross diffusion model. This chapter investigated whether all cross-diffusion system of two interacting species can be derived from these microscopic master equations. First, we presented Ostrander's result that the microscopic master equation can be recovered from the SKT cross-diffusion model [66]. Next, we compared the solution of SKT with the solution of master equation numerically. Then, we also showed that the microscopic master equation could be recovered from the linear cross-diffusion model. Finally, we showed that the microscopic master equation can be recovered from the new non-linear cross-diffusion model. We found out that recovering a system with complex flux does not imply that the jump probabilities are complex. As we see for the SKT cross-diffusion model, where the flux is complex, but jump probabilities are simple. In addition, recovering a system with simple flux does not mean that the jump probabilities are simple. As we see for the linear cross-diffusion model, where the flux is simple, but jump probabilities are complex. Therefore , we conclude that it is not easy to prove that the microscopic master equation (1.3.10) can be derived from all cross-diffusion systems of two interacting species.

Note that the validity of the form of the jump probabilities given in (2.2.33) and (2.3.20) could be verified by comparing numerical solutions of master equation with those for the related PDE models (2.2.1) and (2.3.1), respectively (as is done for the

SKT model and shown in Figure 2.1). Due to the complex form of the jump probabilities we were unable to formulate a stable numerical code for the master equation that would allow such a comparison. The construction of a stable numerical code would form useful future work.

Chapter 3

Effect of Cross-Diffusion on Pattern Formation

In this chapter, we focus on pattern formation for cross-diffusion systems. Our goal is that to follow the ideas of Turing about diffusive instability but to consider the impact of cross-diffusion on the stability of a spatially uniform equilibrium. Suppose we have kinetic where the steady state is stable to all self-diffusions. Can cross-diffusion destabilize it?

A Turing instability arises when a steady state, stable in the absence of diffusion, can be driven unstable in the presence of self-diffusion. It is also known that if cross-diffusion terms are added to the system, the stability of the steady state of the reaction-diffusion system with self-diffusion terms can be reversed. In other words, a steady state, which is stable, either in the absence of any diffusion terms or in the presence of self-diffusion alone can be destabilized when cross-diffusion terms are added to the system. This is called a 'cross-diffusion induced instability' [80], and can also induce pattern formation [10, 101]. On the contrary, a stable steady state that becomes unstable in the presence of self-diffusion (Turing instability) can once again become stable

in the presence of cross-diffusion. This is known as 'cross-diffusion induced stability' [79] and prevents pattern formation. 'cross-diffusion induced stability' investigated for example of models, one example we presented in Chapter 1. However, there are still models where this case has not investigated.

The main purpose of this chapter is that we investigate cross-diffusion induced instability in a class of problems, then we consider two examples. One example is the new non-linear cross-diffusion model which we derive in Chapter 4. We focus in pattern formation for this new model. In particular, we investigate the case of where self-diffusion cannot destabilize the steady state. Thus, we investigate how the non-linear cross-diffusion can affect the steady state. Before investigating the possible pattern for this new model, we investigate an example which is a (simple) linear cross-diffusion with the same kinetic to see how it can affect a stable steady state with self-diffusion.

3.1 Stability for a Class of Cross-Diffusion Models

To investigate the possibility of pattern formation for cross-diffusion systems, we set up a two-species cross-diffusion model and carry out stability analysis. We consider a class of cross-diffusion systems where the general non-dimensional form is

$$\begin{aligned} u_t &= \nabla.[D_{11}(u,v)\nabla u + D_{12}(u,v)\nabla v] + \gamma f(u,v), \\ v_t &= \nabla.[D_{21}(u,v)\nabla u + D_{22}(u,v)\nabla v] + \gamma g(u,v), \end{aligned} \tag{3.1.1}$$

where u and v represent densities of two-species, $f(u,v)$ and $g(u,v)$ are general reaction terms, $D_{12}(u,v)$ and $D_{21}(u,v)$ are cross-diffusion terms, $D_{11}(u,v)$ and $D_{22}(u,v)$ are self-diffusion terms.

3.1.1 Linear Stability Analysis for Diffusion-Driven Instability

Now, we consider the linear stability analysis for a cross-diffusion system. For any steady state to be driven unstable in the presence of diffusion, certain conditions must be satisfied. To formulate the problem mathematically, we need to specify initial conditions and boundary conditions. We take these to be given initial conditions (which will be small perturbations about the steady state) and zero flux boundary conditions. Therefore the mathematical problem is

$$\begin{aligned} u_t &= \nabla.[D_{11}(u,v)\nabla u + D_{12}(u,v)\nabla v] + \gamma f(u,v), \\ v_t &= \nabla.[D_{21}(u,v)\nabla u + D_{22}(u,v)\nabla v] + \gamma g(u,v), \\ (\mathbf{n}.\nabla) &\begin{bmatrix} u \\ v \end{bmatrix} = 0, \quad \mathbf{r} \text{ on } \partial\Omega; \quad u(\mathbf{r},0),\ v(\mathbf{r},0) \text{ given}, \end{aligned} \tag{3.1.2}$$

where $\partial\Omega$ is the closed boundary of the reaction-diffusion domain Ω and n is the unit outward normal to $\partial\Omega$.

The relevant homogeneous steady state (u_0, v_0) of (3.1.2) is the positive solution of

$$f(u,v) = 0, \quad g(u,v) = 0.$$

Note that in Chapter 1 we derived the conditions for diffusion driven instability. For ease of exposition, we rewrite the conditions here (see Chapter 1 for details of the calculations). Linear stability of steady state (u_0, v_0) without any diffusion is guaranteed if $Re\lambda < 0$ where λ satisfy $\lambda^2 - \gamma(f_u^o + g_v^o)\lambda + \gamma^2(f_u^o g_v^o - f_v^o g_u^o) = 0$, that is

$$f_u^o + g_v^o < 0, \tag{3.1.3}$$

$$f_u^o g_v^o - f_v^o g_u^o > 0. \tag{3.1.4}$$

Instability of steady state (u_0, v_0) with self-diffusion is guaranteed if $Re\lambda > 0$ where λ satisfy $\lambda^2 + G(k^2)\lambda + H(k^2) = 0$,

where

$$G(k^2) = k^2 \mathrm{tr}(D) - \gamma \mathrm{tr}(J),$$

and

$$H(k^2) = \det(D)k^4 - \gamma q k^2 + \gamma^2 \det(J),$$

with

$$q := [d f_u^o + g_v^o].$$

Thus, the necessary conditions for self-diffusion-driven instability are

$$f_u^o + g_v^o < 0, \tag{3.1.5a}$$

$$f_u^o g_v^o - f_v^o g_u^o > 0, \tag{3.1.5b}$$

$$\det(D) > 0, \tag{3.1.5c}$$

$$q := [d f_u^o + g_v^o] > 0 \quad \Longrightarrow \; d \neq 1, \tag{3.1.5d}$$

$$(q)^2 - 4 \det(J)\det(D) > 0, \tag{3.1.5e}$$

where $D = \begin{pmatrix} 1 & 0 \\ 0 & d \end{pmatrix}$ is the self-diffusion matrix and the positive constant $d = \frac{D_v}{D_u}$ is the ratio between two self-diffusion coefficients.

Next we consider the following perturbations to the steady state (u_0, v_0)

$$u(x,t) = u_0 + \hat{u}(x,t), \quad v(x,t) = v_0 + \hat{v}(x,t). \tag{3.1.6}$$

where $|\hat{u}| << 1$ and $|\hat{v}| << 1$ are small perturbations.

Substitute equation (3.1.6) into (3.1.2) and apply a Taylor expansion about (u_0, v_0) to $f(u,v)$, $g(u,v)$ and $D_{ij}(u,v)$ to obtain the linearised problem

$$\begin{aligned}
&\frac{\partial \hat{u}(x,t)}{\partial t} = \nabla.[D^o_{11}\nabla\hat{u}(x,t) + D^o_{12}\nabla\hat{v}(x,t)] + \gamma(f^o_u\hat{u}(x,t) + f^o_v\hat{v}(x,t)),\\
&\frac{\partial \hat{v}(x,t)}{\partial t} = \nabla.[D^o_{21}\nabla\hat{u}(x,t) + D^o_{22}\nabla\hat{v}(x,t)] + \gamma(g^o_u\hat{u}(x,t) + g^o_v\hat{v}(x,t)),\\
&(\mathbf{n}.\nabla)\begin{bmatrix} \hat{u}(x,t) \\ \hat{v}(x,t) \end{bmatrix} = 0, \quad \mathbf{r} \text{ on } \partial\Omega,
\end{aligned} \tag{3.1.7}$$

where $D^o_{ij} = D_{ij}(u_0, v_0)$. The subscripts u and v denote differentiation with respect to u and v respectively, and ^{o} indicates evaluation at the equilibrium (u_0, v_0). System (3.1.7) can be written in the form

$$\begin{aligned}
&\mathbf{w}_t = \nabla\cdot(D_c\mathbf{w}\nabla\mathbf{w}) + \gamma J\mathbf{w}, \quad \mathbf{w} = \begin{pmatrix} \hat{u}(x,t) \\ \hat{v}(x,t) \end{pmatrix},\\
&\text{where}\\
&J = \begin{pmatrix} f^o_u & f^o_v \\ g^o_u & g^o_v \end{pmatrix}, \; D^o_c = \begin{pmatrix} D^o_{11} & D^o_{12} \\ D^o_{21} & D^o_{22} \end{pmatrix}.
\end{aligned} \tag{3.1.8}$$

Following the same method in used in Chapter 1, the dispersion relation is

$$\lambda^2 + G_1(k^2)\lambda + H_1(k^2) = 0, \tag{3.1.9}$$

where

$$G_1(k^2) = k^2 \mathrm{tr}(D_c^o) - \gamma \mathrm{tr}(J),$$

and

$$H_1(k^2) = \det(D_c^o)k^4 - \gamma q_1 k^2 + \gamma^2 \det(J), \tag{3.1.10}$$

with

$$q := [D_{22}^o f_u^o + D_{11}^o g_v^o - D_{21}^o f_v^o - D_{12}^o g_u^o].$$

For cross-diffusion driven instability, we require $Re(\lambda) > 0$. It is assumed that $\mathrm{tr}(J) < 0$ and $\mathrm{tr}(D_c^o) > 0$ and so $G_1(k^2) > 0$. Therefore $Re(\lambda) > 0$ if and only if $H_1(k^2) < 0$. The minimum of $H(k^2)$ occurs at

$$k_c^2 := \frac{q_1}{2\det(D_c^o)}, \quad \text{and} \quad H_1(k_c^2) = \det(J) - (q_1)^2/[4\det(D_c^o)].$$

If this minimum is positive, then $Re(\lambda) < 0$. Hence the critical case occurs if $H_1(k_c^2) = 0$, i.e.

$$\det(J) = \frac{q_1^2}{4\det(D_c^o)}.$$

Now, it is assumed that $\det(J) > 0$ hence the only way this equality can hold is if $\det(D_c^o) > 0$ (third condition).

We also require the critical value of $k_c^2 > 0$ (k real). A necessary condition for this is $q_1 > 0$ (fourth condition).

For diffusively-driven instability to occur, the critical case is when $k_\pm^2$ such that $H_1(k_\pm^2) = 0$, and these can be easily shown to occur when

$$k_{\pm}^2 = \frac{q_1 \pm \sqrt{(q_1)^2 - 4\ \det(J)\det(D_c^o)}}{2\det(D_c^o)}. \tag{3.1.11}$$

Thus, requiring $H_1(k^2) < 0$ entails $(q_1)^2 - 4\ \det(J)\det(D_c^o) > 0$ (fifth condition), thereby yielding the fifth and last condition for cross-diffusion-driven-instability.

In summary, the necessary conditions for cross-diffusion-driven instability for system (3.1.1) are given by

$$f_u^o + g_v^o < 0, \tag{3.1.12a}$$

$$f_u^o g_v^o - f_v^o g_u^o > 0, \tag{3.1.12b}$$

$$\det(D_c^o) > 0, \tag{3.1.12c}$$

$$q_1 = [D_{22}^o f_u^o + D_{11}^o g_v^o - D_{21}^o f_v^o - D_{12}^o g_u^o] > 0, \tag{3.1.12d}$$

$$(q_1)^2 - 4\ \det(J)\det(D_c^o) > 0. \tag{3.1.12e}$$

To see how cross-diffusion affects diffusion-driven instability conditions, clearly in the present of cross-diffusion the self-diffusion coefficients can be equal where it is a necessary condition (3.1.5d) to be not equal in absence of cross-diffusion (self-diffusion-driven instability conditions).

Next, we will investigate the choice of kinetics term.

3.2 Kinetics Term

We focus on the effect of cross-diffusion on pattern formation. particularly, can cross-diffusion destabilize a steady state that is stable to all self-diffusion, so cross-diffusion

can induce pattern. Therefore, we need to specify the kinetic term. There are more than one class of kinetic where self-diffusion cannot destabilize the steady state; however, we focus only in one class where Jacobian matrices of kinetic model is

$$J := \begin{pmatrix} f_u^o & f_v^o \\ g_u^o & g_v^o \end{pmatrix} = \begin{pmatrix} - & - \\ + & 0 \end{pmatrix}. \tag{3.2.1}$$

The other classes of kinetics might be discussed in future.

3.3 Patterns Are Not Generated by Self-Diffusion

Here, we check can the conditions (3.1.5) be hold with kinetic (3.2.1) where $f_u^o < 0,\ f_v^o < 0,\ g_u^o > 0$ and $g_v^o = 0$. Thus in this case the conditions become

$$\begin{aligned} & f_u^o < 0, \\ & -f_v^o g_u^o > 0, \\ & \det(D) = d > 0, \\ & d f_u^o < 0. \end{aligned}$$

Hence, conditions (3.1.5) are not satisfied. Thus, we conclude that self-diffusion can not destabilize the uniform steady state , and pattern formation could not rise in presence of self-diffusion only.

However, if we look for conditions (3.1.12) in the presence of cross-diffusion system,

$$
\begin{aligned}
&f_u^0 < o,\\
&-f_v^o g_u^o > 0,\\
&\det(D_c^o) = (D_{11}^o D_{22}^o - D_{12}^o D_{21}^o) > 0,\\
&q_1 = [D_{22}^o f_u^o + D_{11}^o g_v^o - D_{21}^o f_v^o - D_{12}^o g_u^o] > 0,\\
&(q_1)^2 - 4\det(J)\det(D_c^o) > 0.
\end{aligned}
$$

Clearly, in the presence of cross-diffusion, these conditions can be satisfied. Next, we focus on examples of cross-diffusion systems to investigate the role of cross-diffusion in stability and pattern formation.

3.4 A Simple Cross-Diffusion Model

In this section, we investigate the first example of cross-diffusion systems to see how it affects the pattern formation. We consider the non-dimensional cross-diffusion system

$$
\begin{aligned}
u_t &= \nabla.[\nabla u + d_v \nabla v] + \gamma f(u,v),\\
v_t &= \nabla.[d_u \nabla u + d\nabla v] + \gamma g(u,v),
\end{aligned}
\tag{3.4.1}
$$

where d is the ratio of the linear diffusion coefficients, d_u and d_v are cross-diffusion coefficients and the ratio γ is a positive constant. $f(u,v)$ and $g(u,v)$ are kinetics term.

The above system is supplemented with initial conditions and Neumann boundary conditions. The Jacobian of flux coefficients evaluated at steady state is

$$D_c^o := \begin{pmatrix} 1 & d_v \\ d_u & d \end{pmatrix}.$$

3.4.1 Instability Conditions for the Simple Cross-Diffusion Model

We check now the conditions (3.1.12) for system (3.4.1), to see can this example of flux induce instability.

$$f_u^o + g_v^o < 0, \tag{3.4.2a}$$

$$f_u^o g_v^o - f_v^o g_u^o > 0, \tag{3.4.2b}$$

$$\det(D_c^o) = d - d_u d_v > 0, \tag{3.4.2c}$$

$$q_1 = d f_u^o - d_u f_v^o - d_v g_u^o > 0, \tag{3.4.2d}$$

$$(\gamma q_1)^2 - 4\gamma^2 \det(J)(d - d_u d_v) > 0. \tag{3.4.2e}$$

It follows trivially that conditions (3.4.2c), (3.4.2d) and (3.4.2e) can be satisfied by choosing small positive d and d_v and large positive d_u. Note that there are other possibilities for these conditions to be hold, such as negative cross-diffusion. Since all instability conditions can hold, the patterns can form. Next, we investigate system (3.5.1) numerically.

3.4.2 Numerical Simulation

For numerical simulation we consider the following model of predator-prey interaction in a homogeneous environment. This is an example of reaction kinetics for which it satisfies our conditions on kinetics (3.2.1). The model of predator-prey with cross-diffusion is

$$\begin{aligned} u_t &= \nabla^2 u + d_v \nabla^2 v + \gamma u(u-\beta)(1-u) - uv, \\ v_t &= d\nabla^2 v + d_u \nabla^2 u + uv - \delta v, \end{aligned} \tag{3.4.3}$$

where $u(x,t)$ and $v(x,t)$ are the densities of prey and predator, respectively. γ, β and δ are positive constant. The above system is supplemented with initial conditions and Neumann boundary conditions.

The only non-trivial steady state of the reaction term in system (3.4.3) is $(u_0, v_0) = (\delta, \gamma(\delta-\beta)(1-\delta))$, it can be shown that this is stable to standard-diffusion (for more details see Appendix A), and we discuss the outline result here.

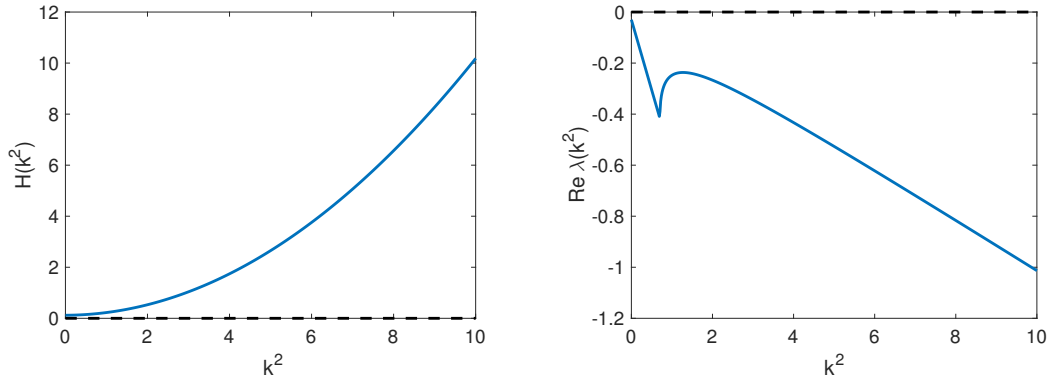

(a) (b)

Figure 3.1: Plots of (a) $H(k^2)$ and (b) $Re(\lambda(k^2))$ in (3.1.9) with parameter values $\beta = 0.1$, $\delta = 0.6$, $\gamma = 1$, $d_v = 0$, $d_u = 0$ and $d = 1$.

Note that the dispersion relation as calculated in (3.1.9) is in the general form, in this section we just substitute the diffusion coefficients partial derivatives from system (3.4.3).

Figure (3.1) shows the dispersion relation for system (3.4.3) with self-diffusion only. We observed no instability for any mode, and $Re(\lambda(k^2))$ remained negative for any value of the diffusion coefficient d. So, self-diffusion can not destabilize the uniform steady state where standard-diffusion.

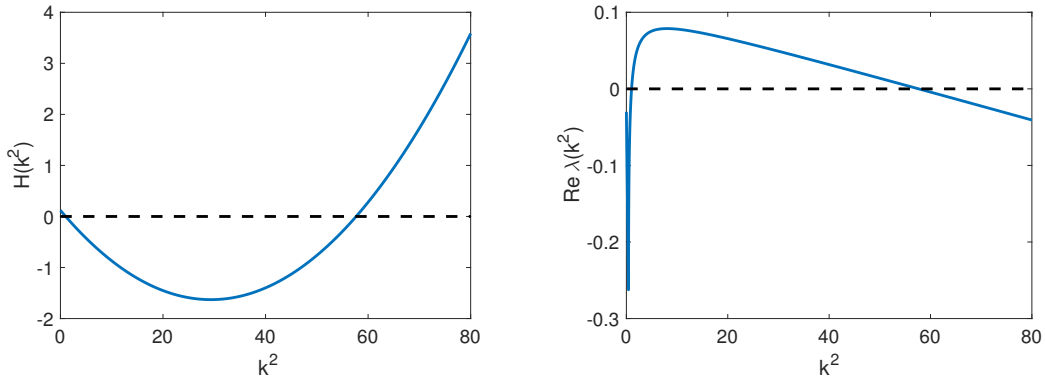

(a) (b)

Figure 3.2: Plots of (a) $H(k^2)$ and (b) $Re(\lambda(k^2))$ in (3.1.9) with parameter values $\beta = 0.1$, $\delta = 0.6$, $\gamma = 1$, $d_v = 0.313$, $d_u = 0.313$ and $d = 0.1$.

Figure (3.2) shows the dispersion relation for system (3.4.3) with self and cross-diffusion. We observed instability in the first and second modes. Next we show the numerical simulation for cross-diffusion system (3.4.1). We test the first mode and the second mode, which are indeed shown to be unstable grow, forming patterns (see Figures 3.3, 3.4).

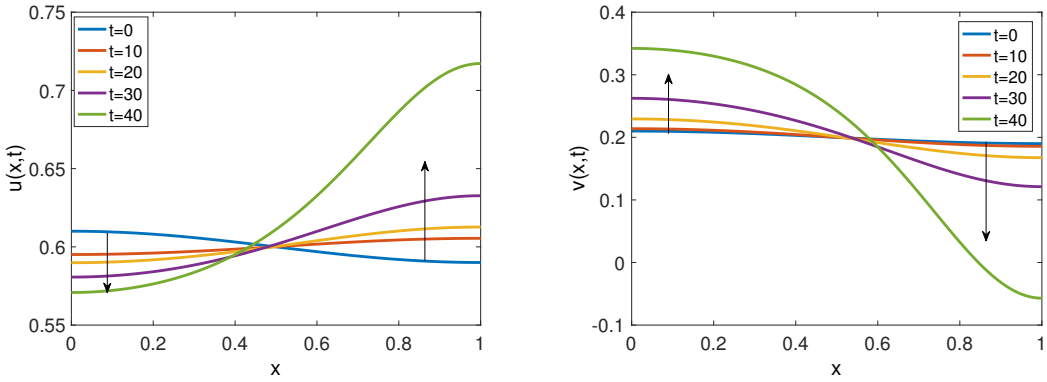

(a) (b)

Figure 3.3: Numerical simulations of (a) species u and (b) species v in system (3.4.1). Figure (a) The initial condition $u(x,0) = 0.6 + .01\cos(\pi x)$. Figure (b) The initial condition $v(x,0) = 0.2 + .01\cos(\pi x)$. Times shown are $t = 0$ (blue), $t = 10$ (orange), $t = 20$ (yellow), $t = 30$ (purple), $t = 40$ (green). Parameter values are shown in Table 3.1.

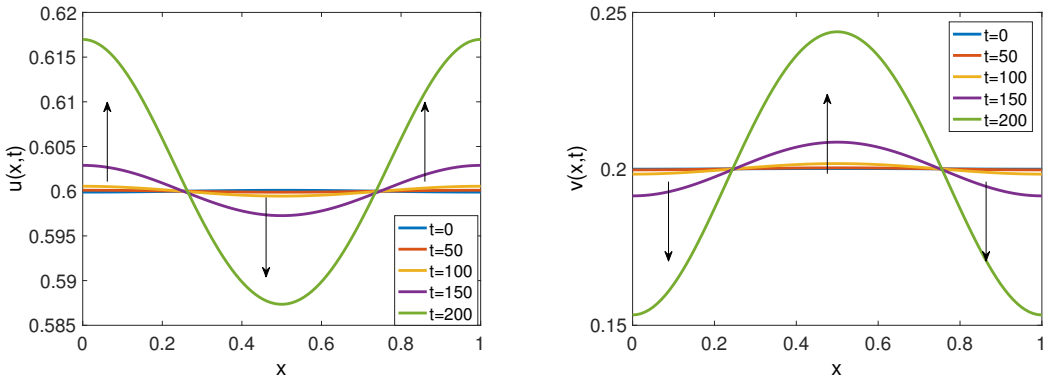

(a) (b)

Figure 3.4: Numerical simulations of (a) species u and (b) species v in system (3.4.1). Figure (a) The initial condition $u(x,0) = 0.6 - .0001\cos(2\pi x)$. Figure (b) The initial condition $v(x,0) = 0.2 - .0001\cos(2\pi x)$. Times shown are $t = 0$ (blue), $t = 50$ (orange), $t = 100$ (yellow), $t = 150$ (purple), $t = 200$ (green). Parameter values are shown in Table 3.1.

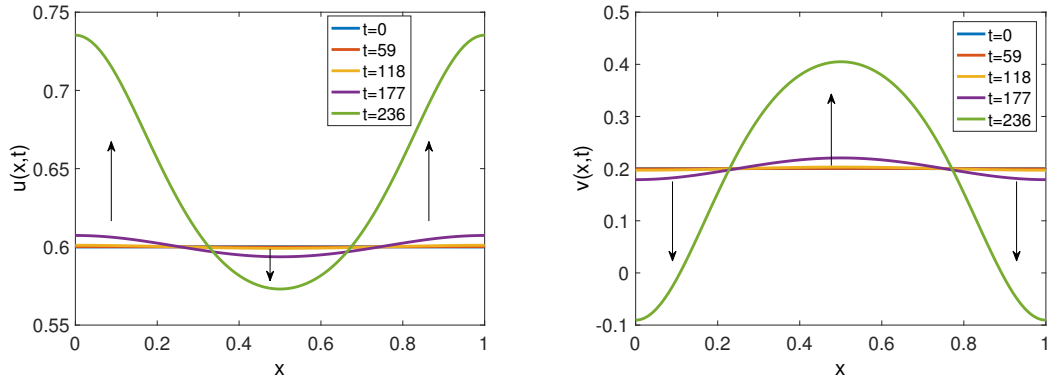

(a)

(b)

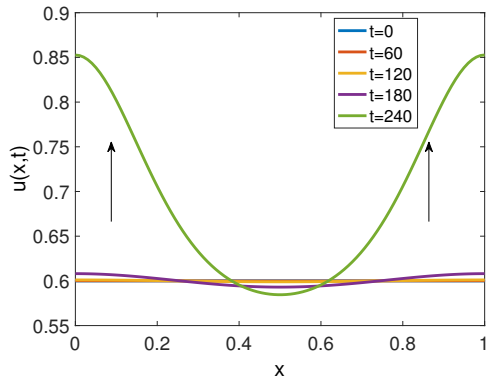

(c)

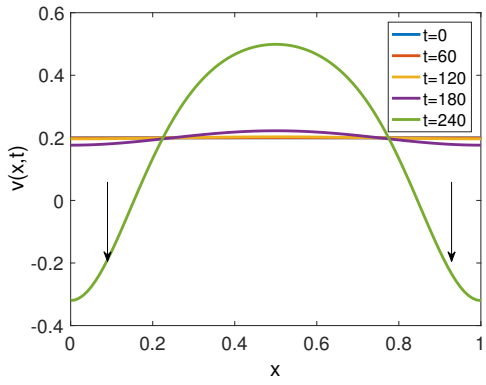

(d)

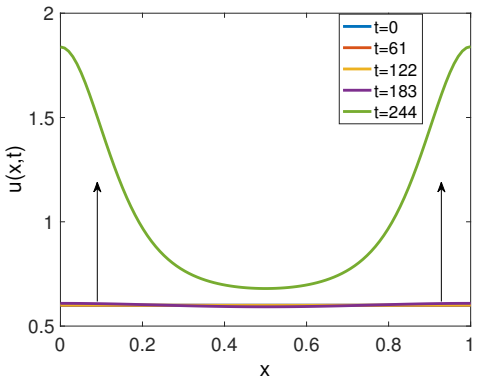

(e)

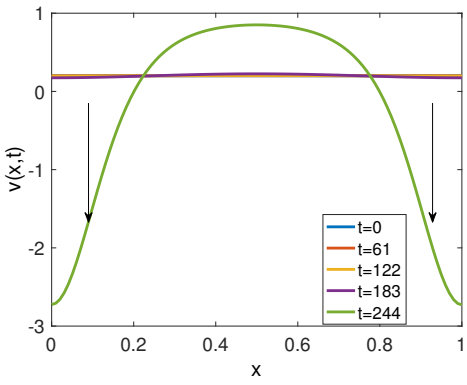

(f)

Figure 3.5: Numerical simulations of (a,c,e) species u and (b,x,f) species v in system (3.4.1). Figure (a) The initial condition $u(x,0) = 0.6 - .0001\cos(2\pi x)$. Figure (b) The initial condition $v(x,0) = 0.2 - .0001\cos(2\pi x)$. Parameter values are shown in Table 3.1.

Parameter	Value
β	0.1
δ	0.6
γ	1
d_v	0.313
d_u	0.313
d	0.1

Table 3.1: Table showing the parameter values that used to solve system (3.4.1).

To understand the behaviour of the solution, we increase the time t, and numerical simulation confirm that the large scale patterns continue to evolve (see Figure 3.5). We conclude linear cross-diffusion can induce the instability where standard-diffusion can not, and that large scale spatio-temporal patterns form. Our numerics suggest that under the effect of cross-diffusion, these patterns continue to evolve.

3.5 Pattern Formation Induced by Non-linear Cross-Diffusion

In previous section, it was shown that a linear cross-diffusion can destabilize the uniform steady state where standard-diffusion can not. Here, we investigate another example of flux. We consider the non-linear cross-diffusion with same predator-prey kinetics as used above. The details of derivation of system (3.5.1) will be in Chapter 4. The full cross-diffusion system is

$$
\begin{aligned}
u_t &= \nabla \,.\, (D_u(1-u)\nabla u - D_v u \nabla v) + \gamma u(u-\beta)(1-u) - uv, \\
v_t &= \nabla \,.\, (D_v(1-v)\nabla v - D_u v \nabla u) + uv - \delta v,
\end{aligned}
\tag{3.5.1}
$$

where D_u and D_v are non-negative constants. The above system is supplemented with initial conditions and Neumann boundary conditions. The Jacobian of flux coefficients evaluated at steady state is

$$
D_c^o := \begin{pmatrix} D_u(1-u_0) & -D_v u_0 \\ -D_u v_0 & D_v(1-v_0) \end{pmatrix}.
$$

3.5.1 Instability Conditions for Non-Linear Cross-Diffusion Model

Here, we investigate the conditions (3.1.12) for system (3.5.1), to see whether this example of flux can derive instability.

$$f_u^o + g_v^o < o, \tag{3.5.2a}$$

$$f_u^o g_v^o - f_v^o g_u^o > 0, \tag{3.5.2b}$$

$$\det(D_c^o) = D_u D_v (1 - v_0 - u_0) > 0, \tag{3.5.2c}$$

$$q_1 = -(D_u(1-u_0)g_v^o + D_v(1-v_0)f_u^o + D_v u_0 g_u^o + D_u v_0 f_v^o) < 0, \tag{3.5.2d}$$

$$q_1^2 > 4\det(J) D_u D_v (1 - v_0 - u_0). \tag{3.5.2e}$$

It follows trivially that condition (3.5.2d) can be satisfied by choosing D_v large and D_u

small, since $f_u^o >$, $f_v^o < 0$, $g_u^o > 0$ and $g_v^o = 0$. The conditions (3.5.2e) become

$$\begin{aligned} q^{*^2} =& (D_u v_0 f_v^o)^2 + (D_v[(1-v_0)f_u^o + u_0 g_u^o])^2 + 2(D_u v_0 f_v^o)(D_v[(1-v_0)f_u^o + u_0 g_u^o]) \\ & > 4D_u D_v (1 - v_0 - u_0)(-f_v^o g_u^o). \end{aligned}$$

This can be satisfied by choosing either D_u or D_v sufficiently small whilst the other is set to be $O(1)$.

We therefore conclude that the non-linear cross-diffusion can induce instability where standard-diffusion can not.

3.5.2 Numerical Simulation

A plot of the dispersion relation of system (3.5.1) is shown in Figure 3.6. We can observe that there is instability in the first, second and third modes.

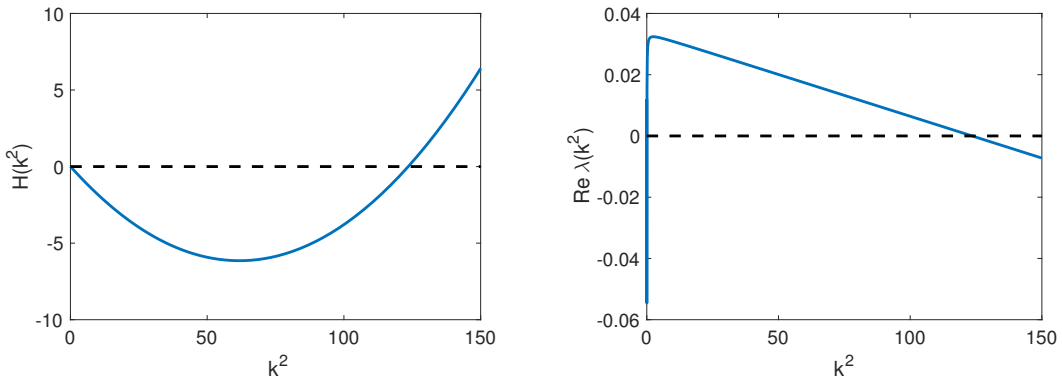

(a) (b)

Figure 3.6: Plots of (a) $H(k^2)$ and (b) $Re(\lambda(k^2))$ calculated from (3.1.9). Reaction parameter values $\gamma = 0.2$, $\delta = 0.6$, $\beta = 0.4$, $D_u = 0.0007$, and $D_v = 6$

Note that the dispersion relation as calculated in (3.1.9) is in the general form. In this section we just substitute the diffusion coefficients partial derivatives from the system (3.5.1).

We test the 1st, 2nd and 3rd modes to confirm our result summarised in Figure 3.6. Numerical test confirms that the 1st (a) 2nd (b) and 3rd (c) modes are unstable (see Figure 3.7). In addition, the standing front pattern in Figure 3.7 (a,b,c) was formed by small perturbation for species u. We observe that $v \approx 0$ (d) when we test the 1st mode, and similar behaviour is observed for the other modes.

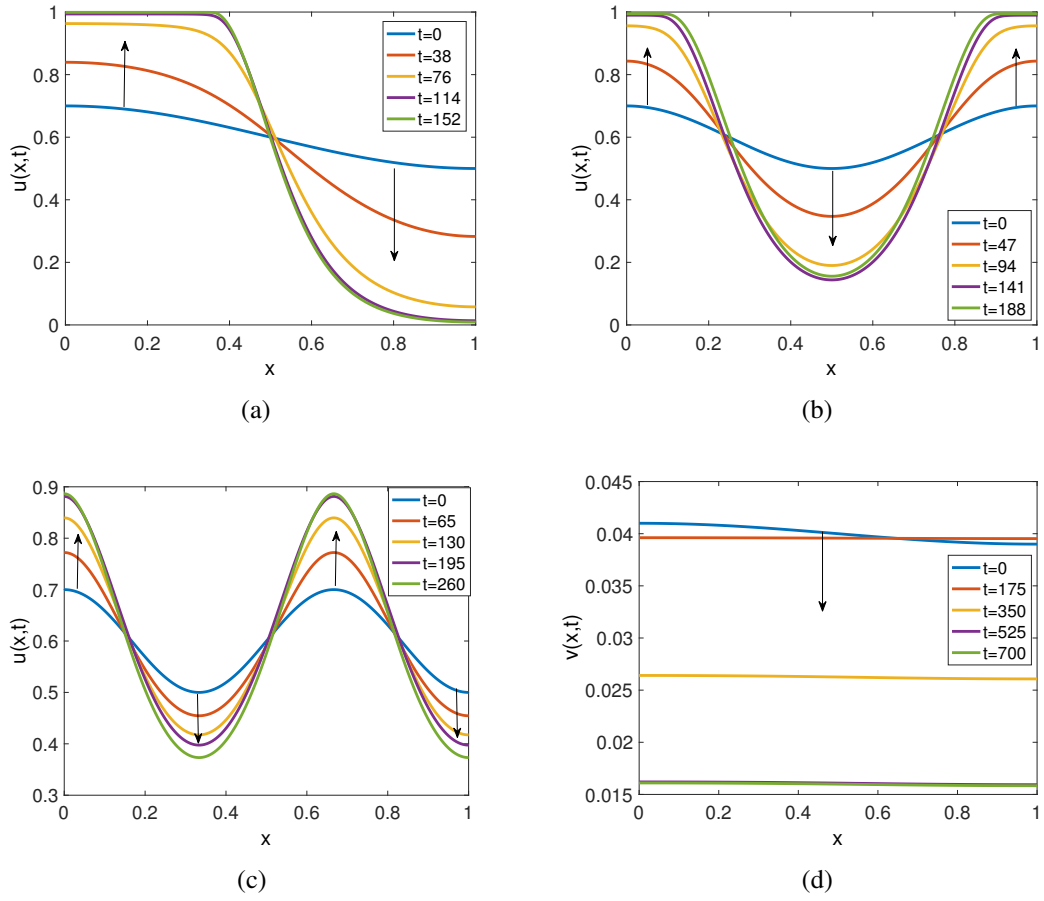

Figure 3.7: Solution of species u as computed by solving (3.5.1), (a) 1st mode: pattern occur, times shown are $t = 0$ (blue), $t = 38$ (orange), $t = 76$ (yellow), $t = 114$ (purple), $t = 152$ (green). (b) 2nd modes: pattern occur, times shown are $t = 0$ (blue), $t = 47$ (orange), $t = 94$ (yellow), $t = 141$ (purple), $t = 188$ (green). (c) 3rd modes: pattern occur, times shown are $t = 0$ (blue), $t = 65$ (orange), $t = 130$ (yellow), $t = 195$ (purple), $t = 260$ (green). Initial condition I.C$= 0.6 + 01\cos(n\pi x)$, $n = 1, 2, 3..$ (d) Solution of species v as computed by solving (3.5.1) with same paramter value we use for u and the initial condition I.C$= 0.04 + .001\cos(\pi x)$. times shown are $t = 0$ (blue), $t = 175$ (orange), $t = 350$ (yellow), $t = 525$ (purple), $t = 700$ (green). Parameter values are shown in Table 3.2.

Parameter	Value
β	0.4
δ	0.6
γ	0.2
D_u	0.0007
D_v	6

Table 3.2: Table showing the parameter values that used to solve system (3.5.1).

We conclude that non-linear cross-diffusion can induce pattern formation where standard-diffusion can not. In addition, numerical simulation confirm that the staple pattern can not generated by the linear cross-diffusion.

3.6 Conclusions

In this chapter, we focused on pattern formation and how it could be affected by cross-diffusion. We found out that cross-diffusion induces patterns where standard-diffusion can not. We have considered the stability analysis for a class of cross-diffusion systems. We focus on one type of kinetics where $f_u^o >$, $f_v^o < 0$, $g_u^o > 0$ and $g_v^o = 0$, with two examples of flux. We derived conditions for linear instability induced by cross-diffusion. Using predator-prey kinetics, we observed that a stable pattern occurs for the non-linear model while for a linear model, the large scale pattern continues to evolve. We conclude that cross-diffusion can induce instability where standard-diffusion can not. In the next chapter, we will discuss the derivation of the non-linear cross-diffusion model.

Chapter 4

Travelling Fronts in a Non-Linear Cross-Diffusion Model for Tightly Packed Populations

In this chapter, we are interested in a non-linear cross-diffusion system used to model tightly packed populations [72]. We first derive the model from a mass-conservation perspective. We investigated the pattern formation process for this model in the previous chapter, and we observed that the stationary front pattern formed. Here, we investigate moving front solutions of this model.

4.1 Model Derivation

Suppose that a biomass can be segregated into three components. Denote the volume fraction of these components by $v = v(x,t)$, $u = u(x,t)$ and $s = s(x,t)$, respectively,

$x \in \Omega \subset \mathbb{R}^3$. We assume that the fractions are subject to the following constraint:

$$v(x,t) + u(x,t) + s(x,t) = 1 \quad \forall x \in \Omega, t \geq 0. \tag{4.1.1}$$

The model we derive below is generic, but for ease of exposition and conception, we have in mind a simple model of a bacterial biofilm - a densely packed community of cells encased in a self-produced extracellular matrix [17, 63]. This volume fraction approach is indeed a common method for dealing with such problems and represents the realistic situation where the depth of the biofilm (in the direction orthogonal to the plane of growth) is nutrient limited and hence the fractions defined above are simply scaled population densities [110]. The components u and v can be considered to represent separate cell populations with s representing the extra cellular polymeric matrix. In the absence of any other processes, conservation of mass demands that the following relationship holds:

$$u_t = -\nabla.J_u; \quad v_t = -\nabla.J_v; \quad s_t = -\nabla.J_s \quad \text{for} \quad (x,t) \in \Omega \times \mathbb{R}^+, \tag{4.1.2}$$

and we consider this system to be augmented with zero flux boundary conditions:

$$J_u.n = J_v.n = J_s.n = 0, \quad \text{for} \quad x \in \partial\Omega, \tag{4.1.3}$$

where n is the outward pointing normal on $\partial\Omega$. Clearly any one of the variables could be computed directly from the other two by invoking (4.1.1), but for clarity, we write the system out in full in the first instance. Moreover, adding the equations in (4.1.2) results in

$$(u+v+s)_t = 0 = -\nabla.(J_u + J_v + J_s).$$

Let us consider the u-subpopulation. Similar arguments hold for the other variables. The conservation equation (4.1.1) combined with the boundary conditions (4.1.3) ensures that a unit of volume in the u-subpopulation e.g. a $u-$cell can move from one spatial location to another only if its place is taken by an equivalent volume. Note that this replacement could be from the $u-$, $v-$ or $s-$populations with only the latter two representing a change in the distribution of the volume fraction (swapping u for u has no net effect on the volume fraction). As a first step suppose that the self-flux J_u^s is proportional to ∇u, i.e. in isolation, the $u-$population exhibits "Fickian-like" behaviour. However, the populations are constrained by (4.1.1) and hence, as outlined above the probability of a change in the u-fraction at a given spatial location is in fact proportional to $1-u$ (i.e. "not u"). Hence, unlike the standard case where the coefficient of proportionality is a positive constant (leading to Fickian diffusion), we set the coefficient of proportionality to be $D_u(u) := D_u(1-u)$, for some positive constant D_u and thus

$$J_u^s = -D_u(1-u)\nabla u = -D_u(v+s)\nabla u.$$

In the absence of other processes, (4.1.1), (4.1.3) demand that this flux of u must be balanced by a flux of v and s. Hence, the terms $D_u v\nabla u$ and $D_u s\nabla u$ must appear in the flux functions for v and s, respectively. Applying similar arguments to v, it follows that the self-flux $J_v^s = -D_v(1-v)\nabla v$ and this component induces the balancing terms $D_v u\nabla v$ and $D_v s\nabla v$ in J_u and J_s, respectively. Finally, the self-flux J_s^s contains the term $-D_s(1-s)\nabla s$ and this component induces the balancing terms $D_s u\nabla s$ and $D_s v\nabla s$ in J_u and J_v, respectively. Hence, the flux terms in system (4.1.2) are

$$\begin{aligned} J_u &= -D_u(1-u)\nabla u + D_v u\nabla v + D_s u\nabla s, \\ J_v &= -D_v(1-v)\nabla v + D_u v\nabla u + D_s v\nabla s, \\ J_s &= -D_s(1-s)\nabla s + D_u s\nabla u + D_v s\nabla v. \end{aligned} \tag{4.1.4}$$

It is easy to confirm that $J_u + J_v + J_s = 0$. Note also that in the special case $D_u = D_v = D_s = D$, then the fluxes collapse to

$$J_u = -D\nabla u; \quad J_v = -D\nabla v; \quad J_s = -D\nabla s.$$

Therefore, the fluxes decouple and standard Fickian diffusion is recovered. We consider this not to be the case as discussed below.

Now that the form of the flux terms has been established, we invoke (4.1.1) to eliminate one of the variables and without loss of generality set $s = 1 - (u + v)$ with $D_s \leq \min\{D_u, D_v\}$. Thus, (4.1.4) becomes

$$\begin{aligned} J_u &= -(D_u - (D_u - D_s)u)\nabla u + D_v u \nabla v, \\ J_v &= -(D_v - (D_v - D_s)v)\nabla v + D_u v \nabla u \end{aligned}$$

From (4.1.1) and the choice of D_s it follows that the coefficients of the self- and cross-gradient terms are negative and positive, respectively. In what follows, for ease of calculation, it is therefore assumed that $D_s = 0$. This choice does not affect the qualitative output of the system. Moreover, If we consider s to represent the sticky extracellular matrix, it may be reasonable to assume this generic self-diffusion rate to be much lower than that of the cell-components.

In summary, we arrive at the flux-driven system

$$\begin{aligned} u_t &= \nabla \,.\, (D_u(1-u)\nabla u + D_v u \nabla v), \\ v_t &= \nabla \,.\, (D_v(1-v)\nabla v + D_u v \nabla u), \end{aligned} \tag{4.1.5}$$

for $(x,t) \in \Omega \times \mathbb{R}^+$ with boundary conditions

$$\begin{aligned} (-D_u(1-u)\nabla u + D_v u \nabla v).n = 0, \\ (-D_v(1-v)\nabla v + D_u v \nabla u).n = 0, \end{aligned} \tag{4.1.6}$$

for $x \in \partial\Omega$.

With the flux terms established, reactions terms $f(u,v)$ and $g(u,v)$ can be added to the right hand side of $u-$ and $v-$ equations in (4.1.5). Note that in general (4.1.1) does not demand that $f+g=0$. Rather, defining $h=-(f+g)$ and adding h to the right hand side of the $s-$equation in (4.1.2) yields the appropriate conservation equation. [The case $s \equiv 0$ would demand $h \equiv 0$ and then $f=-g$. In this case, the system would collapse even further to scalar in u, with $v=1-u$.]

We note that the derivation given above clearly describes the application we have in mind and allows for the possibility of explicitly including the effects of the third variable. Moreover, despite the fact that we reduce the problem to two equations and consider the case $D_s=0$, this case could not have been derived via the route of considering only the u and v populations for which the conditions $u+v \leq 1$ and $u+v \not\equiv 1$ hold. Here, the remaining volume fraction is implicitly defined as $1-(u+v) \not\equiv 0$. As such, it is not possible to partition the relevant component of the fluxes to the "not X" population where $X=u$ or v as we have done using the explicit three variable model.

Finally, we recall that the mass conservation arguments given above are supported by the random walk formulation given in Chapter 2. There, it was shown that jump probabilities could be selected that connect the partial differential equation (4.1.5) with the relevant master equation.

4.2 Moving Fronts

We observed in the previous chapter that with the chosen parameters, the standing front pattern was formed. However if we start with different parameters we have moving front solution. We do numerical simulation for system (3.5.1) with different parameters. As we observed in previous chapter that population u tended to standing front and v tended to small constant. Here, we investigate the same system numerically with a step function as initial condition for species u, and constant initial condition for species v.

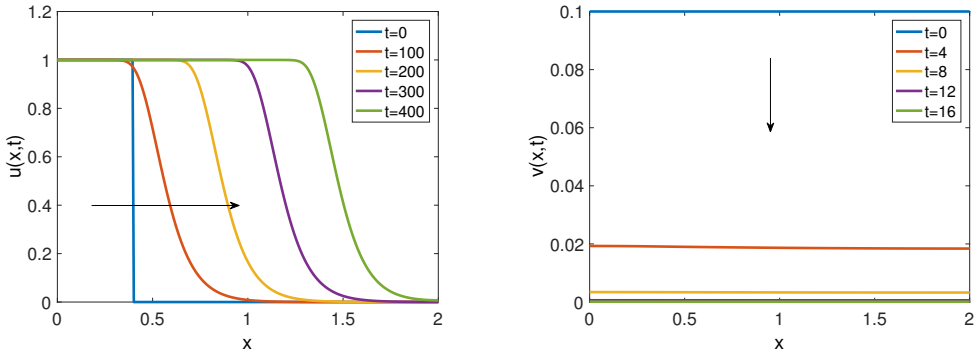

(a) (b)

Figure 4.1: (a) Solution of species u as computed by solving (3.5.1). Times shown are $t = 0$ (blue), $t = 100$ (orange), $t = 200$ (yellow), $t = 300$ (purple), $t = 400$ (green). (b) Solution of species v as computed by solving (3.5.1). Times shown are $t = 0$ (blue), $t = 4$ (orange), $t = 8$ (yellow), $t = 12$ (purple), $t = 16$ (green). Parameter values are shown in Table 4.1.

Parameter	Value
β	0.2
δ	0.6
γ	0.2
D_u	0.0007
D_v	6

Table 4.1: Table showing the parameter values that used to solve system (3.5.1).

Clearly, the model can exhibit a moving front solution for u with certain parameter choices, and $v \approx 0$ (see Figure 4.1). Therefore, in next section, to understand the front formation, we consider the related problem where $v \equiv 0$.

4.3 A Simplified Model

The moving front solution appears for species u while species v is essentially uniform in space and tends to a constant. We observe in Figure 4.1 (b) that $v \approx 0$, thus for ease of analysis and numeric investigation in the following, we take $v \equiv 0$. Thus, the system is reduced to scalar equation as expressed in equation (4.3.1).

$$u_t = \nabla \,.\, (D_u(1-u)\nabla u) + \gamma u(1-u)(u-\beta). \tag{4.3.1}$$

We seek a travelling wave solution of above equation, so we try to understand how the travelling wave solution occur. Two highlighting features of equation (4.3.1) are non-linear diffusion and bistability of the kinetics term. In addition, the kinetic term of equation (4.3.1) is the same as in Nagumo's equation, thus we also focus on the effect of non linear diffusion term and what difference the non-linear diffusion term makes

to the travelling wave solution.

4.4 Travelling Wave Analysis of the Scalar Equation

We consider the reaction-diffusion equation (4.3.1). The stability of steady states of the associated ODE is the same as that in Nagumo's equations (see Appendix A.1.2).

Rewriting equation (4.3.1)

$$u_t = -D_u\Big(\frac{\partial u}{\partial x}\Big)^2 + D_u(1-u)\frac{\partial^2 u}{\partial x^2} + f(u). \tag{4.4.1}$$

Considering the travelling wave ansatz $u(x,t) = W(z) = W(x-ct)$, it follows that the $W(z)$ is required to satisfy

$$-c\frac{dW}{dz} = -D_u\Big(\frac{dW}{dz}\Big)^2 + D_u(1-W)\frac{d^2W}{dz^2} + f(W). \tag{4.4.2}$$

We restrict our attention for the case where $c > 0$. The case where $c < 0$ will be investigated in the future work. Equation (4.4.2) can be re-written as a first order system of ODEs as follows

$$\begin{aligned} &\frac{dW}{dz} = P, \\ &D_u(1-W)\frac{dP}{dz} = D_uP^2 - cP - f. \end{aligned} \tag{4.4.3}$$

When $W = 1$, clearly the left hand side of the second equation is zero. This degeneracy

can be removed by introducing the parameter τ such that

$$\frac{d\tau}{dz} = \frac{1}{D_u(1-W(z))} \Rightarrow \tau(z) = \int_0^z \frac{ds}{D_u(1-W(s))}. \tag{4.4.4}$$

Except at $W = 1$ where $\frac{d\tau}{dz}$ is not defined, $\frac{d\tau}{dz} > 0$ [2, 77].

Thus τ has an inverse τ^{-1}, which in principle can be obtained from (4.4.4). Thus we have

$$W(z) = W(\tau(z)) \text{ and } P(z) = P(\tau(z)), \tag{4.4.5}$$

and we obtain

$$\frac{dW}{dz} = \frac{dW}{d\tau}(\tau)\frac{1}{D_u(1-W(z))} \quad \text{and} \quad \frac{dP}{dz} = \frac{dP}{d\tau}(\tau)\frac{1}{D_u(1-W(z))}. \tag{4.4.6}$$

Clearly, for $0 < W(z) < 1$, $\text{sign}(\frac{dW}{dz}) = \text{sign}(\frac{dW}{d\tau})$ and therefore $W(z)$ is monotone decreasing $\Leftrightarrow W(\tau)$ is monotone decreasing.

Substituting (4.4.6) into (4.4.3) we have a system without the singularity as follows

$$\begin{aligned} \dot{W} &= D_u(1-W)P, \\ \dot{P} &= D_u P^2 - cP - f, \end{aligned} \tag{4.4.7}$$

where "." denotes derivative with respect to τ.

Note that systems (4.4.3) and (4.4.7) are topologically equivalent in the slab $\{(W,P) \mid$

$0 < W < 1,\ -\infty < P < \infty\}$. This is because (4.4.5) defines a re-parametrization of the trajectories which, according to (4.4.6), preserves their orientation.

The steady states of (4.4.7) are $(W_1, P_1) = (0,0)$, $(W_2, P_2) = (1,0)$, $(W_3, P_3) = (\beta, 0)$ and $(W_4, P_4) = (1, \frac{c}{D_u})$.

The Jacobian matrix for system (4.4.7) is given by

$$J(W,P) := \begin{pmatrix} -D_u P & D_u(1-W) \\ -f'(w) & 2D_u P - c. \end{pmatrix}.$$

At steady states (W_j, P_j), the eigenvalues of $J(W_j, P_j)$ are solution of the characteristic polynomial

$$\det(J(W_j,P_j) - \lambda I) = \begin{pmatrix} -D_u P_j - \lambda & D_u(1-W_j) \\ -f'(W_j) & 2D_u P_j - c - \lambda. \end{pmatrix} = 0,$$

$$\Rightarrow \lambda^2 + \lambda[c + D_u P_j - 2D_u P_j] + cD_u P_j - 2D_u^2 P_j + D_u f'(W_j) - D_u W_j f'(W_j) = 0. \tag{4.4.8}$$

Therefore:

$$\lambda_j^{\pm} = \frac{-[c - D_u P] \pm \sqrt{[c - D_u P]^2 - 4D_u[cP - D_u P + f'(W_j) - W f'(W_j)]}}{2}. \tag{4.4.9}$$

We can obtain the eigenvectors associated with the eigenvalues by solving

$$(J - \lambda I)\boldsymbol{W} = \mathbf{0}. \tag{4.4.10}$$

At the steady state $(W_1, P_1) = (0,0)$,

$$\lambda_1^{\pm} = \frac{-c \pm \sqrt{c^2 - 4D_u f'(0)}}{2}. \tag{4.4.11}$$

Since $f'(0) < 0$, we obtain $\lambda_1^- < 0 < \lambda_1^+$ and it is a saddle point. Using (4.4.10), the equations representing the eigenvectors are

$$\Psi_1^{\pm} = \begin{pmatrix} 1 \\ \frac{\lambda_1^{\pm}}{D_u} \end{pmatrix}. \tag{4.4.12}$$

At the steady state $(W_2, P_2) = (1,0)$,

$\lambda_2^+ = 0,\ \lambda_2^- = -c$, so it is non-hyperbolic point for which stability can not be determined using linearisation. However, we look close to $(W_2, P_2) = (1,0)$ with $W^* \lesssim 1$ and $P^* \lesssim 0$, we see from system (4.4.7)

$$\begin{aligned} &\dot{W} = D_u(1-W)P < 0, \\ &\dot{P} = D_u P^2 - cP - f < 0 \quad \text{if} \quad D_u P^2 - cP < f(W). \end{aligned} \tag{4.4.13}$$

Therefore, the trajectory starting at (W^*, P^*) moves away from (W_2, P_2) and hence $(W_2, P_2) = (1,0)$ is unstable.

Using (4.4.10), the equations representing the eigenvectors are

$$\text{for } \lambda_2^+ = 0,\ \Psi_2^+ = \begin{pmatrix} \frac{c}{\gamma(1-\beta)} \\ 1 \end{pmatrix}, \quad \text{for } \lambda_2^- = -c,\ \Psi_2^- = \begin{pmatrix} 0 \\ 1 \end{pmatrix}. \tag{4.4.14}$$

At the steady state $(W_3, P_3) = (\beta, 0)$,

$$\lambda_3^{\pm} = \frac{-c \pm \sqrt{c^2 - 4D_u f'(\beta) - f'(\beta)}}{2}. \tag{4.4.15}$$

Recall $f'(\beta) > 0$. Hence,

$$(\beta,0) - \begin{cases} \text{focus} & \text{if } c^2 < 4D_u f'(\beta) - f'(\beta) \text{ and is stable if } c > 0, \text{ unstable if } c < 0, \\ \text{node} & \text{if } c^2 \geq 4D_u f'(\beta) - f'(\beta) \text{ and is stable if } c > 0, \text{ unstable if } c < 0, \\ \text{centre} & \text{if } c = 0. \end{cases}$$

Using (4.4.10), the equations representing the eigenvectors are

$$\Psi_3^{\pm} = \begin{pmatrix} 1 \\ \frac{\lambda_3^{\pm}}{D_u(1-\beta)} \end{pmatrix}. \tag{4.4.16}$$

At the steady state $(W_4, P_4) = (1, \frac{c}{D_u})$,

$\lambda_4^+ = c,\ \lambda_4^- = -c$, so it is a saddle point. Using (4.4.10), the equations representing the eigenvectors are

$$\text{for } \lambda_4^+ = c,\ \Psi_4^+ = \begin{pmatrix} 0 \\ 1 \end{pmatrix}, \quad \text{for } \lambda_4^- = -c,\ \Psi_4^- = \begin{pmatrix} \frac{2c}{f'(w)} \\ 1 \end{pmatrix}. \tag{4.4.17}$$

To see what effect the non-linear term makes on Nagumo's equation, we compare the eigenvalues $\lambda_j^{\pm}$ in (4.4.9) with the eigenvalues for Nagumo's equation, which are (see e.g. [99])

$$\sigma_j^{\pm} = \frac{-c \pm \sqrt{c^2 - 4f'(W_j)}}{2}. \tag{4.4.18}$$

So, for the steady states $(0,0)$, $(\beta,0)$ and $(1,0)$ equation (4.4.9) become:

$$\lambda_j^{\pm} = \frac{-c \pm \sqrt{c^2 - 4D_u[f'(W_j) - Wf'(W_j)]}}{2}. \tag{4.4.19}$$

$D_u W f'(W_j)$ under square root in (4.4.19) is difference between (4.4.19) and (4.4.18) and that is because of non-linear diffusion term in our equation; however, since $0 < W < 1$ the stability of the steady state should be same in our equation and Nagumo's equation. In summary, the non-linear diffusion term does not affect the stability of steady state and it is similar to Nagumo's equation.

4.5 Sign of the Wave Speed

Let us return to the original formulation (4.4.2), taking the product of equation (4.4.2) and $\frac{dW}{dz}$, and integral over $(-\infty,+\infty)$:

$$\int_{-\infty}^{+\infty} D_u(1-W)\frac{d^2W}{dz^2}\frac{dW}{dz}dz + c\int_{-\infty}^{+\infty}\left|\frac{dW}{dz}\right|^2 dz - D_u\int_{-\infty}^{+\infty}\left|\frac{dW}{dz}\right|^3 dz + \int_{-\infty}^{+\infty} f(W)\frac{dW}{dz}dz = 0. \tag{4.5.1}$$

Using integration by parts to calculate first integral in (4.5.1)

$$\begin{aligned}\int_{-\infty}^{+\infty} D_u(1-W)\frac{d^2W}{dz^2}\frac{dW}{dz}dz &= D_u\left[\frac{dW}{dz}(1-W)\frac{dW}{dz}\right]_{-\infty}^{+\infty} \\ &= D_u\int_{-\infty}^{+\infty}\frac{dW}{dz}\Big(-\frac{dW}{dz}\frac{dW}{dz} + (1-W)\frac{d^2W}{dz^2}\Big)dz \\ &= D_u\int_{-\infty}^{+\infty}\left|\frac{dW}{dz}\right|^3 - (1-W)\frac{d^2W}{dz^2}\frac{dW}{dz}dz.\end{aligned} \tag{4.5.2}$$

Substituting (4.5.2) into (4.5.1), we obtain

$$-\int_{-\infty}^{+\infty} D_u(1-W)\frac{d^2W}{dz^2}dW + c\int_{-\infty}^{+\infty}\left|\frac{dW}{dz}\right|^2 dz + \int_{W(-\infty)}^{W(+\infty)} f(W)dW = 0. \quad (4.5.3)$$

We can rewrite

$$\int_{-\infty}^{+\infty} D_u(1-W)\frac{d^2W}{dz^2}dW = \int_1^0 D_u(1-W)\frac{d^2W}{dz^2}dW = -\int_0^1 D_u(1-W)\frac{d^2W}{dz^2}dW. \quad (4.5.4)$$

Hence,

$$c = \frac{\overbrace{-\int_0^1 D_u(1-W)\frac{d^2W}{dz^2}dW}^{I_1} + \overbrace{\int_0^1 f(W)dW}^{I_2}}{\underbrace{\int_{-\infty}^{+\infty}\left|\frac{dW}{dz}\right|^2 dz}_{I_3}}. \quad (4.5.5)$$

The sign of c depends on the integrals I_1 and I_2 since $I_3 > 0$, so it can be positive (right wave), negative (left wave) and zero (standing wave). With the chosen parameter values the sign of I_1 is negative (we shall show this case in our numerical investigation), then if I_2 is zero or negative the sign of c is negative thus we have left wave, but if I_2 is positive and $I_2 > -I_1$ we get right wave. If $I_2 = -I_1$ we have standing wave.

Comparing expression of c in equation (4.5.5) for non-linear diffusion bistable equation with expression of c in equation (A.1.4) for Nagumo's equation, it can be seen that I_1 does not appear for Nagumo's equation case, which come from non-linear diffusion term in (4.5.5). Thus, I_1 can affect the sign of c. For example with the chosen parameter values taking $\beta = 0.4$ result $I_2 > 0$ which gives right wave for Nagumo's

equation but in non-linear case gives standing wave since $I_1 = -I_2$. Furthermore, taking $\beta = 0.2$ result $I_2 > 0$ which gives right wave for Nagumo's equation and in the non-linear case gives right wave as well since $I_1 < I_2$. In addition, in the case where $\beta = 0.2$ which result right travelling wave for both non-linear and stranded diffusion, the right travelling speed slowed down because of I_1.

As D_u changes, the value of I_1 does not affect or it just have a little effect since the D_u scales z and we integrate $-\infty < z < \infty$; however, as D_u increase, I_3 decrease which result $c \to +\infty$ for right wave (see Tables 4.2, 4.3). In summary, the diffusion coefficient D_u can increase or decrease the wave speed, but it can not change the sign of speed wave.

$\beta = 0.4$ **Standing wave**					
Case	D_u	I_1	I_2	I_3	c
1	1	-0.016	0.016	0.16	0
2	10	-0.016	0.016	0.53	0
3	20	-0.016	0.016	0.37	0
4	200	-0.016	0.016	0.01	0

Table 4.2: Table showing the value I_1, I_2 and I_3 with varying D_u to see the effect on c that calculated in equation (4.5.5) with $\beta = 0.4$.

$\beta = 0.2$ **Right wave**					
Case	D_u	I_1	I_2	I_3	c
1	1	-0.012	0.05	0.14	0.025
2	10	-0.012	0.05	0.04	0.81
3	20	-0.012	0.05	0.32	1.14
4	100	-0.012	0.05	0.041	2.69

Table 4.3: Table showing the value I_1, I_2 and I_3 with varying D_u to see the effect on c that calculated in equation (4.5.5) with $\beta = 0.2$.

We conclude that the sign of c is affected by I_1 which comes from the non-linear diffusion term, in contrast to the classic case (Nagumo's equation) where sign of c depends on I_2 only.

4.6 Proving Heteroclinic Connection via Shooting Method

In order for a travelling wave to exist, it is required that $W(z)$ approaches constant states as $z \longrightarrow \pm\infty$. In other words, trajectory leaves one fixed point at $\tau = -\infty$ and joins another fixed point at $\tau = \infty$. Therefore, we use the shooting method to prove existing of the travelling wave, and we use MATLAB function pplane to develop the phase portraits.

As above, we restrict our attention for the case where $c > 0$. Assume $\int_0^1 (fu)du > 0$,i.e. $c > 0$. For the trajectory T_0 entering $(0,0)$ see Figure 4.2, from the equations in (4.4.7) and the assumptions on f we have

1. If $W \in (0,\beta)$, we have

$$\begin{cases} \frac{dW}{dz} = D_u(1-W)P < 0, \\ \frac{dP}{dz} = D_u P^2 - cP - f(W) > 0, \end{cases}$$

   this implies for $W \in (0,\beta)$, $\frac{dP}{dW} < 0$, since $f(W) < 0$ and $P < 0$. Thus $P(W)$ is always deceasing.

2. If $W = \beta$, we have

$$\begin{cases} \frac{dW}{dz} = D_u(1-W)P < 0, \\ \frac{dP}{dz} = D_u P^2 - cP > 0, \end{cases}$$

   this implies for $W = \beta$, $\frac{dP}{dW} < 0$, since $f(W) = 0$ and $P < 0$. Thus $P(W)$ is always

deceasing.

3. If $W \in (\beta, 1)$, we have

$$\begin{cases} \frac{dW}{dz} = D_u(1-W)P < 0, \\ \frac{dP}{dz} = D_u P^2 - cP - f(W) < 0 \; or \; > 0, \end{cases}$$

this implies for $W \in (\beta, 1)$, $\frac{dP}{dW} > 0$ for small P, and $\frac{dP}{dW} < 0$ for large P, since $f(W) > 0$ and $P < 0$.

Let γ_0 be the first value of $W \in (\beta, 1)$ such that $\frac{dP}{dz} = 0$, then we have

$$\begin{cases} \frac{dP}{dz} > 0 \text{ for all } W \in (0, \gamma_0), \\ \frac{dP}{dz} \mid_{W=\gamma_0} = 0, \end{cases}$$

this implies

$$\begin{cases} \frac{dP}{dW} < 0 \text{ for all } W \in (0, \gamma_0), \\ \frac{dP}{dW} = 0 \text{ for } W = \gamma_0. \end{cases}$$

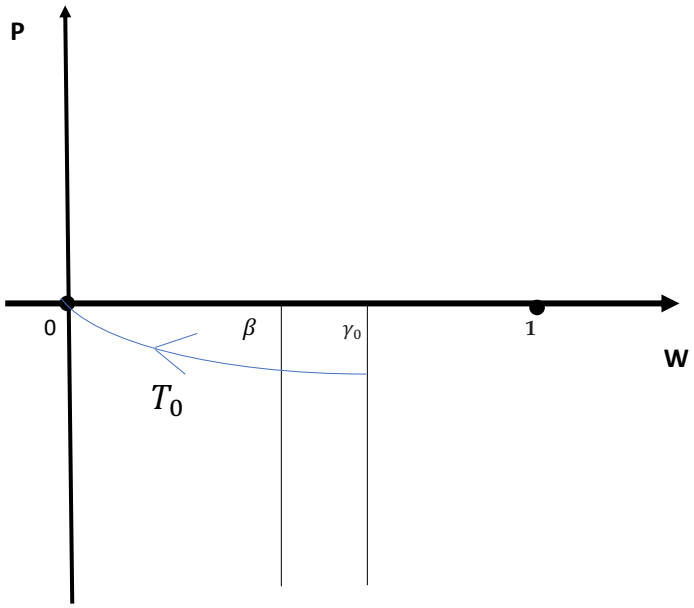

Figure 4.2: An illustration of the trajectories T_0.

Now, for the trajectory T_1 leaving $(1,0)$ see Figure 4.3, with similar calculation from the equations in (4.4.7) and the assumptions on f we have

1. If $W \in (0,\beta)$, we have

$$\begin{cases} \frac{dW}{dz} = D_u(1-W)P < 0, \\ \frac{dP}{dz} = D_uP^2 - cP - f(W) > 0, \end{cases}$$

this implies for $W \in (0,\beta)$, $\frac{dP}{dW} < 0$, since $f(W) < 0$ and $P < 0$. Thus $P(W)$ is always deceasing.

2. If $W = \beta$, we have

$$\begin{cases} \frac{dW}{dz} = D_u(1-W)P < 0, \\ \frac{dP}{dz} = D_uP^2 - cP > 0, \end{cases}$$

this implies for $W = \beta$, $\frac{dP}{dW} < 0$, since $f(W) = 0$ and $P < 0$. Thus $P(W)$ is always

deceasing.

3. If $W \in (\beta, 1)$, we have

$$\begin{cases} \frac{dW}{dz} = D_u(1-W)P < 0, \\ \frac{dP}{dz} = D_u P^2 - cP - f(W) < 0 \; or \; > 0, \end{cases}$$

this implies for $W \in (\beta, 1)$, $\frac{dP}{dW} > 0$ for small P, and $\frac{dP}{dW} < 0$ for large P, since $f(W) > 0$ and $P < 0$.

Let γ_1 be the first value of $W \in (\beta, 1)$ such that $\frac{dP}{dz} = 0$, then we have

$$\begin{cases} \frac{dP}{dz} > 0 \text{ for all } W \in (0, \gamma_1), \\ \frac{dP}{dz} \mid_{W=\gamma_1} = 0, \end{cases}$$

this implies

$$\begin{cases} \frac{dP}{dW} < 0 \text{ for all } W \in (0, \gamma_1), \\ \frac{dP}{dW} = 0 \text{ for } W = \gamma_1. \end{cases}$$

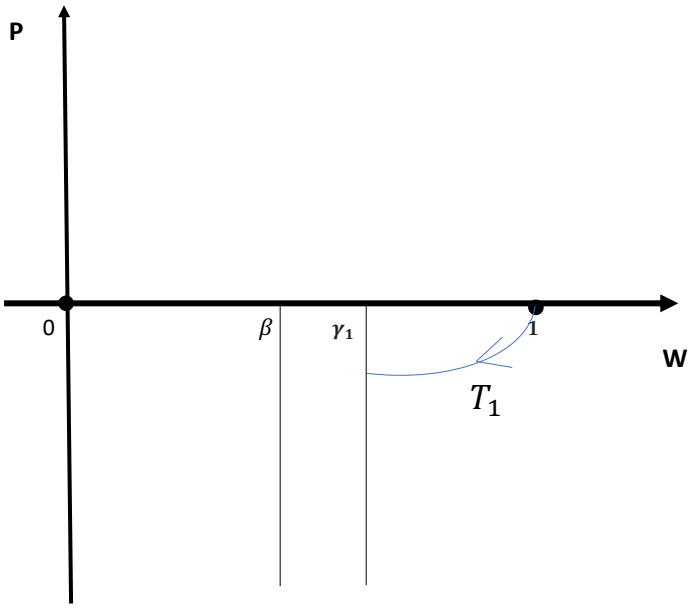

Figure 4.3: An illustration of the trajectories T_1.

We now investigate that either $\gamma_0 = \gamma_1$ or $\gamma_0 \neq \gamma_1$, we have from system (4.4.7)

$$\frac{dP}{dW} = \frac{D_u P^2 - cP - f(W)}{D_u(1-W)P} = 0, \tag{4.6.1}$$

thus,

$$D_u P^2 - cP - f(W) = 0,$$

we get

$$P(W) = \frac{c \pm \sqrt{c^2 + 4D_u f(W)}}{2D_u}.$$

For $W \in (\beta, 1)$ and since $f(W) > 0$, thus this defines a unique value

$$P(W) = \frac{c - \sqrt{c^2 + 4D_u f(W)}}{1D_u},$$

for each value of c. Thus, $\gamma_0 = \gamma_1$ and we rename this point as m.

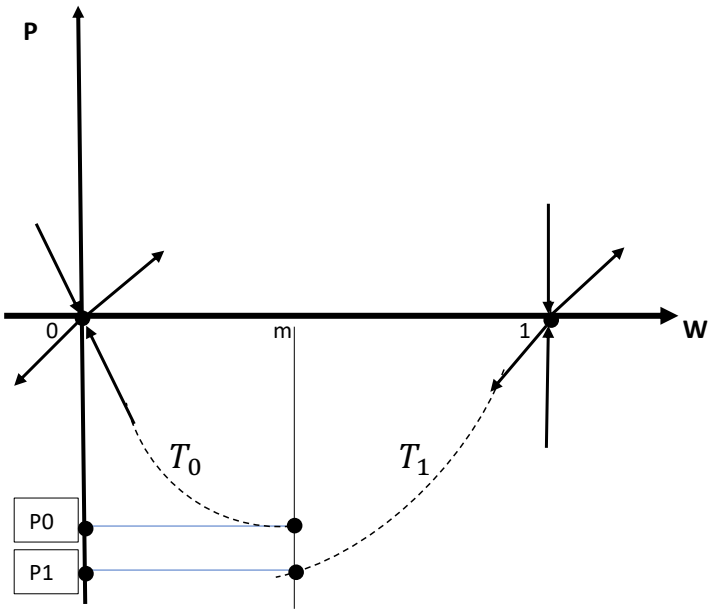

Figure 4.4: An illustration of the trajectories T_0 and T_1

Therefore, there is a travelling wave $\Leftrightarrow$ T_0 and T_1 are the same trajectory. Next, we are going to show that trajectories T_0 and T_1 join. From (4.4.12), the eigenvector for T_0 at $(0,0)$ (see Figure 4.4) is

$$\Psi_1^- = \begin{pmatrix} 1 \\ \frac{\lambda_1^-}{D_u} \end{pmatrix}, \tag{4.6.2}$$

where

$$\lambda_1^- = \frac{-c - \sqrt{c^2 - 4D_u f'(0)}}{2}, \tag{4.6.3}$$

which clearly vary as c varies. A little algebra shows that

$\lambda_1^- \to -\infty$ as $c \to \infty$,

and

$\lambda_1^- \to 0$ as $c \to -\infty$.

The eigenvector for T_1 at $(1,0)$ is

$$\Psi_2 = \begin{pmatrix} \frac{c}{\gamma(1-\beta)} \\ 1 \end{pmatrix}. \tag{4.6.4}$$

Fix m $\in (0,1)$ and let P_0, P_1 be the values of P at which T_0 , T_1 hit the line $W =$ m. Then,

as $c \to \infty$, $\lambda_1^- \to -\infty$, thus $P_0 \to -\infty$ and $P_1 \to \infty$,

and

as $c \to -\infty$, $\lambda_1^- \to 0$, thus $P_0 \to \infty$ and $P_1 \to -\infty$.

Therefore, P_0 and P_1 are the same for exactly one value of $c \Longrightarrow$ there is a travelling wave for this speed only.

4.7 Uniqueness of the Wave Speed

In this section, we investigate the uniqueness of wave speed. We investigate the numerical solution for equation (4.3.1) with different initial condition, and phase plane for system (4.4.7).

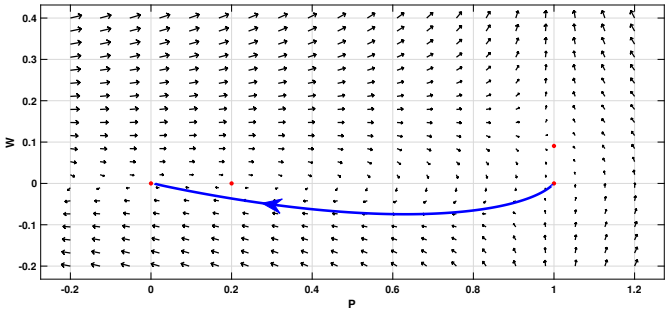

(a)

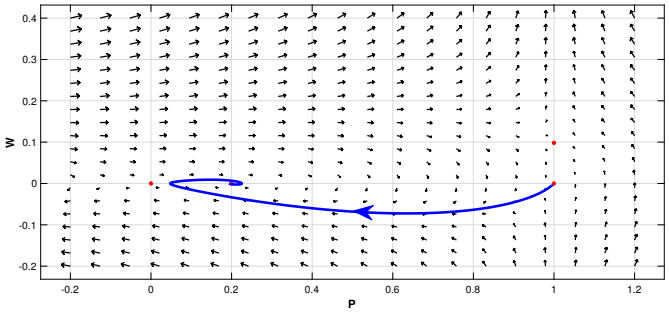

(b)

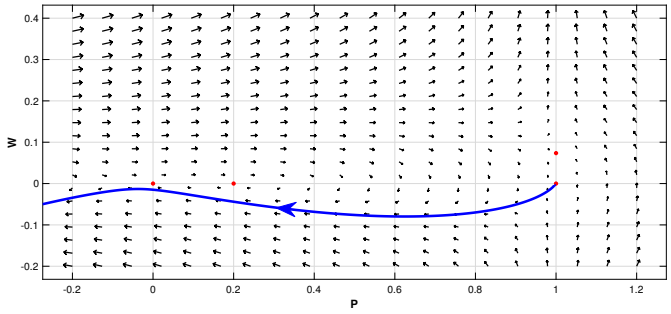

(c)

Figure 4.5: Phase portrait for system (4.4.7) with $D_u = 8.15$ and $\beta = 0.2$. Red circles denote equilibrium points. (a) $c = .7$ there is heteroclinic connection between two steady state $(1,0)$ and $(0,0)$. (b) $c = .8$ there is no heteroclinic connection between two steady state $(1,0)$ and $(0,0)$. (c) $c = .6$ there is no heteroclinic connection between two steady state $(1,0)$ and $(0,0)$.

As it can be seen in phase plane for system (4.4.7) in Figure 4.5 (a), there is trajectory

connection from $(1,0)$ to $(0,0)$ where $c = 0.7$, which mean travelling wave solution exist, and it shall be investigated numerically. From phase plane if c is increased or decreased, there is no trajectory connection from $(1,0)$ to $(0,0)$ (see Figure 4.5 (c,b)).

4.7.1 Numerical Result

Taking $\beta = 0.2$ which implies $\int_0^1 f(W)dW = 0.05 > 0$ and it bigger than $-\int_{-\infty}^{+\infty} D_u(1-W)\frac{d^2W}{dz^2}\frac{dW}{dz}dz = -(-0.0125) = 0.0125$ (numerically calculated), thus we have right waves $c > 0$. For this case we do simulation with different initial conditions using MATLAB (PDEPE). We start with step function Figure 4.6 (a).

By computing the position of a selected level point $(u = 0.5)$ on the solution profile and the velocity of moving boundary position Figure (b) in (4.6, 4.7,4.8), the speed is approximately $c = 0.7$, which is the slope of the line, and it is the same as the speed given by equation (4.5.5).

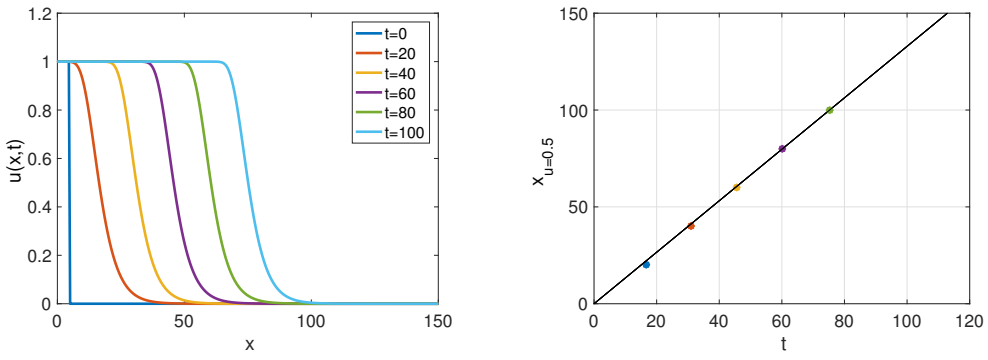

(a) (b)

Figure 4.6: (a) Solution of species u in (4.3.1) with step function as initil condition, times shown are $t = 0$ (blue), $t = 20$ (orange), $t = 40$ (yellow), $t = 60$ (purple), $t = 80$ (green), $t = 100$ (sky blue). (b) Selected level point $(u = 0.5)$ on the solution profile. Parameter values are shown in Table 4.4.

We solve equation (4.3.1) numerically with different initial condition (Figure 4.7, 4.8,(a)).

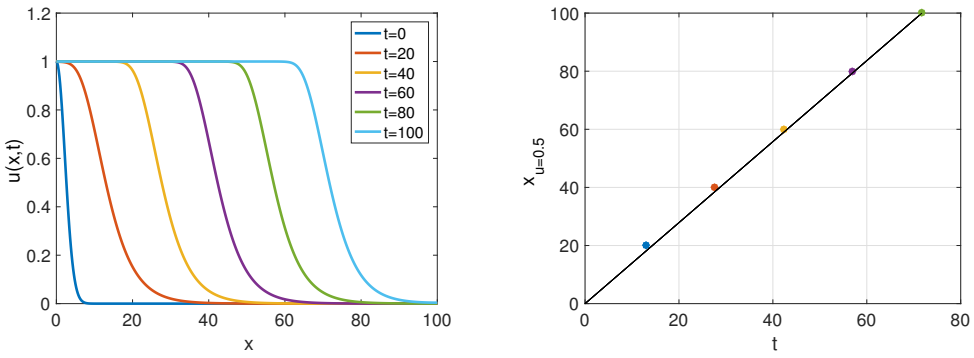

(a) (b)

Figure 4.7: (a) Solution of species u in (4.3.1) with $I.C = exp((-.1x^2))$, times shown are $t = 0$ (blue), $t = 20$ (orange), $t = 40$ (yellow), $t = 60$ (purple), $t = 80$ (green), $t = 100$ (sky blue). (b) Selected level point $(u = 0.5)$ on the solution profile. Parameter values are shown in Table 4.4.

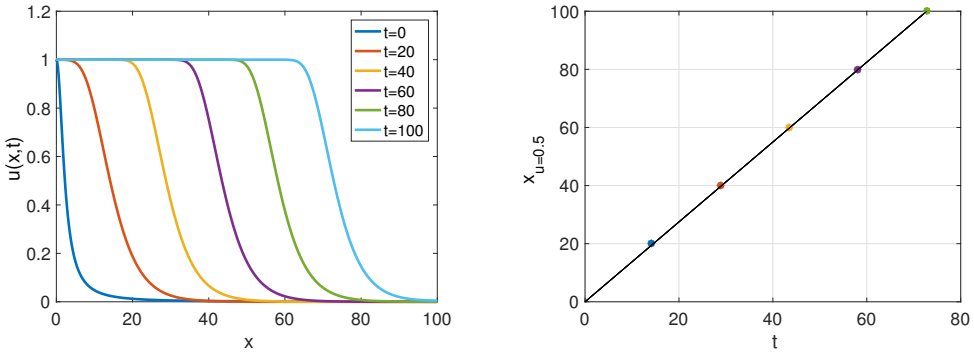

(a) (b)

Figure 4.8: (a) Solution of species u in (4.3.1) with $IC = 1 - (x^2/((5) + x^2))$, times shown are $t = 0$ (blue), $t = 20$ (orange), $t = 40$ (yellow), $t = 60$ (purple), $t = 80$ (green), $t = 100$ (sky blue). (b) Selected level point $(u = 0.5)$ on the solution profile. Parameter values are shown in Table 4.4.

Parameter	Value
β	0.2
γ	1
D_u	8.15

Table 4.4: Table showing the parameter values that used to solve equation (4.3.1).

From all numerical investigations as we started with different initial conditions we end up with same wave speed $c = 0.7$. This support the conjecture that the wave speed is unique.

With chosen parameters, if we take $\beta = 0.4$ implies $\int_0^1 f(W)dW = 0.0166$ and it is equal $-\int_{-\infty}^{+\infty} D_u(1-W)\frac{d^2W}{dz^2}\frac{dW}{dz}dz = -(-0.0166) = 0.0166$ (numerically calculated), so $c = 0$ (standing wave) (Figure 4.9). However, since the sign of c determine by $\int_0^1 f(W)dW$ in Nagumo's equation, thus taking $\beta = 0.4$ implies $c > 0$ (right wave). Phase plane for ODE system (4.4.7) with $c = 0$ is shown in Figure 4.10. We conclude that the non-linear diffusion affect the speed of travelling wave.

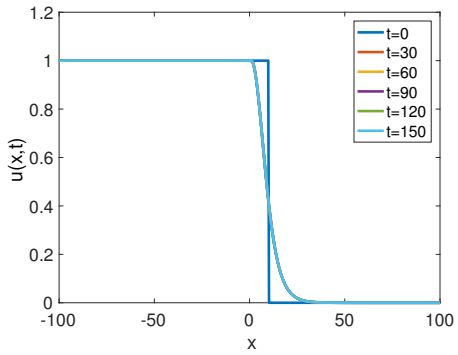

Figure 4.9: Solution of species u in (4.3.1). Times shown are $t = 0$ (blue), $t = 30$ (orange), $t = 60$ (yellow), $t = 90$ (purple), $t = 120$ (green), $t = 150$ (sky blue). Parameter values are shown in Table 4.5.

Parameter	Value
β	0.4
γ	1
D_u	8.15

Table 4.5: Table showing the parameter values that used to solve equation (4.3.1).

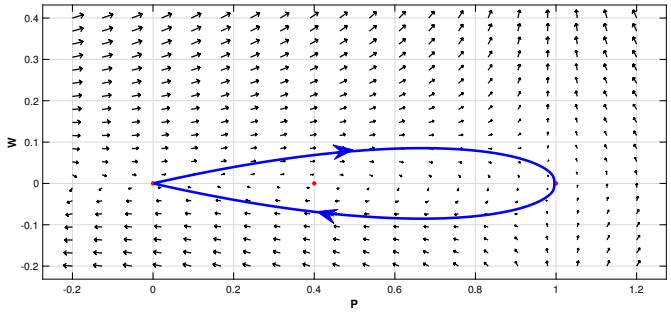

Figure 4.10: Phase portrait for system (4.4.7) with $c = 0$, $D_u = 8.15$ and $\beta = 0.4$. Red circles denote equilibrium points.

4.8 Moving and Standing Front Solution for Full Cross-Diffusion System

We have done a simple calculation for the scalar equation, and we compared equation (4.3.1) with Nagumo's equation. We showed that the sign of the travelling wave speed was affected by non-linear diffusion term in (4.3.1). We use this information in full system and solve tit numerically using step function as initial condition, taking $\beta = 0.2$ is resulting right travelling wave solution for species u see Figure 4.11, and taking $\beta = 0.4$ is resulting standing travelling wave solution for species u see Figure 4.12. We observe that species v is essentially uniform in space and tends to a constant $v \approx 0$

.

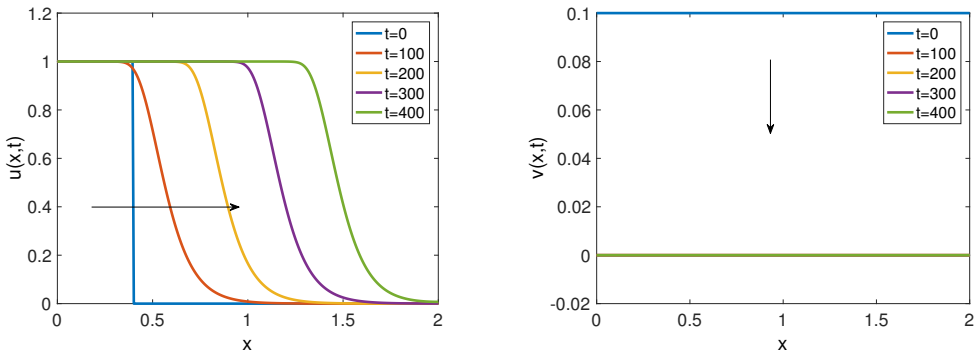

(a) (b)

Figure 4.11: Solution of species (a) u and (b) v in the full system (3.5.1). Times shown are $t = 0$ (blue), $t = 100$ (orange), $t = 200$ (yellow), $t = 300$ (purple), $t = 400$ (green). Parameter values are shown in Table 4.6.

Parameter	Value
β	0.2
δ	0.6
γ	0.2
D_u	0.0007
D_v	6

Table 4.6: Table showing the parameter values that used to solve system (3.5.1).

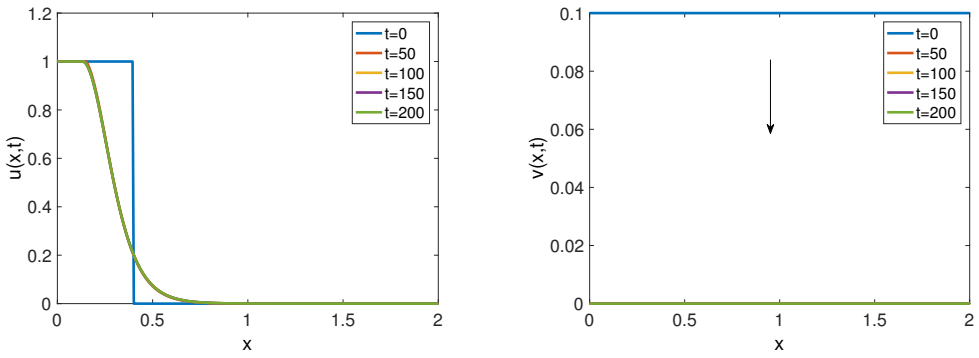

(a) (b)

Figure 4.12: Solution of species (a) u and (b) v in the full system (3.5.1). Times shown are $t = 0$ (blue), $t = 50$ (orange), $t = 100$ (yellow), $t = 150$ (purple), $t = 200$ (green). Parameter values are shown in Table 4.7.

Parameter	Value
β	0.4
δ	0.6
γ	0.2
D_u	0.0007
D_v	6

Table 4.7: Table showing the parameter values that used to solve system (3.5.1).

4.9 Conclusions

In this chapter, we derived a new non-linear cross-diffusion system for tightly packed particles based on mathematical modelling. An important feature of this model is that it leads to pattern formation where standard diffusion does not (see Chapter 3). We found out that this model can exhibit a moving front solution for u with certain parameter choices.

Then, the system was reduced to scalar equation (4.3.1) which is:

$$u_t = \nabla \cdot (D_u(1-u)\nabla u) + \gamma u(1-u)(u-\beta).$$

We investigated the travelling wave solution of this equation. Two highlighting features of this equation were non-linear diffusion and bistability of the kinetics term. We tried to understand how the travelling wave solution could be affected. In addition, it is similar to Nagumo's equation, so we also focused on the effect of non-linear diffusion term and what difference the non-linear diffusion term made to the travelling wave solution. It was proved by shooting method that there exists a travelling wave solution. We calculated the speed of travelling wave, and we established the uniqueness of the wave speed numerically. Most of the analysis showed similarity to Nagumo's equation, but the differences was in the wave speed . The wave speed for equation (4.3.1) depended on $\int_{-\infty}^{+\infty} D_u(1-W)\frac{d^2W}{dz^2}\frac{dW}{dz}dz$ and $\int_0^1 f(W)dW$ in contrast to Nagumo's equation, where it depended only in $\int_0^1 f(W)dW$. Therefore, the non-linear diffusion could change the speed. Using analysis and numerical simulations, we conclude that the non-linear diffusion affected the travelling wave solution and could change the speed's sign of travelling fronts compared to the standard diffusion in Nagumo's equation.

Chapter 5

Conclusions and Future Work

5.1 Conclusions

This thesis investigated cross-diffusion systems to better understand how they impact the formation and characteristics of patterns and fronts in reaction-diffusion systems. In particular, the mechanism of pattern formation and wave fronts. We discussed the derivation of cross-diffusion systems. We discussed the effect of cross-diffusion on pattern formation. In addition, we derived a new cross diffusion model, and we investigated the possible pattern formation and travelling waves solution for that model.

In Chapter 2, we investigated whether all cross-diffusion system of two interacting species can be derived from the following microscopic master equations

$$\frac{du_k}{dt} = \tau^+_{k-1}u_{k-1} + \tau^-_{k+1}u_{k+1} - (\tau^+_k + \tau^-_k)u_k,$$
$$\frac{dv_k}{dt} = \beta^+_{k-1}v_{k-1} + \beta^-_{k+1}v_{k+1} - (\beta^+_k + \beta^-_k)v_k,$$

where u_k is a biomass of u in the location x_k, and the biomass can move to the left or to the right to exit, with the transfer rate τ^-_k or τ^+_k, similarly for v_k. We considered

examples of cross-cross-diffusion models, and we found out that it is not easy to prove that the microscopic master equation (1.3.10) can be derived from all cross-diffusion systems of two interacting species.

In Chapter 3, We derived conditions for linear instability induced by cross-diffusion. We considered a class of cross- diffusion systems which has the form

$$u_t = \nabla.[D_{11}(u,v)\nabla u + D_{12}(u,v)\nabla v] + \gamma f(u,v),$$
$$v_t = \nabla.[D_{21}(u,v)\nabla u + D_{22}(u,v)\nabla v] + \gamma g(u,v).$$

We also focused on one type of kinetics where $f_u^o >$, $f_v^o < 0$, $g_u^o > 0$ and $g_v^o = 0$. We considered two examples of the cross-diffusion system, and we found out that cross-diffusion can induce instability where standard-diffusion could not, thus patterns can generate by cross-diffusion.

In Chapter 4, We derived a new non-linear cross-diffusion system for tightly backed particles from a mass-conservation perspective:

$$u_t = \nabla \,.\, (D_u(1-u)\nabla u - D_v u\nabla v),$$
$$v_t = \nabla \,.\, (D_v(1-v)\nabla v - D_u v\nabla u).$$

An important feature of this model is that it led to pattern formation. We found out that this model can exhibit a moving front solution for u with certain parameter choices. Then, the system was reduced to a scalar equation which is:

$$u_t = \nabla \,.\, (D_u(1-u)\nabla u) + \gamma u(1-u)(u-\beta). \tag{5.1.1}$$

Two highlighting features of this equation were non-linear diffusion and bistability of the kinetics term. We investigated a travelling wave solution of the scalar equation. We

showed that the sign of travelling wave speed was affected by the non-linear diffusion term. We conclude that the non-linear diffusion can affect the travelling wave solution and could alter the speed of travelling fronts compared to the standard case.

5.2 Future Work

In Chapter 2, we found out that it is not easy to prove that the microscopic master equation can be derived from all cross-diffusion system of two interacting species. However the approach in the inverse problem could likely be used to find jump probabilities which recover many other cross-diffusion systems. Also, the validity of the form of the jump probabilities given in (2.2.33) and (2.3.20) could be verified by comparing numerical solutions of master equation with those for the related PDE models (2.2.1) and (2.3.1), respectively (as is done for the SKT model and shown in Figure 2.1). The construction of a stable numerical code would form useful future work.

In Chapter 3, we found out that our new non-linear cross-diffusion model can induce patterns where standard-diffusion can not. In the future, we can investigate other cases, such as how the non-linear cross-diffusion affects unstable steady state with self-diffusion (Turing instability).

In Chapter 4, we proved that the right travelling wave solution exits via a shooting method. However, we did not investigate the left travelling wave case. It would be interesting to attempt to prove this case. We obtain some numeric results of the left travelling wave solution as follows.

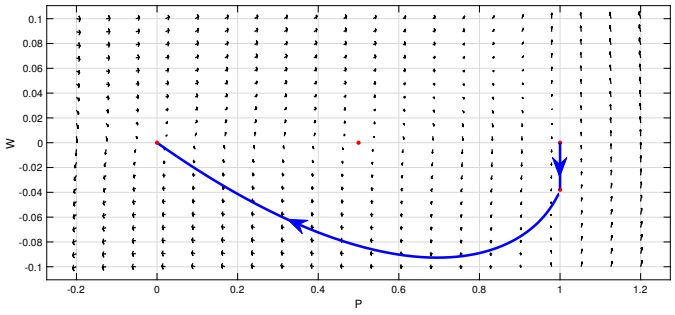

Figure 5.1: Phase portrait for system (4.4.7) with $c = -0.3$, $D_u = 8.15$ and $\beta = 0.5$. The green highlighted curve is heteroclinic connection between two steady state $(1,0)$ and $(0,0)$. Red circles denote equilibrium points.

In the Phase plane of ODE system (4.4.7) with $c < 0$ (see Figure 5.1), we observe that the trajectory that connect steady states $(1,0)$ and $(0,0)$ go through the steady state $(1, \frac{c}{D_u})$ which form non-smooth front, this can be observed in Figure 5.2).

We do numerical simulation where $\beta = 0.5$ so $\int_0^1 f(W)dW = 0$ and since $\int_{-\infty}^{+\infty} D_u(1-W)\frac{d^2W}{dz^2}\frac{dW}{dz}dz = -0.0200 < 0$ (numerically calculated for chosen parameters), so $c < 0$ we get left wave (see Figure 5.2).

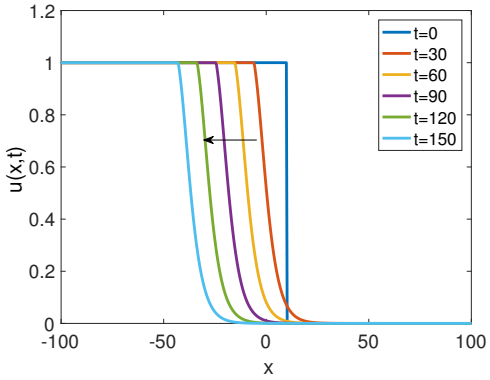

Figure 5.2: Solution of species u in (4.3.1). Times shown are $t = 0$ (blue), $t = 30$ (orange), $t = 60$ (yellow), $t = 90$ (purple), $t = 120$ (green), $t = 150$ (sky blue). Parameter values are shown in Table 5.1.

Parameter	Value
β	0.5
γ	1
D_u	8.15

Table 5.1: Table showing the parameter values that used to solve equation (4.3.1).

Appendix A

Appendix A

A.1 More Background of Travelling Wave

By definition, a travelling wave moves in a certain direction while retaining a fixed shape. Furthermore, the speed of the travelling wave remains constant through out the duration of its propagation. Examples of travelling waves can be found in models for a range of applications such as combustion [98], movement of species [64] and fluid dynamics [82].

Definition 1. *(See e.g. [64]) A travelling wave is a solution of a partial differential equation with a constant profile (shape) and a constant propagation speed.*

A.1.1 Classes of Travelling Waves

- Travelling pulse: $u(x,t) \to a$ as $x \to \pm\infty$
- Travelling front : $u(x,t) \to a$ as $x \to -\infty, u(t,x) \to b$ as $x \to +\infty$, and $a \neq b$
- Periodic travelling wave. (See Figure A.1.)

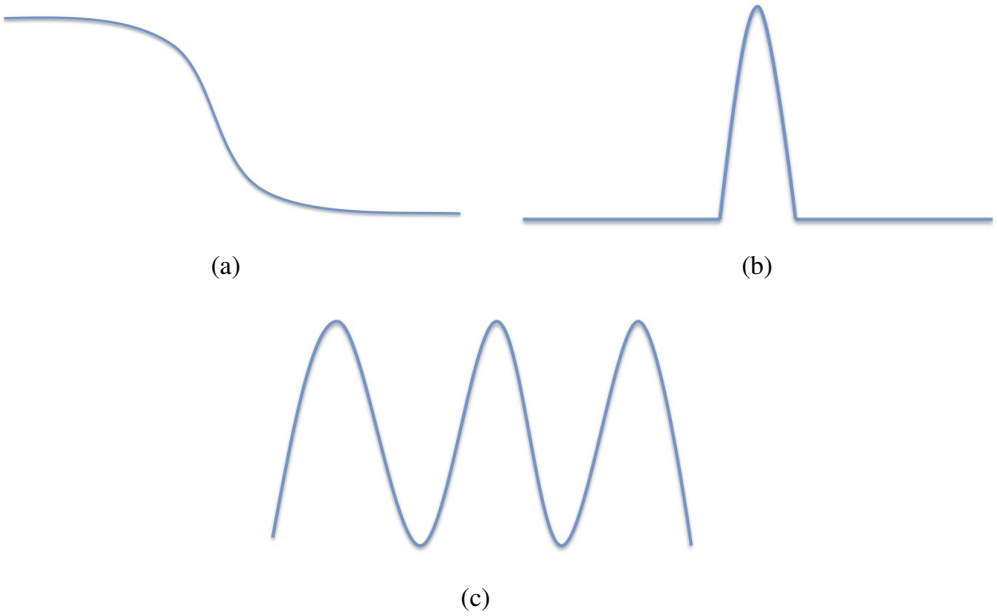

Figure A.1: Forms of travelling waves: (a) wave front, (b) pulse and (c) Periodic travelling wave.

A PDE's travelling wave solution can be presented in the form $u(x,t) = W(z)$, where $z = x - ct$, and $c > 0$, depicts a wave travelling from left to right. The partial derivative of u can calculated as following

$$\frac{\partial u}{\partial t} = \frac{dW}{dz}\frac{\partial z}{\partial t} = -c\frac{dW}{dz}, \tag{A.1.1}$$

and

$$\begin{aligned} \frac{\partial u}{\partial x} &= \frac{dW}{dz}\frac{\partial z}{\partial x} = \frac{dW}{dz}, \\ \frac{\partial^2 u}{\partial x^2} &= \frac{d^2W}{dz^2}\left(\frac{\partial z}{\partial x}\right)^2 + \frac{dW}{dz}\frac{\partial^2 z}{\partial x^2} = \frac{d^2W}{dz^2}. \end{aligned} \tag{A.1.2}$$

A.1.2 Fisher's and Nagumo's Equations

This section covers some well-known properties of simpler reaction-diffusion (R-D) systems. Simplest form of R-D equation in one dimension that represents the travelling wave behaviour can be expressed mathematically as

$$u_t = u_{xx} + f(u), \tag{A.1.3}$$

where u is the concentration, $f(u) = ru(1-u)$ represents the kinetics.

Equation (A.1.3) with $f(u) = ru(1-u)$ is called Fisher's equation, which is known to have monotone travelling wave solution joining $u = 1$ at $x = -\infty$ to $u = 0$ at $x = \infty$ for wave speeds of $c \geq c_0 = 2$ (in terms of the original dimensional equation, the range of wavespeeds satisfies $c_0 = 2\sqrt{rD}$). It is known that rapidly decaying initial data as $x \longrightarrow \infty$ results asymptotically to a wave with minimum speed c_0. Figure A.2 (a) is a solution of Fisher's equation which shows right travelling wave solution, and (b) is phase plane with trajectory connecting $(1,0)$ and $(0,0)$ (phase plane for ODE system obtained by travelling wave analysis for Fisher' equation see [64]. Note two features of Fisher's equation; first that the wave moves the system from unstable to a stable state as expected, second the minimum speed of wave is the function of D, which is the motility parameter. For more details on the analysis of Fisher's equation see [64].

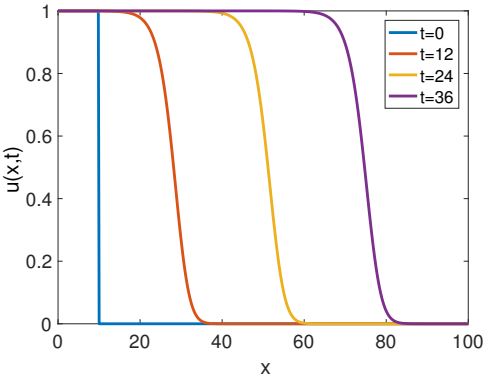

(a)

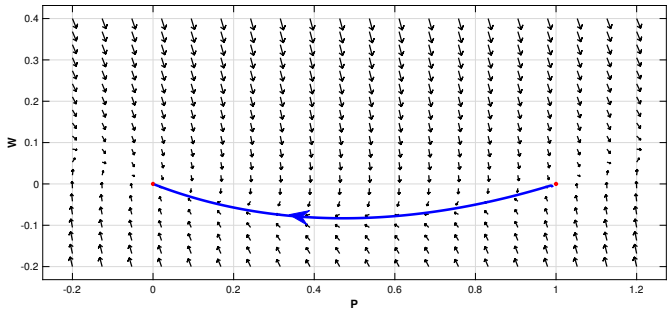

(b)

Figure A.2: (a) Solution of species u for Fisher's equation with a step function as initial condition, Times shown are $t = 0$ (blue), $t = 12$ (orange), $t = 24$ (yellow), $t = 36$ (purple). (b) Phase portrait for Fisher's equation with $c = 3$ where the green highlighted curve shows the heteroclinic connection between $(1,0)$ and (0.0) and red circles denote equilibrium points.

Supposing now that $f(u) = u(1-u)(u-\beta)$, $0 < \beta < 1$, transforms the equation (A.1.3) into Nagumo's equation or bistable Fisher equation. It is called bistable because the associate ODE $\frac{du}{dt} = u(1-u)(u-\beta)$ has two uniform stable steady states $u = 0, 1$, while $u = \beta$ is an unstable state. Figure A.3 (a) is a solution of Nagumo's shows right travelling wave solution. Phase plane with trajectory connecting $(1,0)$ and $(0,0)$ (phase plane for ODE system obtained by travelling wave analysis for Nagumo's equation) is shown in Figure A.3(b). It is an established and well known fact that in the bistable case, there exists a unique travelling wave with speed c. The sign is determined by the

sign of the integral of reaction function over a certain interval (see [23]). For Nagumo's equation, a formula provides the unique wave speed value and the sign from which the direction of wave can be determined, namely, (see e.g. [99]),

$$c = \frac{\int_0^1 f(U)dU}{\int_{-\infty}^{\infty}[U']^2 dz}. \tag{A.1.4}$$

Since $\int_{-\infty}^{\infty}[U']^2 dz > 0$, we conclude that $\int_0^1 f(U)dU$ determines the sign of c

$$\begin{aligned} \int_0^1 f(u)du > 0 \quad &\Longrightarrow \quad c > 0, \\ \int_0^1 f(u)du = 0 \quad &\Longrightarrow \quad c = 0, \\ \int_0^1 f(u)du < 0 \quad &\Longrightarrow \quad c < 0, \end{aligned}$$

which means we can have right $c > 0$, left $c < 0$ or standing $c = 0$ travelling wave.

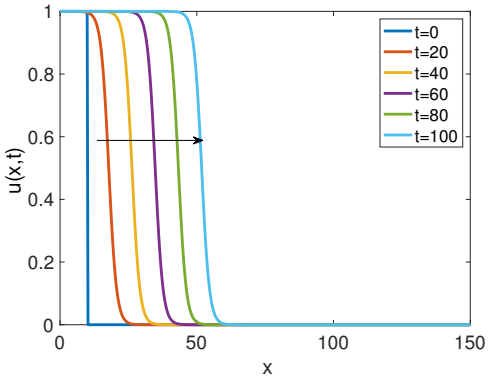

(a)

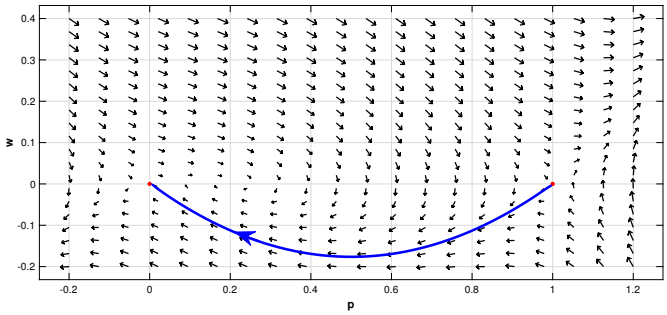

(b)

Figure A.3: (a) Solution of species u for Nagumo's equation with a step function as initial condition, times shown are $t = 0$ (blue), $t = 20$ (orange), $t = 40$ (yellow), $t = 60$ (purple), $t = 80$ (green), $t = 100$ (sky blue). (b) Phase portrait for Nagumo's equation with $c = .426$ where the green highlighted curve shows the heteroclinic connection between $(1,0)$ and (0.0) and red circles denote equilibrium points. Reaction parameter values $\beta = 0.2$.

A.2 Predator-Prey System with Allee Effect

We consider the following model of predator-prey interaction in a homogeneous environment, and it is just example of reaction kinetics for which it is known that they are stable to standard-diffusion. The model of predator-prey with standard-diffusion is

$$\begin{aligned}\frac{\partial H(X,T)}{\partial T} &= D_1\frac{\partial^2 H}{\partial X^2} + F(H) - f(H,P),\\ \frac{\partial P(X,T)}{\partial T} &= D_2\frac{\partial^2 P}{\partial X^2} + \kappa f(H,P) - MP.\end{aligned} \tag{A.2.1}$$

Here, H and P are the densities of prey and predator, respectively, at time T and position X. D_1 and D_2 are diffusivities and is the food utilization coefficient. The function $F(H)$ describes prey multiplication, $f(H,P)$ describes predation, and the term MP stands for predator mortality. To keep the model as simple as possible, we assume that $f(H,P) = AHP$, where A is the predation rate, which corresponds to the classical Volterra scheme. Assuming Allee dynamics for the prey population, its growth rate can be written as (see [47, 62, 69]).

$$F(H) = \frac{4\omega}{(K-H_0)^2}H(H-H_0)(K-H). \tag{A.2.2}$$

Equations (A.2.1) and (A.2.2) contain a large number of parameters, which makes their numerical investigation cumbersome. However, by choosing appropriate scales for the variables following [62], the number of parameters can be lessened. Considering dimensionless variables $u = H/K$, $v = P/(\kappa K)$, $t = aT$, $x = X(a/D_1)^{1/2}$, where $a = A\kappa K$.

From equations (A.2.1) and (A.2.2), we obtain

$$\begin{aligned}\frac{\partial u(x,t)}{\partial t} &= \frac{\partial^2 u}{\partial x^2} + \gamma u(u-\beta)(1-u) - uv,\\ \frac{\partial v(x,t)}{\partial t} &= d\frac{\partial^2 v}{\partial x^2} + uv - \delta v,\end{aligned} \tag{A.2.3}$$

where $\beta = H_0/K$, $\gamma = 4\omega K(A\kappa(K-H_0)^2)$, $\delta = M/a$ and $d = D_2/D_1$.

A.2.1 Linear Stability Analysis of the Associates ODE

In this section, we would like to do stability analysis of system (A.2.3). First, we consider the associate ODE:

$$\begin{aligned} \frac{du}{dt} &= \gamma u(u-\beta)(1-u) - uv, \\ \frac{dv}{dt} &= uv - \delta v, \end{aligned} \tag{A.2.4}$$

where $u(t)$ is the prey density, $v(t)$ is the predator density; $0 < \beta < 1$ corresponds to the strong Allee effect, and assume $\gamma > 0$ and $\delta > 0$.

The steady states (u_0, v_0) of system (A.2.4), are solutions of $\frac{du}{dt} = \frac{dv}{dt} = 0$ which are

$$(u_0, v_0) = (0,0),\ (u_0, v_0) = (1,0),\ (u_0, v_0) = (\beta, 0),\ (u_0, v_0) = (\delta, \gamma(\delta-\beta)(1-\delta)). \tag{A.2.5}$$

Following standard theory (see e.g. [8, 64, 96, 100]), the linear asymptotic stability of the steady states (A.2.5) is determined by the eigenvalues of the Jacobian matrix we have:

$(u_0, v_0) = (0,0)$ is stable, $(u_0, v_0) = (1,0)$ is unstable, $(u_0, v_0) = (\beta, 0)$ is unstable and $(u_0, v_0) = (\delta, \gamma(\delta-\beta)(1-\delta))$ is stable if $0 < \beta < \delta < 1$ and $\frac{\beta+1}{2} < \delta < 1$,

The only nontrivial steady state is $(u_0, v_0) = (\delta, \gamma(\delta-\beta)(1-\delta))$ of kinetic system (A.2.4). We test the stability numerically to support the analysis, we start around the steady state $(u_0, v_0) = (\delta, \gamma(\delta-\beta)(1-\delta))$ and observe that the solution return back to steady state which support our analytical result that the steady state is stable see Figure A.4 (a). This is just an example, and similar behaviour is observed with different initial data. In addition, we start around the steady state $(u_0, v_0) = (\delta, \gamma(\delta-\beta)(1-\delta))$ with different parameter value where the condition $0 < \beta < \delta < 1$ is not hold and observe

that the steady state is unstable see Figure A.4 (b). Next, we investigate the effect of standard diffusion.

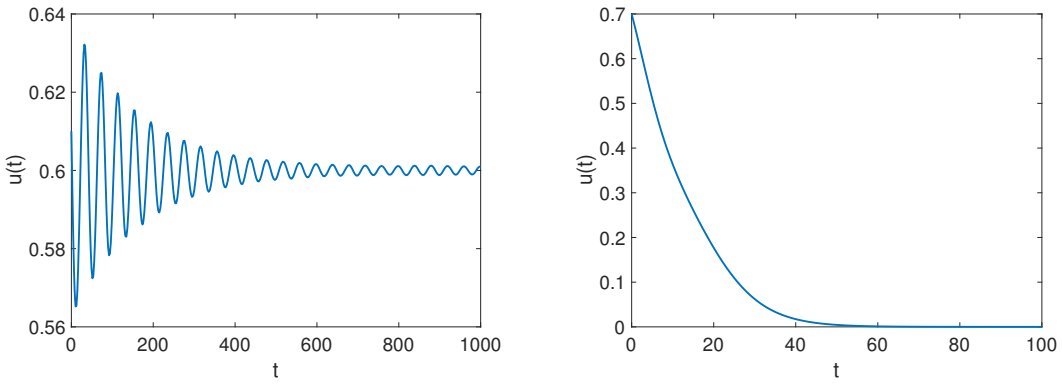

(a) (b)

Figure A.4: (a) The solution $u(t)$ of system (A.2.4) with parameter values $\gamma = 0.2$, $\delta = 0.6$ and $\beta = 0.1$ which shows that the steady states $(u_0, v_0) = (\delta, \gamma(\delta - \beta)(1 - \delta))$ is stable. (b) The solution $u(t)$ of system (A.2.4) with parameter values $\gamma = 0.2$, $\delta = 0.6$ and $\beta = 0.7$ which shows that the steady states $(u_0, v_0) = (\delta, \gamma(\delta - \beta)(1 - \delta))$ is unstable.

A.2.2 Standard Diffusion Does Not Generate Patterns

In previous section, we showed that the steady state of ODE system (A.2.4) $(u_0, v_0) = (\delta, \gamma(\delta - \beta)(1 - \delta))$ is stable. In this section, we investigate it with standard diffusion and see the pattern can occur or not.

By the similar calculation in previous chapter, the dispersion relation associated with the standard diffusion (A.2.3) is

$$\lambda^2 + \lambda \overbrace{\left[k^2[1+d] - [f_u + g_v]\right]}^{c} + \overbrace{dk^4 - (df_u + g_v)k^2 + |A|}^{h(k^2)} = 0. \tag{A.2.6}$$

We already go through stability analysis for reaction-diffusion system in Chapter 3, and we introduce necessary conditions for diffusion driven instability. We show that one of necessary condition ($(df_u + g_v) > 0$) which does not hold for kinetic (A.2.4) :

$$(df_u + g_v) = -d\gamma u_0(2u_0 - (\beta + 1)) = -d\gamma\delta(2\delta - (\beta + 1)).$$

Since $\frac{\beta+1}{2} < \delta < 1$, we have

$$(df_u + g_v) < 0.$$

We conclude that linear instability does not occur with standard diffusion. We solve system (A.2.3) numerically and it supports our analytical result that the steady state is stable (see Figure A.5). Here, the first mode is tested, and similar behaviour is observed for any modes.

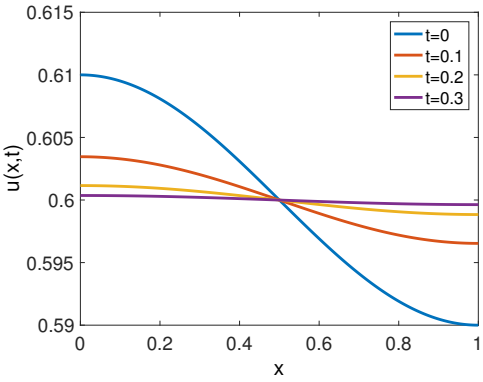

(a)

Figure A.5: Solution of species u in (A.2.3). Times shown are $t = 0$ (blue), $t = 0.1$ (red), $t = 0.2$ (yellow), $t = 0.3$ (purple). Reaction parameter values $\gamma = 0.2$, $\delta = 0.6$, $\beta = 0.1$ and $d = .7$, with initial condition $I.C = 0.6 + .1cos(\pi x)$.

A.3 Calculation Steps

Solution's step for equation (2.3.16).

$$h_1' = h_1\left(\frac{\lambda_1 \bar{D}_u (1-u)}{2\bar{D}_v u \lambda_2} - \frac{1}{2u}\right). \tag{A.3.1}$$

$$\int \frac{dh_1}{h_1} = \int \left(\frac{\lambda_1 \bar{D}_u (1-u)}{2\bar{D}_v u \lambda_2} - \frac{1}{2u}\right) du. \tag{A.3.2}$$

$$\ln h_1 = \int \left[\frac{\lambda_1 \bar{D}_u}{2\bar{D}_v \lambda_2}\left(\frac{1-u}{u}\right) - \left(\frac{1}{2u}\right)\right] du. \tag{A.3.3}$$

$$\ln h_1 = \frac{\lambda_1 \bar{D}_u}{2\bar{D}_v \lambda_2}(\ln u - u) - \frac{1}{2}\ln u + \ln c_1. \tag{A.3.4}$$

Note that $\frac{1}{2}\ln u = \ln u^{\frac{1}{2}} = \ln \sqrt{u}$.

$$\ln\left(\frac{h_1\sqrt{u}}{c_1}\right) = \frac{\lambda_1 \bar{D}_u}{2\bar{D}_v \lambda_2}(\ln u - u). \tag{A.3.5}$$

$$\frac{h_1\sqrt{u}}{c_1} = e^{\left(\frac{\lambda_1 \bar{D}_u}{2\bar{D}_v \lambda_2}(\ln u - u)\right)}. \tag{A.3.6}$$

$$h_1(u) = \frac{c_1}{\sqrt{u}} e^{\frac{\bar{D}_u \lambda_1 (-u + \ln u)}{2\bar{D}_v \lambda_2}}, \tag{A.3.7}$$

Appendix B

Numerical Simulations: MATLAB Codes

B.1 Matlab Code to Solve Equation (1.3.10)

We use this code in section 2.1 to plot Figure 2.1.

```
% Computes the right-hand side
function dx = RHS1(t,x, gamma,n)
    %x=x';
%     n = length(x) /2;

%     % Split the vector x into u and v
%     u = x(1:n);
%     v = x(1,n+1:2*n);
%     p1 = @(u,v) 1;
%     p2 = @(u,v) 0.7071;
```

```
%     q1 = @(u,v) 0.7071*v;
%     q2 = @(u,v) 0.7071*u;
    q1=1; p1=1; q2=1; p2=1;
    % Initialize derivative vectors, tau's and beta's
    du = zeros(n,1);
    dv = zeros(n,1);

    tm = zeros(n,1);          % tau^-
    tp = zeros(n,1);          % tau^+

    bm = zeros(n,1);          % beta^-
    bp = zeros(n,1);          % beta^+

    % tau's and beta's as in  (2.2.2)
    for k=1:n
        % Boundary values
        if k==1
            tp(k) = gamma * q1 * x(n+k) * p1;
            tm(k) = 0;  % is tau^-_0
            bp(k) = gamma * q2 * x(k) * p2;
            bm(k) = 0;  % is beta^-_0
        elseif k == n
            tp(k) = 0;  % is tau^+_n
            tm(k) = gamma * q1 * x(k) * p1;
            bp(k) = 0;
            bm(k) = gamma * q2 * x(k) * p2;
        else
```

```
        tp(k) = gamma * q1 * x(n+k) * p1;
        tm(k) = gamma * q1 * x(n+k) * p1;
        bp(k) = gamma * q2 * x(k) * p2;
        bm(k) = gamma * q2 * x(k)* p2;
    end
end

% Computation of the derivatives by (2.2.1)
for k=1:n
    if k==1     % Since tau^-_1 = 0, the first term
        is missing
        du(k) = tm(k+1)*x(k+1)-(tm(k)+tp(k))*x(k);
        dv(k) = bm(k+1)*x(n+k+1)-(bm(k)+bp(k))*x(n+
           k);
    elseif k == n % Since tau^+_{n+1} = 0, the
       second term is missing
        du(k) = tp(k-1)*x(k-1) -(tm(k)+tp(k))*x(k);
        dv(k) = bp(k-1)*x(n+k-1) -(bm(k)+bp(k))*x(n
           +k);
    else
        du(k) = tp(k-1)*x(k-1) + tm(k+1)*x(k+1)-(tm
           (k)+tp(k))*x(k);
        dv(k) = bp(k-1)*x(n+k-1) + bm(k+1)*x(n+k+1)
           -(bm(k)+bp(k))*x(n+k);
    end
end
```

```
    dx = [du ; dv];
    %size(dx)
end

%  parameters
close
gamma = 1;
n =301;
m = (n-1)/2+1;

%  functions p1, q1, p2, q2
% To test I take them constants
% p1 = @(u,v) 0.7071;
% p2 = @(u,v) 0.7071;
% q1 = @(u,v) 0.7071*v;
% q2 = @(u,v) 0.7071*u;

% Starting values u_i=0 v  i-(n+1)/2
u0 = zeros(n,1);
v0 = zeros(n,1);
for i=1:n
    u0(i) =floor(100*exp(-1*(i-20)^2));
    v0(i)=u0(i);
end
% Starting values v_i=0, except v_m=100
% u0 = zeros(n,1);
% v0 = zeros(n,1);
% v0(m) =100;
```

```
x0 = [u0 ; v0];

% Final time
tmax = 1;

% Produce the solution
[t,x] = ode45(@(t,x) RHS1(t,x, gamma,n), [0,tmax], x0);

% % Plot u an v
% figure(1)
% plot(t,x);

% Plot u
figure(1)
plot(x(1,1:n),'LineWidth',5)
hold on
plot(x(98,1:n),'LineWidth',5)
hold on
plot(x(132,1:n),'LineWidth',5)
hold on
plot(x(157,1:n),'LineWidth',5)
hold on
plot(x(end,1:n),'LineWidth',5)
xlim([5 35])
 xlabel('k','Color','k')
ylabel('u(t)','Color','k')
  set(gca,'FontSize',20)
```

```
% Plot v
% figure(3)
% plot(x(1,n+1:2*n));




% Plot u
figure(4)
plot(x(end,1:n),'LineWidth',7)
xlim([5 35])
 xlabel('k','Color','k')
ylabel('u(t)','Color','k')
  set(gca,'FontSize',20)
```

B.2 Matlab Code to Solve Equation (1.3.2)

We use this code in section 1.3 to plot Figures 1.2, 1.3.

```
close all;clear;


n=100; %number of time  steps;
nwalks=5000; % number of particles
```

```
 %Define an array of uniformly distributed jumps at
    each time step for each particle.
 %x = sing(x) ensures that x is an
 %array of +1 and -1 (right and left jumps resp). Each
    column represents a
 %walker and each row is the jump made by that walke
    rat the specified time
 %step

 alpha = .7;

x = (rand(n,nwalks) - alpha.*ones(n,nwalks));


x=sign(x); %if sign of x postive give 1 if it negative
   give -1

% % At t=0, all particles are at 0.
 x=[zeros(1,nwalks);x(1:end-1,:)];

% Take the cumulative sum of x in the  "row" direction
   (i.e. down each
% column) z is now an array the columns of which
   contain the location of
% each particle at all times reading from t=0 at the
   top to t= n at the
% bottom
```

```
z=cumsum(x,1);

% Compute the average value
z_mean=mean(z,2);



% plot all walks

figure(1)
h=plot(z,0:n-1,'Color', [0.7 0.7 0.7]);
hold on;
%  plot the mean walk
 hmean=plot(z_mean,0:n-1,'b','LineWidth',1.5);

% hold on;0
%  h1=plot((z(1,:)),1:100,'k');
 hold on;
 h2=plot((z(:,50)),0:n-1,'r');
legend([hmean,h2],'Mean','Example Trajectory')
ylabel('Time t')

hold off
```

```
%Generate histogram at time 50
figure(3)
histogram(z(50,:));
%
```

B.3 Matlab Code to Plot the Dispersion Relation

We use this code to plot the dispersion relations in this thesis, and the parameters values generate Figure (3.2) in section 3.4.

```
dd1= [1];%1
dd2=[.313]; %  dv
dd3=[.313];% du
dd4= [.1];% d


% paramters
delta=.6;
gam=1;
beta=.1;



% steady statee
ustar=delta; %u0
 vstar=gam*(delta-beta)*(1-delta); %v0
```

```
 %Jacupain
fu= -gam*ustar*(2*ustar-(beta+1));
fv=-ustar;
gu= vstar;
gv=0;



 ddc=[8.5,1.5625,1.565];
k=linspace(0,100,10000);


for j=1:length(dd4)
    d4=dd4(j);
    d3=dd3(j);
    d2=dd2(j);
    d1=dd1(j);
     dc=ddc(j);
%    lab{j}=sprintf('d1=%.2f,d2=%.2f,d3=%.3f,d4=%.2f,dc
   =%.2f',d1,d2,d3,d4,dc);

    G=@(k)k^2*(d1+d4)-gam*(fu+gv);
    h=@(k)k^4*(d1*d4-d3*d2)-gam*(d4*fu+d1*gv-d3*fv-d2*
       gu)*k^2+gam^2*(fu*gv-fv*gu);
```

```
    pc=@(k)roots([1,(k^2*(d1+d4)-gam*(fu+gv)),k^4*(d1*
       d4-d3*d2)-gam*(d4*fu+d1*gv-d3*fv-d2*gu)*k^2+gam
       ^2*(fu*gv-fv*gu)]);

    %Compute some values for plotting
    for i=1:length(k)
        lam_k(j,i)=max(real(pc(k(i))));
         h_k(j,i)=h(k(i));
         G_k(j,i)=G(k(i));
    end
end
cond1=fu+gv;
cond2=fu*gv-fv*gu;
cond3=(d1*d4-d3*d2);
cond4=(d4*fu+d1*gv-d3*fv-d2*gu)
cond5=(d4*fu+d1*gv-d3*fv-d2*gu)^2-4*(fu*gv-fv*gu)*(d1*
   d4-d3*d2);


figure(1);
plot(k.^2,lam_k,k([1,end]),[0,0],'k--','LineWidth',3)
%    ylim([-10 30])
               xlim([0 80])
%   legend(lab{:})
%  legend('d<dc','d=dc','d>dc');
xlabel('k^2','FontSize',16)
ylabel('Re \lambda(k^2)','FontSize',16)
```

```
% title('Plot of the eigenvalue Re\lambda(k^2)')
set(gca,'FontSize',20)
figure(2)
plot(k.^2,h_k,k([1,end]),[0,0],'k--','LineWidth',3)
%   ylim([-10 65])
       xlim([0 80])
%  legend(lab{:});
%  legend('d<dc','d=dc','d>dc');
xlabel(' k^2','FontSize',16)
ylabel('H(k^2)','FontSize',16)
% title('Plot of H(k^2).')

set(gca,'FontSize',20)
```

B.4 PDEPE

PDEPE is MATLAB function that solve initial-boundary value problems for parabolic-elliptic PDEs in 1-D. We use it to solve all the partial differential equations in this thesis. For example this code used to solve the new non-linear cross-diffusion system.

```
function []=CDpde()
m=0;
xmax=1;
tmax=152;
xstep=200;
tstep=5;
x=linspace(0,xmax,xstep);
```

```
t=linspace(0,tmax,tstep);
%parameters
global d1;
global d2;
global d3;
global d4;
global ri;
global di;
global dm,
global rm;
global beta;
global alpha;
global A;
global B;
global C;
global D;

global kk;
global a;
global b;
global cc;


global gam;
global sig;
global mu;
global rho;
```

```
global p;



%%Yahong model a
global delta;
global gam;
global beta;


% %%pp with alle effect
delta=.6;
gam=.2;
beta=.4;



d1=0.0007;  %du
d2=6;  %dv
d3=6;  %dv
d4=0.0007 ; %du


 options=odeset('RelTol',1e-6,'AbsTol',1e-6);
sol=pdepe(m,@CDfun,@CDinitial,@CDbc,x,t,options);
u=sol(:,:,1);
v=sol(:,:,2);
```

```
% plot u

figure(1);

plot(x,u,'LineWidth',3);
  lgd = legend(['t=' num2str(t(1))],['t=' num2str(t(2))
     ],['t=' num2str(t(3))],['t=' num2str(t(4))],['t='
     num2str(t(5))]);
 xlabel('x','Color','k')
ylabel('u(x,t)','Color','k')
  set(gca,'FontSize',20)

% plot v

figure(2);
plot(x,v,'LineWidth',3);
  lgd = legend(['t=' num2str(t(1))],['t=' num2str(t(2))
     ],['t=' num2str(t(3))],['t=' num2str(t(4))],['t='
     num2str(t(5))]);
 xlabel('x','Color','k')
ylabel('v(x,t)','Color','k')
  set(gca,'FontSize',20)
% %   annotation('arrow', [.2 .2], [.25 .45]);
%  annotation('arrow', [.5 .5], [.8 .6]);
```

```
% % plot of derivative of soln
%  figure(5)
%  plot(x,dif_1,'LineWidth',3)
%  xlabel(' x')
% ylabel('^{du}/_{dx}','Color','k')
%   set(gca,'FontSize',20)
%
%
%   figure(6)
%  plot(x,dif_2,'LineWidth',3)
%  xlabel(' x')
% ylabel('^{du}/_{dx}','Color','k')
%   set(gca,'FontSize',20)
%
%   figure(7)
%  plot(x,dif_3,'LineWidth',3)
%  xlabel(' x')
% ylabel('^{du}/_{dx}','Color','k')
%   set(gca,'FontSize',20)
%
%   figure(8)
%  plot(x,dif_4,'LineWidth',3)
%  xlabel(' x')
% ylabel('^{du}/_{dx}','Color','k')
%   set(gca,'FontSize',20)

function [c,f,s]=CDfun(x,t,u,DuDx)
```

```
%function
global d1;
global d2;
global d3;
global d4;
global beta;
global alpha;
global A;
global B;
global C;
global D;

global kk;
global a;
global b;
global cc;

%%%shi model
global gam;
global sig;
global mu;
global rho;
global p;


%%Yahong model a
global delta;
```

```
global gam;
global beta;


c=[1;1];

%simple c-d flux
%    f=[d1*DuDx(1)+d2*DuDx(2);d4*DuDx(2)+d3*DuDx(1)];

%non-linear c-d flux
f=[d1*(1-u(1))*DuDx(1)-d2*u(1)*DuDx(2);d3*(1-u(2))*DuDx
   (2)-d4*u(2)*DuDx(1)];

%reaction term
        s=[gam*u(1)*(u(1)- beta)*(1-u(1))-u(1)*u(2);u(1)
           *u(2)-delta*u(2)];

function value=CDinitial(x)









% % % % small pret
 u0=.6+.1*(cos(1*pi*x));

v0=.0160+.0001*(cos(1*pi*x));
```

```
 value=[u0;v0];
```

```
%   step function
%  value=[1;.1];
%  if ((x >.5) && (x>.7));
%    value = [0,.1];
%  end;

 function [pl,ql,pr,qr]=CDbc(xl,ul,xr,ur,t)

 %no flux
pl=[0;0];
ql=[1;1];
pr=[0;0];
qr=[1;1];
```

B.5 Pplane Tool

The pplane [24] is software that allows the user to utilize a graphical interface to plot direction fields for differential equations. Instead of defining array vectors of all points in the range of the desired differential equation graph, a user can simply enter their equations in the software, determine the desired range to graph, and the shape of the arrow. This MATLAB package was written and developed by the professor of Rice

University John C. Polking. He made this software free for use in educational institutions [37].

Bibliography

[1] K. Anguige and C. Schmeiser. A one-dimensional model of cell diffusion and aggregation, incorporating volume filling and cell-to-cell adhesion. *Journal of Mathematical Biology*, 58(3):395, 2009.

[2] D. G. Aronson. Density-dependent interaction-diffusion. In *Dynamics and Modelling of Reactive Systems: Proceedings of an Advanced Seminar Conducted by the Mathematics Research Center, the University of Wisconsin-Madison, October 22–24, 1979*, number 44, page 161. Academic Press, 2014.

[3] V. L. Avila. *Biology: Investigating life on earth*. Jones & Bartlett Learning, Boston, MA, USA, 1995.

[4] M. Banerjee, B. Ghorai, and N. Mukherjee. Study of cross-diffusion induced Turing patterns in a ratio-dependent prey-predator model via amplitude equations. *Applied Mathematical Modelling*, 55:383–399, 2018.

[5] E. Barbera, G. Consolo, and G. Valenti. Spread of infectious diseases in a hyperbolic reaction-diffusion susceptible-infected-removed model. *Physical Review E*, 88(5):052719, 2013.

[6] R. Barreira, C. M. Elliott, and A. Madzvamuse. The surface finite element method for pattern formation on evolving biological surfaces. *Journal of Mathematical Biology*, 63(6):1095–1119, 2011.

[7] I. Berenstein. Distinguishing similar patterns with different underlying instabilities: Effect of advection on systems with hopf, Turing-hopf, and wave instabilities. *Chaos: An Interdisciplinary Journal of Nonlinear Science*, 22(4):043109, 2012.

[8] W. E. Boyce, R. C. DiPrima, H. Villagómez Velázquez, et al. *Elementary differential equations and boundary value problems. Ecuaciones diferenciales y problemas con valores en la frontera*. 2004.

[9] N. F. Britton. *Essential Mathematical Biology*. Springer Science & Business Media, New York, USA, 2012.

[10] M. A. Budroni, L. Lemaigre, A. De Wit, and F. Rossi. Cross-diffusion-induced convective patterns in microemulsion systems. *Physical Chemistry Chemical Physics*, 17(3):1593–1600, 2015.

[11] R. A. Cangelosi, D. J. Wollkind, B. J. Kealy-Dichone, and I. Chaiya. Nonlinear stability analyses of turing patterns for a mussel-algae model. *Journal of Mathematical Biology*, 70(6):1249–1294, 2015.

[12] R. S. Cantrell and C. Cosner. *Spatial ecology via reaction-diffusion equations*. John Wiley & Sons, 2004.

[13] V. Capasso and A. Di Liddo. Asymptotic behaviour of reaction-diffusion systems in population and epidemic models. *Journal of mathematical biology*, 32(5):453–463, 1994.

[14] V. Capasso and A. Diliddo. Global attractivity for reaction-diffusion systems. the case of nondiagonal diffusion matrices. *Journal of Mathematical aAnalysis and Applications*, 177(2):510–529, 1993.

[15] Y. Choi, R. Lui, and Y. Yamada. Existence of global solutions for the shigesada-kawasaki-teramoto model with strongly coupled cross-diffusion. *Discrete and Continuous Dynamical Systems*, 10(3):719–730, 2004.

[16] L. Corrias, B. Perthame, and H. Zaag. Global solutions of some chemotaxis and angiogenesis systems in high space dimensions. *Milan Journal of Mathematics*, 72(1):1–28, 2004.

[17] J. W. Costerton, P. S. Stewart, and E. P. Greenberg. Bacterial biofilms: a common cause of persistent infections. *Science*, 284(5418):1318–1322, 1999.

[18] E. Crampin, W. Hackborn, and P. Maini. Pattern formation in reaction-diffusion models with nonuniform domain growth. *Bulletin of mathematical biology*, 64(4):747–769, 2002.

[19] M. C. Cross and P. C. Hohenberg. Pattern formation outside of equilibrium. *Reviews of Modern Physics*, 65(3):851, 1993.

[20] C. M. Dafermos and M. Pokorny. *Handbook of differential equations: evolutionary equations*, volume 4. Elsevier/ North-Holland, Amsterdam, 2008.

[21] F. Davidson, B. Sleeman, A. Rayner, J. Crawford, and K. Ritz. Travelling waves and pattern formation in a model for fungal development. *Journal of Mathematical Biology*, 35(5):589–608, 1997.

[22] L. Edelstein-Keshet. *Mathematical Models in Biology*. Society for Industrial and Applied Mathematics, Philadelphia, USA, 2005.

[23] L. C. Evans. *Partial differential equations*, volume 19. American Mathematical Society, 2010.

[24] O. S. for MATLAB. https://uk.mathworks.com/matlabcentral/fileexchange/61636-pplane.

[25] G. Galiano and V. Selgas. On a cross-diffusion segregation problem arising from a model of interacting particles. *Nonlinear Analysis: Real World Applications*, 18:34–49, 2014.

[26] G. Galiano and J. Velasco. Finite element approximation of a surface–subsurface coupled problem arising in forest dynamics. *Mathematics and Computers in Simulation*, 102:62–75, 2014.

[27] G. Gambino, M. Lombardo, S. Lupo, and M. Sammartino. Super-critical and sub-critical bifurcations in a reaction-diffusion Schnakenberg model with linear cross-diffusion. *Ricerche di Matematica*, 65(2):449–467, 2016.

[28] G. Gambino, M. Lombardo, and M. Sammartino. Cross-diffusion-induced subharmonic spatial resonances in a predator-prey system. *Physical Review E*, 97(1):012220, 2018.

[29] G. Gambino, M. C. Lombardo, and M. Sammartinfile:///Users/maldandani/Downloads/1-s2.0 S1468121812002593-main.pdfo. Pattern formation driven by cross-diffusion in a 2{D} domain. *Nonlinear Analysis: Real World Applications*, 14(3):1755–1779, 2013.

[30] G. Gambino, M. C. Lombardo, and M. Sammartino. Turing instability and traveling fronts for a nonlinear reaction–diffusion system with cross-diffusion. *Mathematics and Computers in Simulation*, 82(6):1112–1132, 2012.

[31] G. Gambino, M. C. Lombardo, and M. Sammartino. Pattern formation driven by cross-diffusion in a 2D domain. *Nonlinear Analysis: Real World Applications*, 14(3):1755–1779, 2013.

[32] G. Gambino, M. C. Lombardo, and M. Sammartino. Pattern formation driven by cross-diffusion in a 2D domain. *Nonlinear Analysis: Real World Applications*, 14(3):1755–1779, 2013.

[33] A. Gierer and H. Meinhardt. A theory of biological pattern formation. *Kybernetik*, 12(1):30–39, 1972.

[34] S. Gourley, M. A. Chaplain, and F. Davidson. Spatio-temporal pattern formation in a nonlocal reaction-diffusion equation. *Dynamical systems*, 16(2):173–192, 2001.

[35] J. Halatek and E. Frey. Rethinking pattern formation in reaction–diffusion systems. *Nature Physics*, 14(5):507–514, 2018.

[36] Y. Han, Z. Li, J. Tao, and M. Ma. Pattern formation for a volume-filling chemotaxis model with logistic growth. *Journal of Mathematical Analysis and Applications*, 448(2):885–907, 2017.

[37] H. Harvey. Pplane (https://www.mathworks.com/matlabcentral/fileexchange/61636-pplane). *MATLAB Central File Exchange*, 2020.

[38] M. Iida, M. Mimura, and H. Ninomiya. Diffusion, cross-diffusion and competitive interaction. *Journal of mathematical biology*, 53(4):617–641, 2006.

[39] H. Khassehkhan, T. Hillen, and H. J. Eberl. A nonlinear master equation for a degenerate diffusion model of biofilm growth. In *International Conference on Computational Science*, pages 735–744. Springer, 2009.

[40] S. Kondo. The reaction-diffusion system: a mechanism for autonomous pattern formation in the animal skin. *Genes to Cells*, 7(6):535–541, 2002.

[41] S. Kondo and T. Miura. Reaction-diffusion model as a framework for understanding biological pattern formation. *science*, 329(5999):1616–1620, 2010.

[42] S. Kovács. Turing bifurcation in a system with cross diffusion. *Nonlinear Analysis: Theory, Methods & Applications*, 59(4):567–581, 2004.

[43] K. Kuto and Y. Yamada. Multiple coexistence states for a prey–predator system with cross-diffusion. *Journal of Differential Equations*, 197(2):315–348, 2004.

[44] K. Kuto and Y. Yamada. On limit systems for some population models with cross-diffusion. *Discrete & Continuous Dynamical Systems-B*, 17(8):2745, 2012.

[45] D. Lacitignola, B. Bozzini, R. Peipmann, and I. Sgura. Cross-diffusion effects on a morphochemical model for electrodeposition. *Applied Mathematical Modelling*, 57:492–513, 2018.

[46] M. Lewis. Spatial coupling of plant and herbivore dynamics: the contribution of herbivore dispersal to transient and persistent" waves" of damage. *Theoretical Population Biology*, 45(3):277–312, 1994.

[47] M. Lewis and P. Kareiva. Allee dynamics and the spread of invading organisms. *Theoretical Population Biology*, 43(2):141–158, 1993.

[48] L. Li, J. Zhen, and S. Gui-Quan. Spatial pattern of an epidemic model with cross-diffusion. *Chinese Physics Letters*, 25(9):3500, 2008.

[49] Z. Lin, R. Ruiz-Baier, and C. Tian. Finite volume element approximation of an inhomogeneous brusselator model with cross-diffusion. *Journal of Computational Physics*, 256:806–823, 2014.

[50] Z. Ling, L. Zhang, and Z. Lin. Turing pattern formation in a predator–prey system with cross diffusion. *Applied Mathematical Modelling*, 38(21-22):5022–5032, 2014.

[51] M. Lizana and V. Padron. A spatially discrete model for aggregating populations. *Journal of Mathematical Biology*, 38(1):79–102, 1999.

[52] M. Lombardo, R. Barresi, E. Bilotta, F. Gargano, P. Pantano, and M. Sammartino. Demyelination patterns in a mathematical model of multiple sclerosis. *Journal of Mathematical Biology*, 75(2):373–417, 2017.

[53] Y. Lou and W.-M. Ni. Diffusion, self-diffusion and cross-diffusion. *Journal of Differential Equations*, 131(1):79–131, 1996.

[54] A. Madzvamuse, H. Ndakwo, and R. Barreira. Stability analysis of reaction-diffusion models on evolving domains: the effects of cross-diffusion. *Discrete & Continuous Dynamical Systems-A*, 36(4):2133, 2016.

[55] A. Madzvamuse, H. S. Ndakwo, and R. Barreira. Cross-diffusion-driven instability for reaction-diffusion systems: analysis and simulations. *Journal of Mathematical Biology*, 70(4):709–743, 2015.

[56] P. Maini. Spatial and spatio-temporal patterns in a cell-haptotaxis model. *Journal of Mathematical Biology*, 27(5):507–522, 1989.

[57] P. K. Maini. Using mathematical models to help understand biological pattern formation. *Comptes Rendus Biologies*, 327(3):225–234, 2004.

[58] H. Matano and M. Mimura. Pattern formation in competition-diffusion systems in nonconvex domains. *Publications of the Research Institute for Mathematical Sciences*, 19(3):1049–1079, 1983.

[59] H. Mehrer. *Diffusion in solids: fundamentals, methods, materials, diffusion-controlled processes*, volume 155. Springer Science & Business Media, 2007.

[60] M. Mimura. Stationary pattern of some density-dependent diffusion system with competitive dynamics. *Hiroshima Mathematical Journal*, 11(3):621–635, 1981.

[61] D. Morale, V. Capasso, and K. Oelschläger. An interacting particle system modelling aggregation behavior: from individuals to populations. *Journal of Mathematical Biology*, 50(1):49–66, 2005.

[62] A. Morozov, S. Petrovskii, and B.-L. Li. Bifurcations and chaos in a predator-prey system with the Allee effect. *Proceedings of the Royal Society of London. Series B: Biological Sciences*, 271(1546):1407–1414, 2004.

[63] J. Muhsin, T. Ufaq, H. Tahir, and A. Saadia. Bacterial biofilm: its composition, formation and role in human infections. *Journal of Microbiology and Biotechnology*, 4:1–14, 2015.

[64] J. D. Murray. *Mathematical biology. II spatial models and biomedical applications, journal = Interdisciplinary Applied Mathematics, volume = 18, year = 2001*. Springer-Verlag New York Incorporated.

[65] A. Okubo and S. A. Levin. *Diffusion and ecological problems: modern perspectives*, volume 14. Springer Science & Business Media, 2013.

[66] S. Ostrander. Macroscopic cross-diffusion models derived from spatially discrete continuous time microscopic models. *SIAM SIURO. doi*, 10, 2011.

[67] S. Ostrander. Macroscopic Cross-Diffusion Models Derived from Spatially Discrete Continuous Time Microscopic Models. *SIAM Undergraduate Research Online*, 4:51–71, 2013.

[68] K. J. Painter and T. Hillen. Volume-filling and quorum-sensing in models for chemosensitive movement. *Quarterly of Applied Mathematicsrahman2015mixed*, 10(4):501–543, 2002.

[69] Y. Peng and T. Zhang. Turing instability and pattern induced by cross-diffusion in a predator-prey system with Allee effect. *Applied Mathematics and Computation*, 275:1–12, 2016.

[70] A. Prieto-Langarica, H. V. Kojouharov, and B. M. Chen-Charpentier. Discrete and continuous approaches to modeling cell movement in the presence of a foreign stimulus. *Computers & Mathematics with Applications*, 64(3):167–174, 2012.

[71] A. Prieto-Langarica, H. V. Kojouharov, and B. M. Chen-Charpentier. Upscaling from discrete to continuous mathematical models of two interacting populations. *Computers & Mathematics with Applications*, 66(9):1606–1612, 2013.

[72] K. A. Rahman, R. Sudarsan, and H. J. Eberl. A mixed-culture biofilm model with cross-diffusion. *Bulletin of Mathematical Biology*, 77(11):2086–2124, 2015.

[73] J. Recknor and S. Mallapragada. The biomedical engineering handbook: Tissue engineering and artificial organs. *Nerve Regeneration: Tissue Engineering Strategies. 3rd. New York: Taylor & Francis*, pages 48–1, 2006.

[74] F. Rossi, V. K. Vanag, E. Tiezzi, and I. R. Epstein. Quaternary cross-diffusion in water-in-oil microemulsions loaded with a component of the belousov-zhabotinsky reaction. *The Journal of Physical Chemistry B*, 114(24):8140–8146, 2010.

[75] W. Ruan. Positive steady-state solutions of a competing reaction-diffusion system with large cross-diffusion coefficients. *Journal of Mathematical Analysis and Applications*, 197(2):558–578, 1996.

[76] R. Ruiz-Baier and C. Tian. Mathematical analysis and numerical simulation of pattern formation under cross-diffusion. *Nonlinear Analysis: Real World Applications*, 14(1):601–612, 2013.

[77] F. Sanchezgarduno and P. K. Maini. Traveling wave phenomena in some

degenerate reaction-diffusion equations. *Journal of Differential Equations*, 117(2):281–319, 1995.

[78] G. Sewell. *The numerical solution of ordinary and partial differential equations*, volume 75. John Wiley & Sons: s: Hoboken, NJ, USA,, 2005.

[79] J. Shi, Z. Xie, and K. Little. Cross-diffusion induced instability and stability in reaction-diffusion systems. *Journal of Applied Analysis and Computation*, 1(1):95–119, 2011.

[80] J. Shi, Z. Xie, and K. Little. Cross-diffusion induced instability and stability in reaction-diffusion systems. *J. Appl. Anal. Comput.*, 1(3):95–119, 2011.

[81] N. Shigesada, K. Kawasaki, and E. Teramoto. Spatial segregation of interacting species. *Journal of Theoretical Biology*, 79(1):83 – 99, 1979.

[82] J. Smoller. *Shock waves and reaction diffusion equations*, volume 258. Springer Science & Business Media, New York/Heidelberg/Berlin, 2012.

[83] A. Stevens and H. G. Othmer. Aggregation, blowup, and collapse: the abc's of taxis in reinforced random walks. *SIAM Journal on Applied Mathematics*, 57(4):1044–1081, 1997.

[84] K. R. Swanson, E. C. Alvord, and J. Murray. Quantifying efficacy of chemotherapy of brain tumors with homogeneous and heterogeneous drug delivery. *Acta biotheoretica*, 50(4):223–237, 2002.

[85] K. R. Swanson, E. C. Alvord, and J. Murray. Virtual brain tumours (gliomas) enhance the reality of medical imaging and highlight inadequacies of current therapy. *British Journal of Cancer*, 86(1):14, 2002.

[86] K. R. Swanson, E. C. Alvord Jr, and J. Murray. A quantitative model for

differential motility of gliomas in grey and white matter. *Cell Proliferation*, 33(5):317–329, 2000.

[87] Y. Tao and M. Wang. Global solution for a chemotactic–haptotactic model of cancer invasion. *Nonlinearity*, 21(10):2221, 2008.

[88] C. Tian, Z. Lin, and M. Pedersen. Instability induced by cross-diffusion in reaction–diffusion systems. *Nonlinear Analysis: Real World Applications*, 11(2):1036–1045, 2010.

[89] C. Tian, Z. Ling, and Z. Lin. Spatial patterns created by cross-diffusion for a three-species food chain model. *International Journal of Biomathematics*, 7(02):1450013, 2014.

[90] R. T. Tranquillo and J. Murray. Mechanistic model of wound contraction. *Journal of Surgical Research*, 55(2):233–247, 1993.

[91] G. Truskey, F. Yuan, and D. Katz. Transport phenomena in biological systems, Pearson Prentice Hall. *NJ, Upper Saddle River*, 2004.

[92] E. Tulumello, M. C. Lombardo, and M. Sammartino. Cross-Diffusion Driven Instability in a Predator-Prey System with Cross-Diffusion. *Acta Applicandae Mathematicae*, 132(1):621–633, aug 2014.

[93] A. M. Turing. The chemical basis of morphogenesis. *Philosophical Transactions of the Royal Society of London. Series B, Biological Sciences*, 237(641):37–72, 1952.

[94] S. Turner, J. A. Sherratt, K. J. Painter, and N. J. Savill. From a discrete to a continuous model of biological cell movement. *Physical Review E*, 69(2):021910, 2004.

[95] V. K. Vanag and I. R. Epstein. Cross-diffusion and pattern formation in reaction–diffusion systems. *Physical Chemistry Chemical Physics*, 11(6):897–912, 2009.

[96] F. Verhulst. *Nonlinear differential equations and dynamical systems*. Springer Science & Business Media, 2006.

[97] A. W. Visser. Lagrangian modelling of plankton motion: From deceptively simple random walks to fokker–planck and back again. *Journal of Marine Systems*, 70(3-4):287–299, 2008.

[98] A. I. Volpert, V. A. Volpert, and V. A. Volpert. *Traveling wave solutions of parabolic systems*, volume 140. American Mathematical Soc., 1994.

[99] V. Volpert and S. Petrovskii. Reaction–diffusion waves in biology. *Physics of Life Reviews*, 6(4):267–310, 2009.

[100] P. Waltman. *Competition models in population biology*, volume 45. Society for Industrial and Applied Mathematics, 1983.

[101] Y. Wang, J. Wang, and L. Zhang. Cross-diffusion-induced pattern in an si model. *Applied Mathematics and Computation*, 217(5):1965–1970, 2010.

[102] J. A. Wiens. Spatial scaling in ecology. *Functional ecology*, 3(4):385–397, 1989.

[103] Y. Wu. Existence of stationary solutions with transition layers for a class of cross-diffusion systems. *Proceedings. Section A, Mathematics-The Royal Society of Edinburgh*, 132(6):1493, 2002.

[104] Y. Wu and Y. Zhao. The existence and stability of traveling waves with transition layers for the skt competition model with cross-diffusion. *Science China Mathematics*, 53(5):1161–1184, 2010.

[105] Z. Xie. Cross-diffusion induced turing instability for a three species food chain model. *Journal of Mathematical Analysis and Applications*, 388(1):539–547, 2012.

[106] Y. Yamada. Positive solutions for lotka–volterra systems with cross-diffusion. In *Handbook of differential equations: stationary partial differential equations*, volume 6, pages 411–501. Elsevier, 2008.

[107] L. Yang, A. M. Zhabotinsky, and I. R. Epstein. Stable squares and other oscillatory Turing patterns in a reaction-diffusion model. *Physical Review Letters*, 92(19):198303, 2004.

[108] E. Zemskov, K. Kassner, M. Hauser, and W. Horsthemke. Turing space in reaction-diffusion systems with density-dependent cross diffusion. *Physical Review E*, 87(3):032906, 2013.

[109] E. P. Zemskov, V. K. Vanag, and I. R. Epstein. Amplitude equations for reaction-diffusion systems with cross diffusion. *Physical Review E*, 84(3):036216, 2011.

[110] W. Zhang, A. Seminara, M. Suaris, M. P. Brenner, D. A. Weitz, and T. E. Angelini. Nutrient depletion in bacillus subtilis biofilms triggers matrix production. *New Journal of Physics*, 16(1):015028, jan 2014.